UPPER BOW RIVER HAZARD STUDY
ICE JAM MODELLING ASSESSMENT AND FLOOD HAZARD IDENTIFICATION

FINAL REPORT

Prepared for:

Alberta Government

Alberta Environment and Parks

17 November 2022

NHC Ref. No. 3001178

nhc
northwest hydraulic consultants
water resource specialists

UPPER BOW RIVER HAZARD STUDY
ICE JAM MODELLING ASSESSMENT AND FLOOD HAZARD IDENTIFICATION

FINAL REPORT

Prepared for:

Alberta Environment and Parks
Edmonton, Alberta

Prepared by:

Northwest Hydraulic Consultants Ltd.
Edmonton, AB

17 November 2022

NHC Ref No. 3001178

Report Prepared by:

Michael Brayall, P.Eng.
Hydrotechnical Engineer

Report Reviewed by:

Gary Van Der Vinne, P.Eng.
Principal

DISCLAIMER

This report has been prepared by **Northwest Hydraulic Consultants Ltd.** for the benefit of **Alberta Environment and Parks** for specific application to the **Upper Bow River Hazard Study in Alberta**. The information and data contained herein represent **Northwest Hydraulic Consultants Ltd.**'s best professional judgment in light of the knowledge and information available to **Northwest Hydraulic Consultants Ltd.** at the time of preparation, and was prepared in accordance with generally accepted engineering practices.

Except as required by law, this report and the information and data contained herein are to be treated as confidential and may be used and relied upon only by **Alberta Environment and Parks**, its officers and employees**. Northwest Hydraulic Consultants Ltd.** denies any liability whatsoever to other parties who may obtain access to this report for any injury, loss or damage suffered by such parties arising from their use of, or reliance upon, this report or any of its contents.

EXECUTIVE SUMMARY

Alberta Environment and Parks (AEP) retained Northwest Hydraulic Consultants Ltd. (NHC) in September 2015 to complete a river hazard study for the Bow River. The roughly 118 km long study reach extends from the Banff National Park boundary, located approximately 5 km upstream of the Town of Canmore, to Bearspaw Dam, near the City of Calgary western boundary. Within the Town of Canmore, the study area incorporates Policeman Creek, a channel roughly 6.5 km long situated on the Bow River floodplain and running parallel to the Bow River main channel. In addition, the study area includes three tributaries: the lower 1 km long reach of Exshaw Creek at the Hamlet of Exshaw; the lower 6 km of Bighill Creek at the Town of Cochrane; and the lower 5 km of Jumpingpound Creek at the Town of Cochrane.

The study is being conducted under the provincial Flood Hazard Identification Program (FHIP). Project stakeholders include the provincial government, local authorities, and the public.

The overall objectives of this project are to identify and assess river related hazards and enhance public safety along the Bow River and the three tributaries included in the study area. The intent is to reduce potential future flood damages and disaster assistance costs to the federal, provincial, and local governments, as well as First Nations. New floodplain maps will inform land use planning decisions, assist with developing flood mitigation options and facilitate emergency response planning.

The Upper Bow River Hazard Study has been structured into eight major project components. This report summarizes the work of the fifth component, Ice Jam Modelling Assessment & Flood Hazard Identification.

The study reach for the ice jam modelling assessment was limited to the reach between Ghost Dam and Bearspaw Dam because areas outside this reach have not previously been affected significantly by ice jam flooding. The most severe ice-affected incident in the historical record occurred in 1973 with a maximum reported stage of 1,119.36 m at River Avenue Bridge. The next highest stage observed was 1,119.18 m in 1970-71, with several other events within one metre of the historical maximum.

Flood hazards due to ice jams are the result of a combination of both ice conditions and discharge. Monte Carlo simulations were carried out to simulate a large number of scenarios with various combinations of ice conditions and discharge to determine the frequency distribution of the flood hazards between Ghost and Bearspaw dams. The input parameters for the Monte Carlo simulation were the maximum discharge during ice production, the annual maximum ice front station, and the deviation from the expected ice jam level. The HEC-RAS model was enhanced to facilitate ice jam modelling through modifications of the model geometry, the selection of ice specific model parameters from literature, and the calibration of an ice roughness value of 0.035 to the maximum ice-affected water level measured in 1988-89. The ice-enhanced HEC-RAS model was used to convert the inputs for each Monte Carlo scenario to water levels along the study reach. An ice production model was developed and calibrated to the observed annual maximum ice front locations in the upper portion of the study reach to generate an unbiased record of annual maximum ice front locations for the Monte Carlo simulation.

Water level frequency curves generated from the Monte Carlo simulation results at each HEC-RAS model cross section were used to generate water surface profiles for the 50-year, 100-year, and 200-year return periods.

Flood inundation mapping was completed to shows areas of ground that would be inundated by water for the 50-year, 100-year, and 200-year ice jam flood scenarios and is provided in the Ice Jam Flood Inundation Map Library. The inundation mapping looked at both direct and indirect areas affected by flooding. The 50-year ice jam flood and larger inundates area around the Cochrane Water Treatment Plant, the backyards of several residences in the Bow Meadows community and along Riverside Place, and recreational areas near the Jumpingpound Creek confluence, the Bighill Creek confluence, and the Girl Guide Camp Jubilee. The 100-year ice jam flood and larger partially inundates several camp buildings in the Girl Guide Camp Jubilee. Minor flooding of the area around the Spray Lake Sawmills Family Sports Centre occurs during the 50-year ice jam flood. The only bridge affected by inundation is the pedestrian bridge at the mouth of Bighill Creek at the 50-year ice jam flood level and higher.

The Ice Jam Floodway Criteria Map Library provided with this report documents the ice jam flood hazard identification criteria and resulting floodway boundary. The governing criteria for the majority of the study reach is the previously defined floodway or the inundation limit when the previously defined floodway is outside the extent of inundation. The floodway includes recreational trails and parks near the Cochrane Water Treatment Plant, the mouth of Jumpingpound and Bighill creeks, and the Girl Guide Camp Jubilee. The flood fringe includes additional parkland and trails around the Cochrane Water Treatment Plant, portions of the Riverfront Park Nature Playground, and several buildings at the Girl Guide Camp Jubilee.

CREDITS AND ACKNOWLEDGEMENTS

Northwest Hydraulic Consultants Ltd. (NHC) would like to express appreciation to Alberta Environment and Parks (AEP) for initiating this project, making available extensive background information and providing advice and support throughout the survey work. Key AEP representatives were Jane Eaket, P.Eng. (Project Manager) and Peter Onyshko, P.Eng. (Alternate Project Manager).

The ice analysis was primarily conducted by Michael Brayall with support from Gary Van Der Vinne and Dan Healy. The ice analysis report was written by Michael Brayall with contributions from Dan Healy and Gary Van Der Vinne. Special thanks are extended to Dave Andres for reviewing the report and providing technical assistance during the project.

TABLE OF CONTENTS

LIST OF TABLES

LIST OF FIGURES

LIST OF MAPS

1 INTRODUCTION

1.1 Project Background

Alberta Environment and Parks (AEP) retained Northwest Hydraulic Consultants Ltd. (NHC) in September 2015 to complete a river hazard study for the Bow River, along a reach defined between the Banff National Park boundary at the upstream end and Bearspaw Dam at the downstream end. The study is being conducted under the provincial Flood Hazard Identification Program (FHIP).

The Bow River has been exposed to severe flooding in the past, with three extreme events occurring from the late 1800s to early 1900s, two around 1930, and, more recently, in 2013.

For the Bow River reach within the current study limits, provincial flood hazard mapping was previously prepared for Cochrane (Alberta Environment, 1990), Canmore (W-E-R Agra, 1993), and Municipal District (M.D.) of Bighorn (Acres, 1996). The Cochrane study was completed by Alberta Environment in 1986 with an addendum issued in 1990. The study reach covered 21 km of the Bow River (from Bearspaw Dam to upstream of the Town of Cochrane boundary) and the lower 4.5 to 5 km reaches of Jumpingpound and Bighill Creeks (two tributaries discharging to the Bow River within the Town of Cochrane limits). The M.D. of Bighorn study, completed by Acres International Ltd., includes a 15 km reach of the Bow River from the west boundary of Bow Valley Provincial Park to Dead Man Flats and includes the lower one kilometre reach of Exshaw Creek. The Canmore study completed by W-E-R Agra Ltd. covered a 20 km reach of Bow River from Dead Man's Flats, through the Town of Canmore (including Policeman Creek), to the Banff National Park boundary.

AEP identified a need to update and expand the coverage of this mapping following the 2013 floods. Stakeholders of the present project are the Government of Alberta, the Town of Canmore, the M.D. of Bighorn, Stoney Nakoda First Nation, Rocky View County, the Town of Cochrane, and the public.

1.2 Project Objectives

The overall objectives of this project are to identify and assess river related hazards and enhance public safety along the Bow River and three tributaries within the study area. The intent is to reduce potential future flood damages and disaster assistance costs to the federal, provincial, and local governments, as well as First Nations. The updated flood mapping will also inform land use planning decisions, assist with developing flood mitigation options and facilitate emergency response planning.

Specific study components, as outlined in the AEP Upper Bow River Hazard Study Terms of Reference, are:

- survey and base data collection;
- hydraulic model development; calibration and validation;
- open water flood inundation map production;

- open water flood hazard identification;
- ice jam assessment and associated flood hazard identification;
- governing flood hazard map production;
- flood risk assessment and inventory; and
- channel stability investigation.

The results of each component will be summarized in individual stand-alone reports. This report describes the outcome of the ice jam modelling assessment and associated flood hazard identification phase of the project and forms the fifth report of the Upper Bow River Hazard Study.

The objectives of the ice jam modelling assessment and associated flood hazard identification phase of the project are to complete the following tasks:

- documentation of the ice jam flood history;
- enhancement of the open water hydraulic model for ice conditions;
- ice jam flood frequency analysis, hydraulic modelling, and inundation mapping;
- sensitivity analysis of the model inputs; and
- ice jam floodway criteria map production.

The ice jam floodway criteria map will be used to determine the governing design flood hazard map and it will form part of the flood risk assessment and inventory.

1.3 Study Area and Reach

From the Bow River headwaters at Bow Lake (Elev. 1940 m), just north of Lake Louise, the river flows in a south-easterly to easterly direction over nearly 600 km before draining into the South Saskatchewan River. The Upper Bow River study area comprises a roughly 118 km long reach, extending from the Banff National Park boundary, located approximately 5 km upstream of the Town of Canmore, to Bearspaw Dam, near the City of Calgary western boundary. Within the Town of Canmore, the study area incorporates Policeman Creek, an inlet controlled high water channel roughly 6.5 km long situated on the floodplain and running parallel to the Bow River main channel. In addition, the study area includes three tributaries:

- the lower 1 km long reach of Exshaw Creek at the Hamlet of Exshaw;
- the lower 6 km of Bighill Creek at the Town of Cochrane; and
- the lower 5 km of Jumpingpound Creek at the Town of Cochrane.

Flow is regulated both on the Bow River main stem and on several tributaries. In addition to the Bearspaw Dam at the downstream end, the Ghost, Horseshoe Falls, and Kananaskis Dams also impound the river. The study area is shown in Figure 1.

The effect of ice on the flood hazards varies throughout the study reach. Upstream of Ghost Dam, water levels can increase during the winter months due to ice accumulation but the potential increase in water levels present little or no risk of flooding (W-E-R AGRA, 1993). A review of the historical flood record shows that ice-affected flooding upstream of Ghost Dam is rare and much less severe than open water flooding. Downstream of Ghost Dam, ice-affected flooding is of similar magnitude to the open water flooding. The Cochrane Floodplain Study (Alberta Environment, 1990) concluded that the ice regime on the Bow River at Cochrane is influenced by Ghost Dam upstream and Bearspaw Dam downstream. Continual releases of warm water from Ghost Reservoir can result in long open water stretches downstream of the dam during the winter months, which can lead to the production of large volumes of frazil ice. Frazil particles flocculate and ultimately become frazil floes (ice pans) that are transported downstream on the water surface and accumulate in the Bearspaw Reservoir. This accumulation progresses upstream through Cochrane at rates and thicknesses that are governed by the ice supply and the local hydraulic characteristics. The relatively steep river slope contributes to the development of thick ice covers that can result in significant increases in water level.

The ice jam modelling assessment and flood hazard identification study was only carried out in the reach between Ghost Dam and Bearspaw Dam because the previous studies indicated that significant ice-affected water levels only occur in this reach. This ice study reach includes several salient features of note. Jumpingpound Creek and Bighill Creek discharge into the Bow River within Cochrane city limits. The two tributaries have no effect on the ice regime of the Bow River and were therefore omitted from the ice-affected hydraulic model. Two bridges cross the Bow River within Cochrane: Highway 22 and River Avenue. The River Avenue bridge is of particular importance as it is the location at which the annual maximum stage was recorded. Additionally, a railway bridge crosses the Bow River upstream of Cochrane within the ice study reach.

2 ICE JAM FLOOD HISTORY

A comprehensive review of past flooding forms an important component of flood hazard assessment. This review provides an understanding of factors that lead to flooding and its severity. It also informs the calibration and validation of the ice enhanced hydraulic model.

An extensive data search was carried out and various local, provincial and federal sources were contacted to obtain hydrometric data, relevant flood narratives, observations, and photographs documenting significant floods (open water and ice jam). Sources contacted include:

- Water Survey of Canada (WSC);
- TransAlta Corporation (TransAlta);
- Alberta Transportation (AT);
- Provincial Archives of Alberta;
- community newspaper archives; and
- local libraries.

2.1 General Information

The flood hazards due to ice on the Bow River between Ghost Dam and Bearspaw Dam are dominated by freeze-up jams. Frazil production downstream of Ghost Dam is significant because of the large stretches of river that remain open during the winter due to warm water released from the reservoir. Furthermore, the Bow River through the study reach is steep and highly turbulent, creating perfect conditions for rapid frazil generation when air temperatures are below freezing. Breakup jams do not create flood hazards in the study reach because breakup is thermal in nature. The regulation of spring flows by Ghost Dam prevent the large flows required to produce mechanical breakups which are the cause of breakup ice jams and flooding. Furthermore, the warm water released from Ghost Reservoir results in rapid melting and downstream progression of the ice front once air temperatures are consistently above zero.

The flood hazard risk due to ice varies throughout the study reach. Ice accumulates in Bearspaw Reservoir and progresses upstream during the winter. The maximum upstream location that the head of the ice accumulation reaches each winter depends on the volume of ice produced throughout the winter. Air temperature is the most important factor affecting ice production. Other factors that have a smaller effect on ice production include discharge and solar radiation. A good understanding of these factors is required to quantify the flood hazard risk due to ice effects throughout the study reach. The risk is generally highest at the downstream end of the study reach and generally decreases towards the upstream end of the study reach.

2.2 Historic and Observed Floods

Both historic and recorded floods were considered in this review. Historic floods refer to major floods that occurred prior to the period of hydrometric data collection and systematic recording of water level and discharge. In some cases, the magnitude of a historic flood can be estimated based on observations or even anecdotal information. Compared to a number of countries, the hydrometric record length is relatively short for most locations in Canada, with stream gauging on the Bow River beginning in 1909. Non-indigenous settlements were first established in the area towards the late 1800s and reported historic floods are limited to this time span, although indigenous anecdotal accounts date back much further.

A search of available sources found no record of historic floods due to ice effects within the study reach. It is worth noting that prior to hydrometric record keeping, the study reach was not regulated by the Ghost and Bearspaw Dams.

2.3 Recent and Recorded Floods

The only source of recent or recorded floods within the study reach was found in the Cochrane Floodplain Study (Alberta Environment, 1990). The following excerpts are quoted from the study:

> "Winter flooding of some low terraces along the Bow River has occurred on a relatively frequent basis following installation of the Ghost Dam and Power Plant in the 1940's and the construction of the Bearspaw Reservoir in 1954. […] The most severe incident appears to have occurred in February, 1973, when a short-term loss in thermal generating capacity necessitated an increase in Ghost Plant output at a time when the ice pack accumulation was building through the Cochrane reach. TransAlta Utilities Corporation's records show that the ice pack water levels on this occasion reached a stage of approximately 4.5 m above normal summer water levels. This is high enough to cause flooding of low-lying areas bordering the river."

The 1973 peak stage recorded at River Avenue Bridge in TransAlta records is 1,119.36 m, which is the highest stage on record (Section 3.1). The next highest stage observed is 1,119.18 m in 1970-71, which suggests that the 1973 observation is not an outlier. Furthermore, there are several other observed stages within 1 m of the highest recorded stage.

Another quote from the Cochrane Floodplain Study (Alberta Environment, 1990) suggests localized flooding upstream of Highway 1A:

> "Winter flooding in the vicinity of the Cochrane Ranch Historic Site, located just upstream of Highway 1A, is believed to be caused by ice dams (aufeis) which form in the spring fed creek, particularly in years with sudden and frequent temperature changes."

Aufeis can develop on top of the intact ice cover when runoff collects on top of the ice and freezes, rather than draining through the ice. The increased ice thickness from this additional freezing raises water levels locally. This localized flooding was not analysed in this report.

3 AVAILABLE DATA

3.1 Ice-Related Water Level Measurements and Observations

Ice-related highwater levels in the study reach were summarized in the most recent floodplain study (Alberta Environment, 1990). A record of the maximum winter stage at the River Avenue Bridge is available in many years between 1947 and 1992 as summarized in Table 1. The annual maximum ice front location was also described in the 1990 floodplain study. The corresponding HEC-RAS river stations estimated for each observation are also presented in Table 1. The river stationing was developed during the hydraulic model creation portion of this study and is documented in the Hydraulic Model Creation and Calibration Report (NHC, 2018a).

Table 1 Maximum Observed Winter Water Levels on the Bow River at River Avenue Bridge in Cochrane

Ice Year	Description of Annual Maximum Ice Front Location	River Station of Annual Maximum Ice Front Location (m)	Maximum Stage (m)
1947-48	Ice did not reach Cochrane	<19,500	A
1948-49	above Mitford	30,000 - 31,000	1,118.48
1949-50	2.5 miles d/s of Ghost plant	37,800	1,116.83
1950-51	to #2 line crossing		B
1951-52	Ice did not reach Cochrane	<19,500	A
1952-53	Ice did not reach Cochrane	<19,500	A
1953-54	u/s of old Cochrane bridge	21,230 - 21,730	1,117.96
1954-55	just above Old Cochrane bridge	21,230 - 21,330	B
1955-56	4.7 miles d/s of Ghost plant	34,260	1,118.17
1956-57	to old Cochrane bridge	21,220	B
1957-58	no observations		B
1958-59	below mouth of Jumpingpound Creek.	24,379 - 24,879	1,118.87
1959-60	no observations		B
1960-61	no observations		B
1961-62	not observed		1,118.90
1962-63	1/2 mile d/s of Horse Creek	26,310	1,118.60
1963-64	no observations		B
1964-65	above CPR bridge	27,372 - 27,872	1,118.23
1965-66	no observations		B
1966-67	1 mile d/s of old Cochrane bridge	19,615	A
1967-68	not observed		1,117.72
1968-69	0.4 mile above CPR bridge	28,015	1,118.39
1969-70	above Hwy #22 bridge (new in 1969)	23,401 - 23,901	B
1970-71	above Jumpingpound Creek	24,879 - 25,379	1,119.18
1971-72	somewhere above CPR bridge	>28,000	1,118.72
1972-73	at Bighill Creek	22,890	1,119.36
1973-74	above Jumpingpound Creek	24,879 - 25,379	1,118.23
1974-75	1000' u/s of #22 Hwy bridge	23,705	1,117.99

Ice Year	Description of Annual Maximum Ice Front Location	River Station of Annual Maximum Ice Front Location (m)	Maximum Stage (m)
1975-76	d\s of Old Cochrane bridge (Griffith ranch)	20,224	A
1976-77	did not reach Cochrane	<19,500	A
1977-78	above Jumpingpound Creek	24,879 - 25,379	1,117.75
1978-79	between mouth of Jumpingpound Creek. & #22 Hwy bridge	23,890 - 24,390	1,118.78
1979-80	no observations		A
1980-81	no observations		B
1981-82	above Jumpingpound Creek	24,879 - 25,379	1,118.17
1982-83	no observations		A
1983-84	no observations		
1984-85	above #22 Hwy bridge	23,401 - 23,901	1,118.04
1985-86	no observations		B
1986-87	no observations		B
1987-88	no observations		B
1988-89	above #22 Hwy bridge	23,401 - 23,901	1,117.43
1989-90	ice did not reach Cochrane area	<19,500	1,114.93
1990-91	Backwater from heavy flows of slush ice only, no packing		1,116.45
1991-92	No observation of ice packing		A

A – Year in which the ice pack did not reach Cochrane.

B – Year for which no observations were recorded.

Ice profiles were surveyed by Alberta Environment three time during the winter of 1981-82 at eight different sites near Cochrane. The profiles were documented in the 1990 floodplain study. To compare the surveyed profiles to results from this study, the HEC-RAS river station was estimated for each survey site. The surveyed profiles are summarized in Table 2.

Table 2 Profile Surveys by Alberta Environment during the Winter of 1981-82.

Site	River Station (m)	December 15, 1981		January 25, 1982		February 22, 1982	
		Water Level (m)	Ice Level (m)	Water Level (m)	Ice Level (m)	Water Level (m)	Ice Level (m)
1	17,960	1,108.01	A	1,109.50	1,110.93	1,109.88	1,110.87
2	18,934	1,110.34	A	1,112.99	1,113.88	1,113.31	1,113.82
3	20,174	1,112.65	A	1,115.29	1,116.21	1,114.84	1,116.08
4	21,170[1]	1,114.78	A	1,117.30	1,118.17	1,116.88	1,117.93
5	22,399	B	A	B	B	1,118.99	1,120.34
6	23,317[2]	1,118.71	A	1,121.36	1,122.32	1,120.90	1,122.33
7	24,263	B	A	B	B	1,122.53	1,124.52
8	24,684	B	A	B	B	1,123.30	1,125.16

[1] River Avenue Bridge [2] Highway 22 Bridge

A – Ice cover not formed yet.

B – Measurement not taken at the river station during the day of survey.

3.2 Gauge Data and Rating Curves

Water levels (stage) and rating curves from hydrometric gauging stations located on the Bow River within the study area were obtained and used to support calibration of the ice-affected hydraulic model. The gauge names, locations, gauge operation and other gauge details are shown in Figure 1 and summarized in Table 3.

Table 3 Summary of Gauging Stations in the Study Reach

Source	Gauge Number	Gauge Name	Gauge Status	Period of Record	
				Measurements	Rating Curves
WSC	05BE999	Ghost Tailrace	Active	1989 - 2015	1979 - 2015
	05BH005	Bow River near Cochrane	Active	2006 – 2014[1]	2006 - 2014
	05BE006	Bow River below Ghost Dam	Discontinued	1933 – 1936[1], 1937 – 1962, 1968 – 1979, 1980 - 1989[1]	1933 - 1973
TransAlta	N/A	Ghost Plant	Active	1985 - 2014	N/A

[1]Seasonal measurements generally extending from March 1 to October 31 each year.

Discharge in the study area is regulated by the Ghost Dam and has been monitored by Water Survey of Canada (WSC) at three different gauge locations since 1933. The gauges were operated seasonally, generally between March 1 and October 31, for numerous years. As can be seen in Table 3, there are gaps in the discharge record.

TransAlta reported the discharge exiting Ghost Plant at hourly intervals starting in 1985. Winter discharge values are reported at Calgary but were not utilized for the study as they reflect operating conditions at Bearspaw Dam and not the discharge in the study reach.

3.3 Regulated Discharges

Golder Associates (Golder) was commissioned by AEP to conduct an assessment of the flood hydrology for the Bow River basin, including the Bow, Elbow, Highwood, and Sheep Rivers, as well as major tributaries (Golder, 2017). As part of this study, naturalized daily discharge series from 1930 to 2015 were developed. The naturalization of discharge in the study reach included discharges from Jumpingpound Creek and Bighill Creek when discharge data was available. Using available current operating rules, reservoir routing, channel discharge routing, and estimates of current water use, the effect of regulation from Ghost Dam was applied to the naturalized daily discharge series between Ghost and Bearspaw dams.

As part of the current study, the regulated discharges were compared to reported discharges from the three WSC gauges within the study reach to assess the difference between the regulated and measured discharges. Figure 2 provides a comparison of the variation in winter discharge (October to March) between the regulated discharge at both the Ghost Reservoir Outflow and the Bow River at Cochrane with the reported discharge from WSC 05BE999 Ghost Tailrace from the winter of the year 2000. The

regulated discharge generally follows the trend of the reported discharge but includes large daily fluctuations not shown by the reported discharge. Figure 3 shows the year-over-year variation of the mean winter (October to March) regulated discharge and the reported discharge. The reported discharge record is a combination of the reported discharges at the three gauges operated historically by WSC in the study reach. The regulated mean winter discharge was on average 10 m^3/s larger than the reported discharge for the period of record between 1937 and 1950. After 1950, the regulated mean winter discharge was less than the reported discharge for the majority of the years with an average difference of 6 m^3/s.

3.4 Winter Discharge

Simulation of ice conditions requires an understanding of discharge during the freeze-up period. The daily discharge is important for modelling water temperature and ice production (Section 4.2). As the Bow River discharge is regulated through the study reach by Ghost Dam, significant variation in discharge can occur throughout the day. Hourly outflows from Ghost Reservoir are available from TransAlta at the Ghost Plant. Analysis of both daily and hourly discharges is required to simulate the thickness of the ice cover that develops.

Ice production and accumulation generally occurs in December, January, and February each winter. The mean monthly flow is generally quite constant throughout the winter, with an average variation from the December to February mean discharge of only ± 6% (Figure 4). The monthly flows have increased systematically from a low of around 30 m^3/s in 1935 to a high about 75 m^3/s in 1961. The winter flows have decreased since 1961 and the winter flow regime has been quite constant since 1975, with an average winter discharge of 60 m^3/s.

The hourly discharges reported by TransAlta at Ghost Plant were analysed to determine the maximum discharge each day, as the thickness of the jam is more likely to reflect the effects of the maximum discharge as opposed to the mean daily discharge. Ghost Dam is used to generate hydropower; therefore, the maximum discharge from the dam occurs when power requirements are at a maximum. The term hydropeaking refers to the time during which the discharge is a distinct maximum due to power requirements. An example of hydropeaking and the day to day variation of releases from Ghost Reservoir during the first half of January 2015 is shown in Figure 5. Hydropeaking tended to occur between the hours of 19:00 and 23:00 at a maximum discharge of about 142 m^3/s. Between the hours of 00:00 and 08:00 each day, the discharge was at a minimum of about 32 m^3/s and then increased to a moderate value of approximately 53 m^3/s after 08:00 each day. Also shown on Figure 5 is the mean daily discharge each day. In 2015, it was generally between 55 and 60 m^3/s, except on the days when hydropeaking did not occur. The operating procedure used in 2015 is similar to the operating procedure in most years but the magnitudes of the low, moderate, and maximum discharges, and the times when each occurred, varied from year to year. For example, in 1995, the low, moderate, and maximum discharges were around 4 m^3/s, 96 m^3/s, and 150 m^3/s, respectively. In 2012, only a low and moderate discharge were included in the operating procedure, and a discharge above the moderate value was never employed.

It is expected the maximum ice levels each year will occur while the discharge is at its maximum. The maximum discharge for each year during the ice production period is listed in Table 4. The mean maximum discharge during ice production is about 150 m^3/s. The maximum of 216 m^3/s occurred in 1997 and the minimum of 80 m^3/s occurred in 2012. It is evident that substantial year to year variations in maximum discharge could result in significant differences in the maximum ice elevations each year.

Table 4 Summary of maximum discharge each year during ice production period.

Ice Year	Maximum discharge during ice production period (m^3/s)	Ice Year	Maximum discharge during ice production period (m^3/s)
1985-86	110	2000-01	163
1986-87	140	2001-02	173
1987-88	133	2002-03	165
1988-89	143	2003-04	173
1989-90	122	2004-05	156
1990-91	166	2005-06	164
1991-92	161	2006-07	166
1992-93	159	2007-08	168
1993-94	202	2008-09	169
1994-95	157	2009-10	149
1995-96	155	2010-11	112
1996-97	121	2011-12	112
1997-98	216	2012-13	80
1998-99	167	2013-14	145
1999-2000	167	2014-15	142

3.5 Air Temperature Data

The air temperature record is required to simulate ice production from year to year as discussed in Section 4.2. Environment Canada operates numerous climate stations within the vicinity of the study reach. The usefulness of a given climate station depends on both its proximity to the study reach and the length of the measurement record. Three climate stations were utilized in the analysis and are summarized in Table 5.

Table 5 Summary of Climate Stations Utilized for the Study

Station Name	Climate ID	Latitude (degrees)	Longitude (degrees)	Location Description	Elevation (m)	Record Length
Wildcat Hills	3037550	51.27	-114.72	6 km north of Ghost Dam	1268.0	2005-2016
Cochrane	3031676	51.20	-114.43	4 km northeast of River Ave Bridge	1332.0	1991-2004[1]
Calgary International Airport	3031093	51.11	-114.02	18 km east of Bearspaw Dam	1084.1	1881-2016

[1] Data collection at Cochrane began in 1961 but temperatures were not recorded until 1991.

Both the Wildcat Hills and Cochrane climate stations are near the study reach, but neither station has measurement records that span the entire ice observation record. As well, the two records do not overlap, so the records cannot be compared directly. The climate record at the Calgary International Airport spans the entire ice observation record and the measurement records of the other two climate stations. Daily temperature measurements between the months of October and March were correlated between the Calgary station and the Wildcat Hills (Figure 6) and Cochrane (Figure 7) stations. On the average, Calgary is slightly colder (0.3°C) than Cochrane and slightly warmer (1.6°C) than Wildcat Hills, which indicates that there is a 1.9°C difference between the Cochrane and Wildcat Hills air temperature on average; therefore, air temperatures cannot be appended to the Cochrane air temperatures to create a single unbiased record. The Calgary air temperatures are quite similar to those at Cochrane and provide a consistent air temperature record over the entire ice observation record, so the Calgary station record was selected to represent the air temperatures in the study reach.

3.6 Water Temperature Data

Water temperature measurements are important to determine when ice production begins on the Bow River each year between Ghost and Bearspaw Dams. Water temperature measurements are collected by AEP as part of the surface water quality monitoring program and stored as part of the Long Term River Network (LTRN) project. Water temperatures were measured periodically at Cochrane as part of LTRN at gauge AB05BH0010. The water temperature measurements are plotted relative to date for the October to January period in Figure 8. The dataset shows that by about the end of November, the water temperature reaches 0°C at Cochrane.

Figure 8 also shows simulated water temperatures at Ghost Dam based on heat transfer simulations discussed in Section 4.2.2. The simulated water temperature also reaches 0°C around the end of November. A best fit curve of the simulated water temperature at Ghost Dam was developed and adopted as the input water temperature for the ice production model (Section 4.2).

3.7 Solar Radiation

Solar radiation can have a significant effect on ice production. Solar radiation data is available from the Canadian Weather Energy and Engineering Datasets (CWEEDS) at Calgary International Airport from 1953 to 2005. The solar radiation is provided as daily global horizontal irradiance. The variation in solar radiation during months of ice production for the measurement record is shown in Figure 9. The lowest values of solar radiation typically occur around the winter solstice.

4 ICE RELATED MODELLING

Flood hazards are typically defined by the discharge frequency during open water flooding because, under open water conditions, it is possible to ascribe an unique water level to each flood frequency discharge. However, for ice jam floods, there is a range of water levels that can be associated with the same discharge depending on the ice conditions. Ice conditions vary each year with winter severity and the discharge during ice formation. As a result, there is a large combination of discharge and ice condition scenarios that contribute to the flood hazard. A Monte Carlo simulation was conducted to determine the distribution of flood hazards resulting from these combinations. Monte Carlo simulation involves generating a series of random values of input parameters from which a joint probability distribution is generated for the resultant parameter based on the combinations of input values. The value of the input parameters for each scenario are randomly generated from the observed probability distribution of each parameter.

The input parameters for the Monte Carlo simulation were (1) the maximum discharge during ice production, (2) the annual maximum ice front station, and (3) the deviation from the expected ice jam level. The maximum discharge during ice production was discussed in Section 3.4. The observed annual maximum ice front station record (Section 3.1) is biased because observations were only collected when the ice front reached at least as far as Cochrane. Therefore, an ice production model was developed and calibrated to the observed record to provide unbiased inputs to the Monte Carlo simulation (Section 4.2). The HEC-RAS model developed and discussed in the Hydraulic Model Creation and Calibration Report (NHC, 2018a) was enhanced to simulate ice jam water levels in the study reach (Section 4.1). A deviation from the simulated ice jam water level based on water level measurements at the WSC gauge was then applied to account for other processes that could not be simulated using the available data. Water level frequency curves generated from the Monte Carlo simulation results at each HEC-RAS model cross section were then used to establish water surface profiles for the 50-, 100-, and 200-year return periods.

4.1 Hydraulic Model Enhancement

4.1.1 HEC-RAS Program and Model

The U.S. Army Corps of Engineers computer program “HEC-RAS River Analysis Program” Version 5.0.3, developed in September 2016, was used to calculate the ice jam thickness and water surface profiles along the study reach. HEC-RAS is able to solve for water levels under ice covered conditions for two different scenarios. The first being when the ice thickness of the ice cover is known and the second when solving for the thickness of an ice jam. Ice jam thicknesses are a function of river width and slope, which can vary significantly along the study reach, so HEC-RAS was used to solve for the ice jam thickness. The inputs required to conduct an ice simulation with HEC-RAS include those documented in the Hydraulic Model Creation and Calibration Report (NHC, 2018a) (i.e., river cross sections along known lengths of channel, roughness coefficients for the channel and overbank areas at each cross section, a specified or computed water level at the downstream model boundary, and a discharge at all upstream model boundaries). In addition to these inputs, an ice enhanced model requires the following at each model

cross section: a prescribed ice cover condition, under-ice roughness, and a set of ice parameters characterizing the properties of the ice jam. These ice parameters are used to solve the wide channel ice jam stability equation and energy equation concurrently.

The HEC-RAS model allows the user to specify the ice cover condition as an option within the HEC-RAS cross section data editor. If no information is provided for the ice cover, then an open water condition is presumed. If the user assigns a value to the ice cover thickness, then the model assumes an ice cover condition. When an ice cover condition is defined, the user must provide the following:

- Ice cover thickness in the left overbank, main channel, and right overbank
- Ice cover roughness values in the left overbank, main channel, and right overbank
- Ice cover specific gravity
- Ice cover thickness
- Ice cover condition (stable ice cover or ice jam)
- If ice cover condition is set to ice jam, ice jam strength parameters (internal friction, ice jam porosity, and stress ratio constants) and maximum under-ice velocity
- Option to use either a fixed ice cover roughness or one that scales with the thickness of the ice cover

Additional detail on these parameters and how the model was enhanced for ice-cover simulations is provided in the following sections.

4.1.2 Enhancement Methodology

Beginning with the calibrated open water model, the following steps were undertaken to develop the ice enhanced model:

1. Adjust and refine the open water geometry for improved performance of the ice jam thickness profile computation.
2. Define ice specific model parameters.
3. Calibrate the ice enhanced model to observed ice-affected water levels by adjusting the under ice roughness.

Interpolated cross sections: Cross sections were interpolated throughout the length of the ice enhanced model to decrease cross section spacing. Ice jam modelling research (Beltaos and Tang, 2013; Flato and Gerard, 1986) suggests that the ice jam solution algorithm requires a maximum cross section spacing approximately one quarter of the main channel width to adequately resolve the computed ice jam thickness profile. The main channel width is defined as the width of the channel through which the ice cover moves and develops. It is less than the channel width between bank stations established for the open water model and does not change significantly along the reach. Furthermore, the ice jam algorithm

converges best when cross section spacing is regular and changes in shape between successive cross sections occurs gradually.

For the purposes of developing the ice enhanced model, it was required to establish a reach averaged main channel width to define the maximum cross section spacing when interpolating cross sections. A reach averaged main channel width of 100 m was chosen for the study. It was found that when setting the maximum cross section spacing to 25 m (one quarter of the main channel width) stable ice jam profiles could not be achieved, and a maximum cross section spacing of 100 m was required to achieve stable ice jam profiles. The resultant spacing of the interpolated cross sections in the ice enhanced model varied from 52 m to 99 m with an average spacing of 85 m. For comparison, the cross section spacing through the ice study reach for the open water model varied from 80 m to 973 m with an average spacing of 273 m.

The final step for adjusting cross section geometry was to remove closely spaced cross sections at bridges. Model tests found that the presence of bridge structures introduced instabilities in the ice thickness computations. The removal of the bridges was deemed to have no discernable effect on the computed ice jam profiles because the bridge structures span the main channel (i.e., the embankments only encroach the overbank areas) and do not impact the ice jam width used for the ice thickness computation. In total, the geometry improvement of the ice enhanced model increased the number of cross sections in the model from 158 to 490, and the average space between cross sections was decreased from about 270 m to 85 m.

Main channel widths: The main channel width is important for ice jam calculations as it affects the ice jam stability calculation directly and it indirectly affects the flow distribution between the main channel and the overbank area. The ice jam profile computations were found to be sensitive to abrupt changes in the main channel width for these reasons. Bank stations were adjusted along the study reach to improve model stability and to provide for a more representative ice jam width. Adjustments were made so that the modelled main channel was representative of an average ice jam width along the river and so that changes in the ice jam widths were gradual. This required constraining the main channel to a single channel alongside islands and the placement of bank stations within the open water main channel when transitioning from a cross section with a single channel to a cross section with an island. This provides a reasonable approximation of field observations on ice jam widths, which are indicated by the presence of longitudinal shear walls. Observed shear wall lines generally follow a smooth pattern with gradual transitions. As ice jams form alongside islands, it is common for the ice to accumulate and shove first down one side of the island and then the other. Bank stations within the open water main channel were necessary to allow for the transition between single channels and split channels with islands and to ensure gradual changes in ice jam widths for model stability.

The cross section interpolation routine within the HEC-RAS geometry editor was found to not adequately represent the main channel width for some interpolated cross sections. The largest errors were seen in areas where the channel shape changed significantly (i.e., single channel to split channel with island or single entrenched channel to single channel with a wide floodplain). Therefore, an alternative approach was developed to provide a better representation of the main channel width at poorly interpolated cross sections. The channel banks and overbank areas were replaced with geometry from the digital terrain

model (DTM) and the main channel portion of the cross section was interpolated from the main channel portion of the neighbouring cross sections. The interpolation process was therefore quite laborious and required manual adjustment of each interpolated cross section through the problem reaches.

Bed Roughness: Open water modelling allows for the variation of bed roughness across each cross section. Ice jam modelling requires a single roughness value in the main channel and each of the left and right overbanks. All bed roughnesses in the ice enhanced model were set to 0.035, which is the bed roughness calibrated at low flow from the open water modelling.

Ineffective flow areas: Ineffective flow areas defined in the open water model were outside the wetted area of the maximum water levels in the ice enhanced model, so they did not affect the simulations. Therefore, no changes were made to the ineffective flow areas in the ice enhanced model.

4.1.3 Ice-Specific Model Parameters

To evaluate the formation of an ice cover, a number of calibration parameters are required. The primary parameters required to solve the jam stability equation are described as follows.

Composite Roughness

The composite ice roughness is the combined bed and ice roughness factor resisting flow under the ice cover. HEC-RAS computes the composite roughness, n_o, following the familiar Sabeneev relationship Nezhikhovskiy (1964) as follows:

$$n_o = \left(\frac{{n_1}^{3/2}+{n_2}^{3/2}}{2}\right)^{2/3} \quad [1]$$

where n_1 and n_2 are the bed and bottom of ice roughness values, respectively.

Jam Stability Parameters

The jam stability parameters required as input to the HEC RAS model to solve the ice jam stability equation include: the internal friction angle of the jam, ϕ; the ice jam porosity (fraction of voids between ice floes), p; the maximum allowable flow velocity underneath the jam (V_{max}); and the coefficient of lateral to longitudinal stress in the jam, k_1. All other parameters are solved internally by the model. Ice jam strength properties cannot be measured directly in the field and consequently they are not reported for observed events. However, for an idealized *equilibrium* thickness condition, the suite of jam stability parameters can be lumped into a single *jam stability* parameter (dimensionless coefficient of internal friction), commonly denoted as μ. Some estimates for the magnitude of the jam stability parameter have been reported in the literature, but these values have been deduced by assuming equilibrium jam conditions, ice jam width, and hydraulic properties.

Beltaos (1978) deduced that the equilibrium jam stability relationships presented by Uzner and Kennedy (1976) could be made equivalent to those of Pariset et. al. (1966) by expressing the jam stability parameter as:

$$\mu = \tan\phi\,(1\text{-}p) \qquad [2]$$

Flato and Gerard (1986), following the work of Uzner and Kennedy (1976), presented the following definition of the jam stability parameter:

$$\mu = k_1 k_x \tan\phi(1\text{-}p) \qquad [3]$$

where the passive pressure ratio, k_x, is defined as:

$$k_x = tan^2\left(45 + \frac{\varphi}{2}\right) \qquad [4]$$

Equivalence between Equations 1 and 2 is found when $k_1 k_x$=1 (Healy and Hicks, 1997). With these assumptions, it was possible to estimate the required input parameters ϕ and k_1, given the more familiar jam stability parameters μ and p. The variable naming conventions presented herein are consistent with those in the HEC-RAS manual. An expanded overview of these formulations is provided by White (1999).

Ice Jam Porosity: Ice jam porosity represents the volume fraction of the interstitial spaces in the ice jam. It is assumed to be the same above and below the water surface. No information is available regarding the porosity of ice jams on the Bow River upstream of Bearspaw Dam. Ice accumulates on the Bow River as frazil pans consolidate due to the shear stress on the underside of the ice. A review of White (1999) shows that the porosity of frazil ice jams can range from 0.33 to 0.77. A value of p = 0.4 was chosen for the ice enhanced model based on the work by Majewski and Grzes (1986), who observed porosity of frazil accumulated by shoving and Shen and Wang (1992) who observed porosity of freeze-up jams.

Jam Stability Parameter: Previous investigators have estimated μ in the range of 0.8 to 2.0, with the larger values being associated with smaller ice jams (Andres, 1995a). A value of 0.93 was estimated by Neill and Andres (1984) for a large 1982 ice jam on the Peace River. As this value was obtained on a regulated river in Alberta, it was deemed to be appropriate for ice jam simulations in the study reach and was, therefore, adopted for this study.

Internal Friction and Coefficient of Lateral to Longitudinal Stress: The internal friction and stress coefficients were found by substitution of the adopted values for p = 0.4 and μ = 0.93 into equations [2] through [4], resulting in adopted values of ϕ = 57.17° and k_1 = 0.0868.

Maximum Allowable Flow Velocity Underneath the Jam: The model assumes that ice will be transported along the bottom of the ice cover if the velocity exceeds the maximum. The maximum velocity is most applicable at the ice jam toe where the thickness is typically at a maximum. If the computed velocity for a given ice thickness exceeds the maximum velocity, the ice thickness is reduced. Setting the maximum velocity at the default value of 1.5 m/s results in ice jam profiles with implausible shapes. The HEC-RAS ice jam routine produces the most plausible ice jam profiles when the maximum velocity is set artificially high (Beltaos and Tang, 2013); V_{max} = 10 m/s.

Overbank Ice Thickness

The ice jam stability equation for this study was only solved in the main channel portion of each cross section. This requires manually adjusting the ice thickness in the left and right overbank. The geometry modification to the main channel bank stations results in significant portions of the overbank at certain cross sections carrying a large percentage of the flow under the ice. Therefore, ice thickness in the overbank has a significant effect on the flow distribution between the main channel and the overbanks. There are several islands and gravel bars within the study reach that split the flow under ice conditions and the flow distribution around the island is affected by the ice thickness in the main channel and the overbank. Therefore, a methodology for establishing the ice thickness in the secondary channel was required. The general effect of varying the ice thickness in the secondary channel is that thicker ice in the secondary channel increases the flow in the main channel. Increased flow in the main channel increases the shear stress, which in turn increases the ice thickness. If the ice is thin or not present in the secondary channel, a large portion of the discharge will be pushed from the main channel into the secondary channel and main channel ice thickness will be less.

No ice thickness measurements are available to quantify the ice thickness variation between the main channel and the overbank channel at islands, but it is possible to develop estimates based on the mechanism of ice jam formation around islands. Ice pans generally follow the deepest part of the channel where the surface velocity is highest. Around flow splits, ice will first fill the main channel side of the island. As ice packs into the main channel, the water level in the main channel will rise and the percentage of the flow in the main channel will reduce and be forced down the secondary channel. The ice front will eventually reach the upstream end of the island and ice will begin going into the open water of the overbank channel. At this point, the discharge in the overbank channel will be at its maximum. The ice moving down the overbank channel will then develop an ice cover and the ice front will continue upstream of the island once the overbank channel is covered with ice. As the overbank channel fills with ice, the flow distribution will readjust and it is possible for additional packing of ice to occur in the main channel. Incremental adjustments in the ice thickness will continue until an equilibrium condition is reached. The final ice thickness in each channel will reflect the maximum formation discharge in each channel.

The ice cover formation process around islands is quite dynamic and beyond the capabilities of HEC-RAS. The HEC-RAS ice jam routine assumes a wide channel jam forms in the main channel only. It is evident that a reasonable ice thickness must be specified in the overbank channel to achieve realistic ice thicknesses in the main channel. The effect of the ice thickness in the overbank channel is largest when the flow split between the main and overbank channel is similar. When the overbank channel is much smaller than the main channel, the overbank channel ice thickness has less effect on the simulated main channel ice thickness. Therefore, the approach adopted for assigning the overbank channel ice thickness was to equate it to the main channel ice thickness. This required the development of an iterative modelling approach where the overbank channel ice thickness was gradually adjusted until it was equal to the main channel ice thickness within a chosen tolerance.

4.1.4 Calibration Results

The HEC-RAS ice model was calibrated to the maximum ice-affected water level measured in 1988-89 as this was the only year of water level measurements during which hourly discharge measurements were available from TransAlta. Based on temperature records from that winter, sustained temperatures below zero did not occur until 19 December 1988 and remained below zero until 18 January 1989. The maximum hourly discharge due to hydropeaking between 29 December 1988 and 23 January 1989 was 109 m^3/s. After 23 January 1989, the maximum hourly discharge during hydropeaking was increased to 143 m^3/s for the remainder of the winter. It was assumed that the ice cover formed while the maximum hourly discharge was 109 m^3/s and that the maximum water level occurred later in the winter while the maximum hourly discharge was 143 m^3/s. This assumption is based on experience with ice cover formation on regulated rivers. It is common practice to develop an ice cover at a lower maximum discharge when the ice cover is comprised of loose frazil. Once the interstitial spaces within the frazil cover freeze, the strength of the cover increases and the cover is able to withstand higher discharges without collapsing. Therefore, the maximum discharge is often increased after the frazil ice jam has had a chance to freeze due to increased power production. The model boundary conditions and the calibrated input parameters are presented in Table 6.

Table 6 Calibrated Ice Inputs

Parameter	Simulated Value
Discharge during Ice Cover Formation (m^3/s)	109
Discharge during Stage Measurement (m^3/s)	143
Maximum Water Level at River Avenue Bridge (m)	1,117.43
Manning's Roughness, Bed	0.035
Manning's Roughness, Ice	0.035
Composite Roughness	0.035
Dimensionless Internal Strength Coefficient, μ	0.93
Ice Porosity, p	0.40
Internal Angle of Friction, ϕ (°)	57.2
Ratio of Lateral to Longitudinal Stress, K_1	0.087
Maximum Flow Velocity Under Ice (m/s)	10

The calibration ice jam profile is plotted on Figure 10. The calibrated ice jam profile matches the maximum water level from 1988-89. The calibrated ice roughness is 0.035, which is consistent with roughness coefficients reported by White (1999) for loose slush accumulations with thicknesses between 2.0 and 3.0 m. The composite roughness based on the calibrated ice roughness is 0.035. The mean simulated ice thickness for the ice cover throughout the study reach is 2.4 m with a thickness varying between 1.6 and 3.1 m.

The calibrated ice model was used to simulate the measured ice jam profiles from the winter of 1981-82 to validate the calibrated ice roughness. Hourly discharge measurements were not collected by TransAlta in 1981, so the maximum discharges during the profile measurements were not known. The simulated 1981-82 ice jam profile is shown in Figure 11. The maximum discharge that best matches the surveyed profiles was 160 m^3/s. Looking at Table 3-4, this discharge is typical of the median

hydropeaking discharge within the measurement record and is therefore plausible for the profiles measured in 1981-82.

4.1.5 Uncertainty and Confidence

The levels of uncertainty and confidence in the ice-enhanced HEC-RAS model water level simulations are functions of the amount of data that were available for calibration. Calibration was carried out with a single ice-affected water level measurement for which the discharge could reasonably be estimated. Water levels simulated at other discharges and at other locations are extrapolated from this calibration and are therefore less certain. These extrapolated water levels are a function of ice jam width, ice jam stability parameters, and ice roughness.

The variability of ice jam width was controlled to improve the stability of the model and to reflect that rapid variations in width are not observed in ice jams. The ice jam width was limited by confining the ice jam to the main channel and adjusting the bank station locations to vary smoothly from section to section. These adjustments were made based on observations of ice jam behavior in other rivers and may not reflect the precise behaviour of ice jams in the study reach. This may affect the estimates of ice jam thicknesses and water levels, particularly in transition zones upstream and downstream of islands. However, the simulated ice jam thicknesses based on these adjustments are consistent with thicknesses observed in other rivers, so there is a reasonable degree of confidence in the results.

Independent evaluation of the jam stability parameters requires detailed measurements of ice characteristics. Even when jam thicknesses are available, the jam stability parameters are lumped together during the calibration so that the ultimate uncertainty of the calibration is less than the uncertainty of the individual stability parameters. When ice thickness data is not available, as is the case for the present study, the stability parameters are adopted to produce an internal strength coefficient, μ, that is representative of similar conditions. This results in some uncertainty and reduced confidence in the ice thickness values predicted by the model; however, the effects of this uncertainty on simulated water levels is reduced by the ice roughness calibration process.

The ice roughness is also difficult to independently calibrate because ice jam water levels are also dependant on the jam stability parameters and the bed roughness. The general accepted practice is to assume that the bed roughness calibrated during open water conditions is the same as that under ice conditions, although the bed roughness under ice conditions may be different. The calibration process tends to reduce the effects of uncertainty in the individual parameters because the model is calibrated to simulate the correct water level. Uncertainty increases and confidence decreases as the water level deviates more from the calibrated value due to changes in discharge. Fortunately, due to regulation of discharge on the Bow River in the study reach, discharge variation each winter is generally small.

4.2 Ice Production Modelling

4.2.1 Methodology

The descriptions of the annual maximum ice front location were documented by Alberta Environment from 1947 to 1992 (Section 3.1). Descriptions of the annual maximum ice front location were only provided during years when the ice front progressed close to or beyond Cochrane. Therefore, the documented ice front locations tend to be biased towards the more severe ice years. To remove this bias and to increase the number of years for the statistical analyses, an ice production and ice advance model was created to produce estimates of the annual maximum ice front station for each year.

To simulate the annual maximum ice front location, ice production was simulated daily each winter. Ice production generally begins when the river water temperature reaches 0°C. When this occurs, the model begins producing ice within the domain and advancing an ice cover, with a specified thickness, from the downstream end of the study reach. The amount of ice produced is directly related to the length of open water through which energy is lost to the air. As the ice cover progresses upstream, the amount of ice produced each day decreases. Melting of the ice cover was also included in the simulation. At some point during each winter, the ice cover reaches its most upstream position. The inputs of the model were adjusted so that the mean and standard deviation of the simulated annual maximum ice front station matched as closely as possible the mean and standard deviation for the years during which the annual maximum ice front location was recorded. The annual maximum ice front location was then simulated for the years without ice observations described.

The simulation was developed using daily input values and reach averaged parameters. Ice production is a gradual process and the rate of production changes more slowly than the variation in river hydraulics along the reach. Therefore, the rate of ice production can be simulated well using daily input values and reach averaged parameters. Furthermore, any error introduced by simulating using daily input values and reached averaged parameters is acceptable because the results are being analyzed statistically.

4.2.2 Ice Production Model Components

The inputs required to simulate the annual maximum ice front location include winter hydraulic conditions, water temperature, border ice, ice production and ice accumulation. These inputs are summarized and discussed in the following sections.

Winter Hydraulic Conditions

To simulate ice production, it is important to specify inputs that define the reach averaged winter hydraulic conditions and determine how they vary with discharge. The inputs required by the model are the mean depth, mean velocity and open water top width.

When the air temperature is below freezing, the mean daily discharge is typically about 60 m^3/s . The calibrated open water HEC-RAS model was run for this discharge with a Manning's roughness of 0.035 to determine the variations of the mean depth (Figure 12), mean velocity (Figure 13), and top width

(Figure 14) throughout the study reach. The plots show the effect of the Bearspaw Reservoir, with the mean depth and top width being significantly higher in the reservoir than the reach average upstream, and the mean velocity being significantly less than the average. The plots also show that reach averaged values of mean depth, mean velocity and top width for stations more than 10,000 m upstream of Bearspaw Dam are representative of the study reach upstream of the reservoir.

The variation of the reach averaged mean depth, mean velocity, and open water top width with discharge was determined by running the open water HEC-RAS model for discharges ranging from 20 m^3/s to 120 m^3/s. The reach averaged values were determined for stations more than 10,000 m upstream of Bearspaw Dam to eliminate the effect of the reservoir. Using discharge intervals of 10 m^3/s, best fit curves were developed for each input. Power curve relationships fit the simulated inputs very well. The best fit curves and equations are presented in Figure 15.

Water Temperature

The Ghost Reservoir provides a consistent source of warm water throughout the winter. Downstream of the reservoir, the water temperature changes with variations in air temperature as the water flows downstream. The initial water temperature at Ghost Dam on each day for each year of the simulation was obtained from the best fit curve of the measured water temperatures in Ghost Reservoir shown in Figure 8. The change in water temperature in response to changing air temperature prior to the formation of frazil ice can be calculated reasonably well using the energy balance equation below.

$$\frac{dT_w}{dx} = \frac{1}{\rho C_p q}[-\phi_{Rw} + H_{wa}(T_w - T_a)] \qquad [1]$$

where: T_w = water temperature at a given distance x downstream of the reservoir; ρ = density of water (1,000 kg/m^3); C_p = specific heat of water (4220 J/kg/°C); q = the unit discharge; φ_{Rw} = the net solar radiation penetrating the water surface; H_{wa} = heat transfer coefficient at the air-water interface; and T_a = air temperature.

The water temperature varies with distance and the calculation is valid over a domain that the water can travel during which the meteorological conditions are more or less constant. The typical travel time based on the mean velocity from Ghost Dam to Bearspaw Dam is around 12 hours, so mean daily air temperatures were used.

The net solar radiation is determined by reducing the measured solar radiation by the effects of albedo and the degree of exposure of the water surface. The albedo during the winter months is quite high because the low angle of the sun causes a higher percentage of incoming solar radiation to be reflected from the water surface. The albedo of the water surface is also affected by the degree of surface turbulence, as water absorbs less energy when the water surface is flat. The degree of exposure of the water surface is very important during the winter months due to the low sun angle. Depending on the height and slope of the river banks, a large percentage of the water surface can be in shadow. This is of particular note as the Bow River between the Ghost and Bearspaw Dams generally has an East-West flow direction.

The steps for the daily water temperature simulation were as follows:

1. Determine the water temperature leaving Ghost Reservoir each day from the best fit curve on Figure 8.

2. From the daily air temperature (Section 3.5) and solar radiation (Section 3.7), calculate the distance downstream of Ghost Reservoir where the water temperature first reaches 0°C (the zero degree isotherm).

3. Compare the zero degree isotherm location to the location of the ice front. If the zero degree isotherm is located upstream of the ice front on the current simulation day, the distance between the zero degree isotherm and ice front locations is taken as the length over which frazil is generated each day. If the zero degree isotherm location is downstream of the ice front, no ice production occurs that day.

Attempts were made to incorporate melting of the ice cover into the ice production simulation, but this process is quite different from ice production. The ice front location was found to deteriorate too quickly during warm days when simple approximations were used . Furthermore, the ice production model was calibrated to the maximum ice extent and not the rate of accumulation and deterioration; therefore, ice melt was not a significant factor in simulating the maximum ice extent.

Ice Production

Ice production begins within the water column as ice crystals following the onset of supercooling and subsequent nucleation. Supercooling occurs in turbulent open water reaches exposed to sub-zero air temperatures. The Bow River is a shallow river with high turbulence so there is no significant vertical water temperature gradient through the actively flowing portions of the channel. The ice crystals that form are referred to as frazil, and frazil production is possible as long as the water is supercooled. In the case of a regulated river, such as the Bow River downstream of Ghost Dam, a longitudinal temperature gradient develops and frazil production begins downstream of the zero degree isotherm. Algorithms to calculate the frazil production have been derived by Shen et al. (1995) and Andres (1995b).

1. Frazil production occurs downstream of the zero degree isotherm at a rate that is proportional to the rate of energy flux from the air to the water.

2. Frazil ice particles within the water column combine together to form frazil flocs. The frazil flocs continue to grow in size until the buoyancy forces acting on the flocs is stronger than the turbulence forces responsible for the continuous mixing of the water column. The frazil flocs then rise to the surface to form ice floes.

3. As the ice floes move further downstream, they increase in both size and thickness as additional frazil flocs rise to the surface. As the surface ice concentration increases in the downstream direction, the rate of frazil production within the water column decreases, due to the reduced

open water area. When the surface ice concentration approaches 100%, frazil production ceases.

Simulation of ice production is a complex process that requires calibration of numerous parameters. Shen et al. (1995) summarizes the equations for the generation of frazil ice, the concentration of the suspended frazil, and the formation and growth of the ice floes for unsteady hydraulic and meteorological conditions. The CRISSP1D Ice Simulation model includes various ice production and melt algorithms; however, this model is not suitable for this study as it is unstable on gravel bed rivers like the Bow River, where there are rapidly changing flow conditions between pool and riffle sections. Instead, a simplified approach developed by Andres (1995b) was employed for this study.

The ice production algorithm is as follows:

1. The thickness of the surface ice floes was assumed to be constant and frazil flocs reaching the surface were assumed to only increase the surface ice concentration.

2. Reach average values for depth and flow velocity were assumed over the time that it takes water to move through the model domain.

3. The meteorological conditions were assumed to be constant over the length of the model domain and constant over the time it takes water to move through the domain.

The approximations employed during the ice simulation provide a first order estimate of ice generation that was calibrated to historical ice observations.

The simulation of ice production requires the assignment of three unknown parameters: the rise velocity of suspended frazil, the frazil floe thickness, and the frazil floe porosity. The other simulation parameters are known from the hydraulic and meteorological characteristics of the study reach.

Border Ice

Border ice develops from the edge of the water in areas where the flow velocity is low. Due to the temperature differential between the water and the bank, it is possible for border ice growth to begin while the ambient water temperature is above freezing. Border ice growth reduces the open water surface area of the channel resulting in reduced heat loss from the water to the air and reduced production of frazil ice.

Border ice growth occurs through two mechanisms, with the first generally beginning before the second.

1. Growth first occurs due to lateral heat loss into the bank as the temperature of the bank can be well below the freezing temperature of the water. As the border ice grows laterally from the bank, it also increases in thickness. The resulting ice is very smooth on the top and bottom. The thickness is greatest along the bank and decreases moving away from the bank, depending upon the relative growth rates in the lateral and vertical directions.

2. Once the water temperature begins to supercool and frazil ice begins to form frazil pans on the water surface, the lateral growth of the border ice increases as the frazil pans brush up against the existing border ice and deposit frazil onto the border ice. This process is known as "buttering". Border ice growth through this mechanism only occurs when surface ice concentrations are low to moderate and there is adequate time for the deposited frazil to freeze onto the border ice edge. When the surface ice concentration becomes substantial, there is a marked reduction in the rate of border ice growth due to abrasion between the moving frazil pans and the stationary border ice.

The mechanisms which control the growth of border ice are not well understood, and equations to simulate the growth of border ice are not well advanced. The air temperature and the local surface velocity are the two most important parameters. On a steep gravel bed river like the Bow River, the surface velocity can vary substantially due to the variability of the channel depth. The one-dimensional model utilized for this study is not capable of providing the level of velocity variation detail required to predict border ice growth rates. Instead, a cursory assessment was conducted; Google Earth aerial photographs and the shape of channel cross sections were evaluated to determine the importance of border ice growth in the study reach and its expected effect on ice production.

Border ice growth first occurs in regions of low velocity through thermal growth from the edge of water. Typical regions of low velocity occur on the inside of a channel bend or downstream of an island in the recirculation zone between the converging flows. Split flows around islands are a special case, as typically the flow distribution around an island is significantly skewed. When this is the case, border ice development can be expected in the secondary channel, sometimes across its entire width. It is difficult to quantify the percentage of the study area occupied by zones of low velocity. Border ice growth in the low velocity zones can occur quite quickly. Dynamic border ice growth can also occur when frazil pans adhere directly to the existing border ice. The amount of dynamic border ice growth is limited by high flow velocity.

Due to the complexity of simulating border ice coverage with time and the spatial variability of the channel shape throughout the domain, border ice growth was treated on a reach average basis. Most of the border ice is produced as skim ice in low velocity areas, where the depth is significantly less than the mean depth. A review of channel cross sections throughout the study area indicated that the border ice width would typically be about 15% of the open water top width.

Ice Accumulation

To simulate the position of the ice front over the winter, the ice produced in the model was accumulated to form an ice cover. The accumulated ice cover has a thickness defined by the hydraulic conditions of the reach through which the ice cover is passing. Two accumulation types were used in the model: a juxtaposed cover and a consolidated cover represented by an ice jam.

A juxtaposed cover occurs when the surface ice floes accumulate against each other to occupy the entire channel width with minimal deformation of the floes. The cover gains its strength as the ice floes freeze together and has a thickness more or less equal to that of the contributing ice floes. Juxtaposed covers

typically occur when the channel Froude number is very low. A juxtaposed cover is expected on the Bearspaw Reservoir for a length approximately 5 km upstream of the dam.

An ice jam occurs when the internal strength of the ice cover is less than the streamwise forces caused by the shear on the underside of the ice and mass of the cover. The ice cover collapses, increasing in thickness until the internal strength is equal to the streamwise forces. The resulting ice thickness is referred to as the equilibrium ice jam thickness. The thickness of the equilibrium ice jam varies from section to section, depending on the hydraulic conditions. For this study, it was assumed that the ice jam thickness was constant and equal to the reach-averaged thickness determined from the simulation of the 1988-89 ice jam profile, as discussed in Section 4.1.4.

The area in which the ice cover accumulated on a day-to-day basis was determined based on the channel surface area during low flow extracted from aerial photographs. The mean top width between successive model sections was adjusted to match the simulated reach averaged top width from the HEC-RAS model for a discharge of 60 m^3/s.

4.2.3 Model Calibration

The ice production model was calibrated to the observed annual maximum ice front stations presented in Table 1. The calibration was only conducted for observations occurring after the construction of Bearspaw Dam in 1954. The mean and standard deviation of the observed annual maximum ice front stations, along with results of the calibrated model, are presented in Table 7. The mean of the simulated maximum ice front station matches the observed very well but the standard deviation is larger by 1.6 km (50%). The main reason for the difference in standard deviation is the number of unknowns that were not simulated, due to the simplifications required to run the ice production model.

For the complete record, the mean of the simulated annual maximum ice front location is 20.6 km, 4.0 km further downstream than the observed mean. This is consistent with the fact that the observation record only includes years in which the ice front reached at least as far as Cochrane. Furthermore, the standard deviation of the simulated annual maximum ice front location increased to 6.0 km; this is likely due to removing the bias of the observed record. A summary of the ice production parameters used in the calibrated ice production model are summarized in Table 8.

The ice production simulation results are summarized in Table 9 and compared to the observed ice location when available. The maximum simulation error was 8.6 km downstream of the observed ice location in 1962-63. Figure 16 compares the observed versus the simulated ice location. The mean error of the modelled ice front location is 3.3 km.

Table 7 Summary of Mean and Standard Deviation of Maximum Ice Position Upstream of Bearspaw Dam

Description	Years	Distance Upstream of Bearspaw Dam	
		Mean (km)	Standard Deviation (km)
Observed Maximum Ice Front Location	1953-56, 58, 62, 64, 66, 68-75, 77-78, 81, 84, 88	24.6	3.3
Simulated Maximum Ice Front Location (Observed Years)	1953-56, 58, 62, 64, 66, 68-75, 77-78, 81, 84, 88	24.4	4.8
Simulated Maximum Ice Front Location (Full Record)	1953-2005	20.4	5.9

Table 8 Summary of Calibrated Ice Production Parameters

Parameter	Calibrated Value
Heat transfer coefficient	12.0
Ice thickness; consolidated cover (m)	2.4
Ice thickness; juxtaposed cover (m)	0.2
Frazil floe thickness (m)	0.2
Accumulation porosity (%)	40
Frazil floe porosity (%)	70
Rise velocity of suspended frazil (m/s)	0.0008
Length of juxtaposed cover (m)	5,000
Percentage of top width covered by border ice (%)	15
Albedo	0.30
Exposure (%)	75

Table 9 Comparison of Ice Production Simulation Results to Observed Maximum Annual Ice Position

Ice Year	Observed Annual Maximum Ice Front Location (m)	Simulated Annual Maximum Ice Front Location (m)	Simulation Error (m)
1953-54	21,230 - 21,730	23,622	-1,898
1954-55	21,230 - 21,330	18,482	2,842
1955-56	34,260	31,290	2,970
1956-57	21,220	25,262	-4,038
1957-58		16,311	
1958-59	24,379 - 24,879	22,662	1,717
1959-60		18,493	
1960-61		12,424	
1961-62		26,712	
1962-63	26,310	17,444	8,867
1963-64		18,216	
1964-65	27,372 - 27,872	31,103	-3,231
1965-66		27,407	

Ice Year	Observed Annual Maximum Ice Front Location (m)	Simulated Annual Maximum Ice Front Location (m)	Simulation Error (m)
1966-67	19,615	23,649	-4,034
1967-68		22,178	
1968-69	28,015	32,678	-4,662
1969-70	23,401 - 23,901	19,178	4,723
1970-71	24,879 - 25,379	26,555	-1,176
1971-72	>28,000	30,460	-2,588
1972-73	22,890	20,754	2,140
1973-74	24,879 - 25,379	22,659	2,720
1974-75	23,705	20,000	3,706
1975-76	20,224	18,557	1,667
1976-77	<19,500	11,511	
1977-78	24,879 - 25,379	29,243	-3,864
1978-79	23,890 - 24,390	27,644	-3,504
1979-80		19,878	
1980-81		14,710	
1981-82	24,879 - 25,379	28,435	-3,056
1982-83		12,495	
1983-84		19,666	
1984-85	23,401 - 23,901	20,769	3,132
1985-86		17,139	
1986-87		6,468	
1987-88		14,661	
1988-89	23,401 - 23,901	21,344	2,557
1989-90	<19,500	14,530	
1990-91		19,654	
1991-92		8,315	
1992-93		23,206	
1993-94		19,903	
1994-95		17,361	
1995-96		27,707	
1996-97		26,744	
1997-98		18,422	
1998-99		15,694	
1999-2000		15,777	
2000-01		14,082	
2001-02		21,386	
2002-03		18,154	
2003-04		16,296	
2004-05		17,740	
2005-06		16,281	

4.2.4 Uncertainty and Confidence

Uncertainty in the ice production model results are a function of uncertainty in the ice observations as well as in the inputs to the model. The observed location of the annual maximum ice position upstream

of Bearspaw Dam was estimated from available descriptive records, so it could deviate from actual locations by ±500 m or more. As well, the observations were biased to colder years because the downstream portion of the reach was not monitored; however, this effect was mitigated by the use of the model to simulate the entire record.

The inputs to the ice production model are river-specific, and since no observations of ice cover development along the study reach were available, the inputs were assigned based on general experience. The inputs to the ice production model are interrelated and require significant field observations to independently calibrate each parameter. The uncertainty of each input parameter is quite high, but due to the reach averaged approach employed, uncertainty in the simulated annual maximum ice front location upstream of Bearspaw Dam is less than the overall uncertainty of the input parameters. Furthermore, the simulation results were used to generate a mean and standard deviation for the Monte Carlo simulation, which were similar for the observed and calibrated data. Therefore, even though the confidence in the simulation of the annual maximum ice front location upstream of Bearspaw Dam for any given year is relatively low, it ultimately does not reduce the confidence in the results of the Monte Carlo simulation.

4.3 Ice-Related Flood Frequency Analysis

4.3.1 Monte Carlo Simulation

Ice-related flood frequencies are more complex than open water flood frequencies, as there are factors in addition to discharge that influence water levels. The factors that must be accounted for in an ice-related flood frequency analysis include the maximum discharge during ice production, the annual maximum ice front location, and secondary consolidations of the ice cover. The maximum discharge during ice production and the annual maximum ice front location can be used to calculate the expected freeze-up level at a particular location. A stable ice cover on a river regulated for hydropower production typically does not form without undergoing some degree of secondary consolidation, characterized by surges of ice and water that occur when an ice cover advances upstream and then collapses. The reasons for secondary consolidations include large daily variations in air temperature and discharge along the study reach. Secondary consolidations can produce surges of ice and water greater than the maximum discharge during ice production and can have the effect of increasing the ice thickness and water level above what is expected from considerations of the hydropeaking discharge alone. Current knowledge and techniques available to simulate ice jam levels are unable to quantify these dynamic events. Therefore, an additional factor must be added to the expected ice jam levels to account for these limitations. This factor is referred to as the deviation from the expected ice jam level.

The number of input factors greatly increases the complexity of the analysis, and typically field measurements of the inputs are not available for each maximum event or the length of record is insufficient to make useful predictions. To artificially extend the record length and improve peak flood level predictions, a Monte Carlo simulation was conducted. Monte Carlo simulation involves generating a series of random values for each given input parameter that match the probability distribution of the input parameters. The simulations can then be extrapolated beyond the measured data record to

predict extreme events. The main assumption of the Monte Carlo simulation is that the input parameters are independent of each other. The input parameters that were utilized in the Monte Carlo simulation were the maximum annual ice front location, the maximum annual discharge during ice production periods, and the deviation from the expected ice jam level.

A water level was calculated at each model cross section from 2,000 random combinations of input parameters. To calculate the water level at a given cross section, a rating curve relationship was required. Generally speaking, the water level at a given cross section will be governed by: (1) fully developed ice cover conditions, (2) open water conditions, or (3) the transition from a fully developed ice cover downstream to open water conditions. The transition region is comprised of two parts depending on whether the head of the ice cover is upstream or downstream of a given location. The *ice transition zone* is defined as the zone between the head of the ice cover and the start of fully developed ice conditions. The *open water backwater zone* is defined as the zone between the head of the ice cover and the end of ice-affected open water conditions (Figure 17). To ensure continuous profiles and avoid discontinuities, ice jam profiles for a range of discharges were generated with varying ice jam head locations. In total, 107 ice jam head locations ranging from 5,064 m to 40,850 m upstream of the Bearspaw Dam were simulated for nine discharges, ranging from 40 m^3/s to 280 m^3/s, for a total of 963 simulations. The water level was estimated at each model cross section by linearly interpolating between the simulated discharges and ice front stations generated from the suite of generated rating curves, the maximum discharge during ice production, and the annual maximum ice front location. This process was repeated for each Monte Carlo scenario. An example of the suite of rating curves generated for each model cross section is shown in Figure 17. This figure presents the variation in water level with discharge at the WSC gauge (River Station 21,170), transitioning from an open water condition to a fully developed ice cover condition. If the annual maximum ice front location is further downstream than the locations presented in the figure, the open water rating curve is applicable. If the annual maximum ice front location is further upstream, then the fully developed ice cover rating curve is used. The final water level is determined by adding the deviation from the expected ice jam level to the simulated ice level if an ice cover is present at that location. If the cross section was upstream of the annual maximum ice front location, the deviation was not applied to the calculated water level.

The process to determine the water level at each cross section for each Monte Carlo scenario is outlined below:

1. A frequency analysis was conducted on the annual maximum discharges during ice production**.** The data shown in Figure 18 are best represented by a normal distribution with a mean of 145 m^3/s and a standard deviation of 28.2 m^3/s.
2. A frequency analysis of the simulated annual maximum ice front location is shown in Figure 19. The data shown in this figure are best represented by a normal distribution with a mean of 20,400 m and a standard deviation of 5,900 m.
3. A series of 2,000 random maximum annual peaking discharges and maximum annual ice front locations were synthesized based on the means and standard deviations of the respective normal distributions.

4. The water level for each event in the series was determined for the cross section at River Avenue Bridge, since that is where historical maximum ice levels were measured. The suite of rating curves for the range of possible ice conditions used to determine the water level for each random event is shown in Figure 17. A frequency analysis of the simulated water levels indicated that simulated annual maximum ice front location distribution did not correctly simulate the steep portion of the measured water level frequency distribution, as shown in Figure 20. This steep portion of the measured distribution at the bridge provides a more accurate measure of the maximum ice front location in the vicinity of the gauge. Since the bridge is located near the mean ice front location, only the mean value could be refined. The mean of the annual maximum ice front location was therefore adjusted to 22,000 m. Figure 20 also compares the upper portion of the frequency distribution of the measured maximum water levels and the maximum water levels simulated using the refined annual maximum ice front location frequency distribution. The difference between the simulated and measured maximum water levels illustrates the need to include the deviation from the expected ice jam water level as an additional parameter.
5. The deviation from expected ice jam water level varies with return period, increasing as the return period increases. A series of 2,000 random deviations from expected ice jam water level were generated with an assumed normal distribution and applied to the calculated water level. The mean and standard deviation of this distribution were adjusted to minimize the sum of the squared differences between the simulated and observed water levels at the WSC gauge. It was found that a mean of 0.53 m and a standard deviation of 0.54 m provided the best fit. Figure 20 also shows the calibrated water level frequency curve with the deviation from expected ice jam water level at River Avenue Bridge.
6. The water level for the 2,000 random generated events was then determined for all of the HEC-RAS model cross sections within the ice study reach. Water levels were only determined for the surveyed model cross sections and not the interpolated cross sections. Frequency curves were established for each cross section. Samples of the frequency curves throughout the study reach are presented in Figure 21 The figure shows that the transition between open water and ice-affected conditions occurs at a lower annual probability of exceedance closer to Ghost Dam. The result is that water levels close to Ghost Dam are dominated by open water conditions rather than ice-affected conditions.
7. Water surface profiles corresponding to the 50-, 100-, and 200-year return periods were then constructed from the frequency curves at each cross section as discussed in Section 4.3.2.

4.3.2 Computed Ice Jam Flood Frequency Profiles

The simulated profiles for the 50-, 100-, and 200-year return periods are shown in Figure 22. The simulated water surface at each model cross section for each profile is summarized in Appendix A. Comparing the 50-, 100-, and 200-year profiles, it is worth noting that as the return period increases, the length of the profile under ice-affected conditions increases. The ice-affected conditions extend about 33 km upstream of Bearspaw Dam for the 50-year return period, about 35 km upstream for the 100-year return period, and about 37 km upstream for the 200-year return period.

4.3.3 Uncertainty and Confidence

At the River Avenue Bridge, the confidence in the Monte Carlo simulation results is high, as the results match the observed annual maximum water levels very well. The uncertainty in the water levels simulated from the enhanced HEC-RAS model is reduced because the mean and standard deviation of the deviation from the expected ice jam level were calibrated to match the observed levels. Furthermore, the mean of the annual maximum ice front location was adjusted to match the location of annual probability of exceedance of the ice transition region at River Avenue Bridge.

The confidence in the results of the Monte Carlo simulation are generally proportional to the distance from River Avenue Bridge. The simulation assumes that the deviation from the expected ice jam level is the same at all locations in the study reach; however, the deviation likely varies depending on the local hydraulic conditions at a given location. Furthermore, as there was only one location with observed water levels, which was near the mean annual maximum ice front location, it is not possible to make adjustments to the standard deviation of the annual maximum ice front location. The simulated standard deviation was higher than the observed value so the simulation may slightly overpredict the frequency of jamming in the upstream part of the study reach. This may result in slightly conservative estimates of ice jam water levels in this reach. Additional ice observations along the study reach over a series of the winters would provide additional confidence in the simulation results.

4.4 Comparison to Previous Studies

Two previous studies on the Bow River at Cochrane have attempted to identify the ice-related risks at Cochrane: the “Cochrane Floodplain Study” (Alberta Environment, 1990) and a letter report entitled “Ice-Related Flood Levels: Riversong Development, Bow River at Cochrane” (NHC, 2011). The methodology used in both studies was analysed and is presented below. The limitations of each method are highlighted.

The ice analysis in the “Cochrane Floodplain Study” utilized the ice observations presented in Table 1; however, the observations used were limited to those gathered between the winters of 1947-48 and 1982-83. Additionally, the eight years when the ice pack did not reach the measurement site (River Avenue Bridge) were neglected from the analysis. A frequency analysis was conducted on the resulting 18 ice-affected water levels. The analysis assumed that the 18 years of ice measurements were representative of an 18 year period, when in fact the 18 years of measurements represent a period of 26 years. Furthermore, the analysis assumed that the ice conditions and resulting water levels were representative of the entire study reach between Ghost Dam and Bearspaw Reservoir. The calculated design ice level was translated upstream and downstream of the measurement site using the reach averaged slope of the simulated open water 100-year flood. The analysis did not assess the variation in climate each year, its effect on the ice cover throughout the study reach, and the fact that the ice cover generally progresses further upstream during colder winters.

The ice analysis conducted for the Riversong Development (NHC, 2011) focused on ice-related water levels within Cochrane. The hydropeaking discharge was assumed to be constant for the observed maximum annual water levels at River Avenue Bridge, and the annual variation in maximum water level

was due to consolidation of the ice cover. A deviation from the expected ice-affected water level was applied, which is similar to the current study. The analysis did not look at annual variation of the maximum ice extent, so the ice levels could not be extrapolated beyond the vicinity of River Avenue Bridge.

4.5 Model Sensitivity Analysis

4.5.1 Ice Enhanced Hydraulic Modelling

The sensitivity of the calibrated ice enhanced hydraulic model to the roughness of the ice was evaluated. The roughness of the ice in the channel and the overbank were evaluated simultaneously because the overbank area through specific segments of the study reach occupied a significant portion of the main channel due to the adjustments made to bank stations (discussed in Section 4.1.2).

The open water sensitivity analysis of roughness was conducted on the 100-year flood profile. Due to the fact that the 100-year ice jam flood profile was developed using a Monte Carlo simulation, it is not possible to use the same methodology as the open water sensitivity analysis. Instead, the ice jam sensitivity analysis was conducted on an equivalent simulated ice jam profile, which produced water levels similar to the 100-year ice jam flood profile. This equivalent ice jam profile was simulated with a discharge of 280 m^3/s.

Based on a review of roughness of freeze-up ice jams by White (1999), sensitivity runs were conducted where the ice roughness was varied by about ±15% from the calibrated value (0.030 and 0.040) . The maximum and average difference in water level due to changing the ice roughness by ±15% were ±0.11 m and ±0.09 m, respectively. The change in water level was nearly constant along the study reach except for within Bearspaw Reservoir where there was very little change in water level for both sensitivity runs because the water level is not affected by ice roughness.

4.5.2 Ice Production Modelling

The sensitivity of the mean and standard deviation of the simulated annual maximum ice front location to the model inputs was analyzed. This was important because the calibrated Monte Carlo simulation showed that the annual probability of exceedance of the ice transition zone at River Avenue Bridge was quite sensitive to the mean. The model inputs analyzed in the sensitivity analysis are summarized in Table 10. The ice thickness of the juxtaposed cover and the frazil floe ice thickness were analyzed together as they reflect the same input.

Table 10 Sensitivity Analysis Results of Ice Production Input Parameters

Parameter	Inputs			Difference from baseline (m)			
				Low		High	
	Baseline	Low	High	Mean	Std Dev	Mean	Std Dev
Heat transfer coefficient	12.0	11.0	13.0	-1,550	-240	1,480	190
Ice thickness; consolidated cover (m)	2.4	2.16	2.64	1,540	270	-1,310	-270
Frazil floe/juxtaposed ice thickness (m)	0.2	0.1	0.3	-1,080	-330	180	140
Accumulation porosity (%)	40	30	50	-2,200	-440	2,820	390
Frazil floe porosity (%)	70	60	80	380	70	-730	-140
Length of juxtaposed cover (m)	5,000	4,000	6,000	-1,260	190	1,420	-250
Percentage of top width covered by border ice (%)	15	5	25	1,530	240	-1,630	-300
Albedo	0.3	0.2	0.4	-660	-30	680	30
Exposure (%)	75	65	85	670	30	-660	-30

To understand the results of the sensitivity analysis, it is important to understand the effect that each parameter has on ice production in the model. The parameters can be divided into two categories based on whether they affect the rate of ice production or the rate of ice accumulation. It should be noted that the rates have an indirect effect on each other, so the categories are not exclusive with respect to how they affect the annual maximum ice front location. The parameters affecting the ice production are the heat transfer coefficient, the percentage of top width covered by border ice, the albedo, and the exposure. The parameters affecting the rate of ice accumulation are the ice thicknesses, the porosity (accumulation and frazil), the length of the juxtaposed cover, and the percentage of top width covered by border ice.

Due to the connection between ice production and ice accumulation, it is not possible to definitively say which input parameter the results are most sensitive too, but it is possible to generally identify the most important parameters. For the ice production parameters, the most important are the heat transfer coefficient and the percentage of top width covered by border ice with the mean and standard deviation changing by about ±1,500 m and ±250 m, respectively. The ice front location was not sensitive to changes in the albedo and exposure as these parameters operate on solar radiation which generally has a small effect on ice production during the months that the majority of the ice is produced. The most important ice accumulation parameter is the accumulation porosity with a mean and standard deviation of about ±2,500 m and ±400 m, respectively, which were used to assess the sensitivity of the Monte Carlo simulation. Ice production results were also sensitive to the ice thickness of the consolidated cover. Both of these parameters directly relate to how the model converts the volume of ice produced into accumulated ice; therefore, the importance of these parameters is expected.

Based on the results of the sensitivity analysis, the adjustment that was applied to the calibrated mean of the maximum ice front locations during the Monte Carlo simulation is of a reasonable magnitude.

4.5.3 Monte Carlo Simulation

The results of the sensitivity analysis of the ice roughness and the ice production parameters were applied to the Monte Carlo simulation to determine the effect on the ice jam flood frequency profiles. The ice roughness and the ice production parameters affect the Monte Carlo simulation results in different ways. Ice roughness impacts the higher water levels within the fully developed ice jam region of the frequency curve, while the ice production parameters impact the location of the transition region of the frequency curve where, due to the proximity of the ice front, water levels shift rapidly from lower open water values to higher ice jam water levels.

As stated in Section 4.5.1, changes to the ice roughness generally change the water level uniformly throughout the domain. Due to the computation time required, it was not feasible to run the ice jam simulations required to generate new rating curves with the ice roughness changed ±15% (0.030 and 0.040). Instead, the average water level change found in Section 4.5.1 of ±0.10 m was applied to the Monte Carlo simulation results. The effect of this water level change on the water level frequency curve at River Avenue Bridge in the fully developed portion of the flood frequency curves is shown in Figure 23.

Figure 23 also shows the effect of varying the calibrated mean ice front location of 22,000 m by ±2,500 m on the water level at River Avenue Bridge. Increasing the mean ice front location increases the annual probability of occurrence of an ice cover at River Avenue Bridge. For the calibrated simulation results, the transition region at River Avenue Bridge begins at an annual probability of exceedance of about 60%. Increasing the mean ice front location by 2,500 m results in the transition region beginning at an annual probability of exceedance of about 75%. Conversely, decreasing the mean ice front location by 2,500 m results in the transition region beginning at an annual probability of exceedance of about 40%.

Varying the standard deviation of the ice front location has little effect on the annual probability of exceedance of the transition region, but it does affect the distance upstream that ice affects the flood frequency profile. The effect on the flood frequency profile of varying the calibrated standard deviation of 5,900 m by ±400 m is shown in Figure 24. Reducing the standard deviation by 400 m results in the ice-affected portion of the profile being shortened by about 2 km. Increasing the standard deviation by 400 m lengthens the ice-affected portion of the profile by about 1 km.

5 ICE JAM FLOOD INUNDATION MAPS

Flood inundation mapping shows areas of ground that could be covered by water under one or more flood scenarios for existing conditions. For this study, one flood inundation map series was created for each of the 50-, 100-, and 200-year ice-related floods and are provided in the Ice Jam Flood Inundation Map Library under sperate document. The process to produce the ice jam flood inundations maps is analogous to the production of the open water flood inundation maps documented in the Open Water Flood Inundation Mapping Report (NHC, 2018b). Additional information concerning the production of the ice jam flood inundation maps is provided below.

5.1 Methodology

The simulated profiles generated with the Monte Carlo simulation for the 50-, 100-, and 200-year ice-related floods, and the supplied DTM were used to determine the inundated areas for each scenario. Cross section lines were prepared in ArcGIS as follows to support the flood inundation mapping:

- An attribute field containing the water surface elevation for each of the flood scenarios was populated using the flood frequency water levels found in Appendix A.
- Left and right endpoints were extended outward, as needed, so that straight lines connecting the endpoints of adjacent cross sections remained outside the 200-year flood extents.

A boundary polygon was generated that enclosed all of the cross sections; this polygon defined the clipping extents for inundated areas. Automated routines were then used to complete the following tasks in ArcGIS for each of the flood scenarios:

- A triangular irregular network (TIN) representing a continuous water surface elevation (WSE) profile along the study reach was generated for each flood scenario, based on the computed WSE at each cross section; between cross sections, the WSE was linearly interpolated.
- The WSE TIN was converted to a tiled set of preliminary WSE grids. The WSE grid tiles matched the alignment and horizontal resolution of the LiDAR-derived bare earth DTM tiles supplied by AEP.
- Each bare earth DTM grid tile was subtracted from the corresponding WSE grid tile to generate a tiled set of flood depth grids. Grid cells with depth values less than 0 m, which represent dry areas, were assigned a value of NoData.
- Based on the depth grids, all areas with depths greater than 0 m were converted to inundation polygons. A simplification was applied in the raster to polygon conversion, so that the polygon boundaries do not exactly follow the edge of each raster cell.
- Filtering was used to remove isolated inundation areas smaller than 100 m^2. Holes in the inundation extent with areas less than 100 m^2 were also removed.

The resulting inundation polygons were then reviewed to identify direct overtopping in overbank areas, as described in Section 5.2. An adjusted version of the WSE TIN was created to reflect any edits made, and the above steps were repeated to produce adjusted WSE grids, depth grids, and inundation polygons.

The adjusted inundation polygons were smoothed in ArcGIS. A *PAEK* smoothing algorithm was applied with a 20 m tolerance. This allowed for an inundation boundary that is smoothed, but remains very similar to the original inundation polygon output. The smoothed inundation polygons were further reviewed in ArcGIS and classified to identify inundation of isolated areas and areas of potential flood control structure failure.

The final smoothed inundation extent polygons were used to clip the WSE grid tiles. The resulting WSE grids have *NoData* values for all dry areas but retain WSE values wherever inundation is shown.

5.1.1 Water Surface Elevation TIN Modifications

There are two complex areas that were not adequately represented by the WSE TIN based directly on the computed water surface elevations at each cross section. TIN modifications, as described below, were required in these locations.

Jumpingpound Creek and Bighill Creek Confluences

The WSE TIN was adjusted to represent backwater inundation on both Jumpingpound Creek and Bighill Creek. The water surface elevation from the Bow River model cross section at the confluence of each creek was applied to the creek until the inundation extents ended.

Areas Adjacent to Dams

Immediately upstream and downstream of Ghost Dam and Bearspaw Dam, additional WSE isolines were inserted to ensure that the adjacent model cross section water surface elevation extended to the dam structure and to other nearby structures such as spillways and powerhouses.

5.1.2 Representation of Water Bodies

As the LiDAR-derived bare earth DEM has not been hydro-flattened, water bodies (rivers, streams, lakes, and ponds) may not be represented as consistently flat surfaces. In some cases, this means that mapped flood inundation extents derived from the flood depth grids are discontinuous over water bodies.

To compensate for this issue, polygons were digitized to represent some of the water bodies, as required. These polygons were merged into the flood extent polygons before final polygon smoothing. This approach ensured that inundation extents are complete over water bodies.

5.1.3 GIS Deliverables

GIS deliverables include (for each flood scenario):

- Model cross sections with computed ice-related flood frequency levels attached as attributes. Polyline layer in Esri file geodatabase format.
- WSE TIN – preliminary, based directly on ice-related flood frequency levels . Esri TIN format.
- WSE TIN – adjusted, including any applicable revisions to account for overtopping areas. Esri TIN format.
- Tiled ice-related flood depth grids. Esri file geodatabase grid feature class format.
- Smoothed ice-related flood inundation extent polygons, with polygons classified as inundation extents, isolated areas, or potential flood control structure failure areas. Polygon layer in Esri file geodatabase format.
- Tiled WSE grids, clipped to the inundation extent polygons. Esri file geodatabase grid feature class format.

5.2 Direct Flood Inundation Areas

Direct flood inundation areas were identified as either being part of the actively-flowing river channel or flooded overbank areas connected to the actively-flowing river channel. Areas showing extensive overbank flooding connected to the channel at one distinct location (overtopping point) were adjusted such that the water surface elevation across that area was set equal to the water surface elevation at the overtopping point. This generally reduced the size of the inundated area extending upstream of an overtopping point and increased the size of the inundated area extending downstream of the overtopping point. In any instance where these adjustments resulted in a new overtopping point forming downstream, the water surface elevations in the overbank area were re-adjusted such that they were interpolated linearly between the upstream overtopping point and the ground elevation at the new downstream overtopping point.

Railway embankments were considered to be permeable, due to the presence of culverts and porous fill material within them. Therefore, it was assumed that the water surface elevation behind railway embankments would be equal to that of the adjacent actively-flowing river channel in front of them. No adjustments were made to the water levels or inundation extents for potential overtopping areas separated from the actively-flowing river channel by a railway embankment.

All adjustments were made to the water surface TINs so that inundation polygons could be re-generated from the data using the procedure described in Section 5.1 above.

5.3 Indirect Flood Inundation Areas

Indirect flood inundation areas were identified as having ground elevations below the water surface but no direct overland connection to the actively flowing river channel based on the surrounding topography. Two types of indirect flood inundation areas were identified for mapping purposes: isolated areas and areas of potential flooding due to flood control structure failure.

5.3.1 Inundation of Isolated Areas

Isolated areas, mapped using water surface elevations interpolated between cross sections, could potentially become inundated during a flood due to subsurface flow through porous media or flooding of buried pipes and culverts. Inundated areas behind embankments not identified as dedicated flood control structures or railways, such as roads and berms, were considered isolated areas.

5.3.2 Inundation Due to Potential Flood Control Structure Failure

No inundation areas due to potential flood control structure failure were identified for the ice jam flood inundation analysis.

5.4 Areas Affected by Flooding

5.4.1 Flooding of Residential Areas

Residential areas in Cochrane have the potential to be impacted by flooding.

- At the 50-year return period, some inundation would occur along the north (left) bank of the Bow River, upstream of the Jumpingpound Creek confluence. The inundation would extend nearly to the paved area around the Cochrane Water Treatment Plant and the backyards of several residences in West Terrace Point. The inundation would cover several recreational trails passing through this area.

- Along the south (right) bank of the Bow River, near the Jumpingpound Creek confluence, the backyards of residences in the Bow Meadows community would experience some inundation starting at the 50-year return period. Some parkland and recreational trails along Jumpingpound Creek and Bow River would also be inundated.

- Inundation of the Riverfront Park area, upstream and downstream of the Highway 22 bridge along the north bank of the Bow River, would start to occur at the 50-year return period.

- At the Bighill Creek confluence, the backyard of several residences along Riverside Place would be partially inundated, starting at the 50-year return period, along with a recreational trail.

- Downstream of Highway 22, the Girl Guide Camp Jubilee recreational area would be inundated starting at the 50-year return period. At the 100-year return period, the camp buildings would be partially inundated.

5.4.2 Flooding of Commercial & Industrial Areas

There are very few commercial or industrial buildings within the floodplain in Cochrane. The exception is a few industrial buildings near the Spray Lake Sawmills Family Sports Centre, located on the left bank of the Bow River downstream of the River Avenue Bridge. This area would experience some flooding at the

50-year return period. Further details regarding impacted structures are provided with the Flood Risk Assessment and Inventory Report (NHC, 2018c), provided under separate cover.

5.4.3 Flooding of Bridges & Culverts

For the purposes of this study, bridges are assumed to experience impacts from flooding if flood levels reach the highest low chord of the bridge. Similarly, culverts are assumed to be impacted by flooding if the road surface above the culvert is inundated. The pedestrian bridge at the mouth of Bighill Creek would be impacted at the 50-year return period, and a culvert in the north (left) floodplain of the Bow River, just upstream of the Highway 22 bridge, would also be impacted at the 50-year return period.

6 ICE JAM FLOOD HAZARD IDENTIFICATION

Flood hazard identification involves delineation of the floodway and flood fringe zones for a specified design flood. A description of key terms from the FHIP Guidelines (Alberta Environment, 2011), incorporating technical changes implemented in 2021 regarding how floodways are mapped in Alberta, is provided in Sections 6.1 and 6.2 below.

6.1 Ice Jam Design Flood Selection

The 100-year ice jam flood (as presented in Section 4.3) was selected as the ice jam design flood for flood hazard identification. The ice jam design flood is not meant to represent an actual single, static, ice jam flood event. In fact, no single, fully developed ice jam accumulation reproduces the design flood levels along the entire study reach. The more appropriate way to interpret the ice jam design flood event is that, anywhere along the study reach, a 100-year ice jam may develop and produce the 100-year ice jam flood levels. The flood levels would extend over some distance along the river within the study reach. Additionally, the ice jam design flood is not defined by a discharge, since that is not the only input to the Monte Carlo simulation, but is defined by a number of parameters, including the maximum discharge during ice production, the annual maximum ice front location, and secondary consolidation of the ice cover.

6.2 Ice Jam Floodway and Flood Fringe Terminology

Flood Hazard Area

The flood hazard area is the area of land that would be flooded during the design flood. It is composed of the floodway and the flood fringe zones, which are defined below.

Flood Hazard Mapping

Flood hazard mapping identifies the area flooded for the design flood and is typically divided into floodway and flood fringe zones. Flood hazard maps can also show additional flood hazard information, including areas of high hazard within the flood fringe and incremental areas at risk for more severe floods, like the 200-year and 500-year floods. Flood hazard mapping is typically used for long-term flood hazard area management and land-use planning.

Floodway

When a floodway is first defined on a flood hazard map, it typically represents the area of highest flood hazard where flows are deepest, fastest, and most destructive during the 100-year design flood. The floodway generally includes the main channel of a stream and a portion of the adjacent overbank area. Previously mapped floodways do not typically become larger when a flood hazard map is updated, even if the flood hazard area gets larger or design flood levels get higher.

Flood Fringe

The flood fringe is the portion of the flood hazard area outside of the floodway. The flood fringe typically represents areas with shallower, slower, and less destructive flooding during the 100-year design flood.

However, areas with deep or fast moving water may also be identified as high hazard flood fringe within the flood fringe. Areas at risk behind flood berms may also be mapped as protected flood fringe areas.

Design Flood Levels

Design flood levels are the computed water levels associated with the design flood.

6.3 Ice Jam Floodway Determination Criteria

In areas being mapped for the first time, the floodway typically represents the area of highest hazard. For ice-affected flood hazard identification, modified floodway determination criteria are used compared to open water flood hazard identification. Given the backwater associated with a wide channel ice jam, flow velocities are typically not considered when defining the ice-affected floodway. Therefore, the governing criterion under ice jam conditions is typically flood depths of 1 m or greater. If the overbank depths are less than 1 m or if there is no overbank flooding, the edge of the main channel area would define the floodway boundary.

When a flood hazard map is updated, an existing floodway will not change in most circumstances. Exceptions to this would be: (1) a floodway could get larger if a main channel shifts outside of a previously-defined floodway or (2) a floodway could get smaller if an area of previously-defined floodway is no longer flooded by the design flood.

Areas of deeper water outside of the ice jam floodway are identified as high hazard flood fringe. These high hazard flood fringe zones are identified in all areas, whether they are newly-mapped or have an existing floodway. The criterion used to define high hazard flood fringe zones will be aligned with the 1 m depth floodway determination criterion for newly-mapped areas.

All areas protected by dedicated flood berms that are not overtopped during the design flood are excluded from the floodway. Areas behind flood berms will still be mapped as flooded if the berms are overtopped, but areas at risk of flooding behind dedicated flood berms that are not overtopped will be mapped as a protected flood fringe zone.

Appendix B presents the left and right floodway stations and governing criteria for the ice jam flood hazard identification. The 1 m depth and previously mapped floodway govern throughout the majority of the study reach; when the previously mapped floodway falls outside the extent of inundation, the inundation limit was used to define the floodway boundary. For Bearspaw Reservoir, flood fringe was considered impractical and the inundation limits were also adopted for the floodway boundary in this area.

6.4 Ice Jam Design Flood Levels

The ice jam design flood levels are equivalent to the 100-year ice jam flood levels derived from the Monte Carlo simulation. Figure 25 presents the ice jam design flood profile and Appendix C provides a tabular summary of the associated water levels for the Bow River. Along Jumpingpound and Bighill creeks, backwater inundation was considered by applying the ice jam design flood level from the Bow

River immediately upstream of the confluence to tributary cross sections, where the thalweg is below this water level.

6.5 Ice Jam Floodway Criteria Maps

The ice jam floodway criteria maps depict the results of the ice jam flood hazard assessment and delineation of the proposed floodway boundary. The Ice Jam Floodway Criteria Map Library illustrates the following:

- inundation extents for the 100-year ice jam design flood;
- areas where the depth of water is 1 m or greater and the corresponding 1 m depth contour;
- the proposed floodway boundary for the ice jam design flood, as well as the associated floodway stations corresponding to the floodway determination criteria;
- isolated areas of non-flooded, high ground (i.e., “dry areas”) within the design flood extent;
- the location and extent of all cross sections used in the HEC-RAS model; and
- the previously-mapped floodway boundary (where it exists).

Additional information concerning the floodway criteria map production is provided below.

6.5.1 Methodology

The extent of inundation was mapped using the general procedure described in Section 5.1; a WSE TIN, WSE grid, and flood depth grid for the ice jam design flood levels were also generated as part of the process. Between HEC-RAS cross sections, a hydraulically-smooth floodway boundary was delineated using the adjacent governing criteria as a guide.

6.5.2 Areas in the Floodway

The following areas are within the ice jam floodway:

- A portion of the recreational trail near the Cochrane Water Treatment Plant.
- Parkland and recreational trails along the south (right) bank of the Bow River near the Jumpingpound Creek confluence.
- Portions of the Riverfront Park Nature Playground along north (left) floodplain of the Bow River downstream of the Highway 22 bridge.
- Recreational trails on the west (right) floodplain adjacent to the Girl Guide Camp Jubilee.

More information regarding existing infrastructure and property within the floodway can be found in the Flood Risk Assessment and Inventory Report (NHC, 2022), provided under separate cover.

6.5.3 Areas in the Flood Fringe

The flood fringe includes all inundated areas outside the floodway at ice jam design flood levels.

Areas behind flood control structures are mapped as flooded if they are overtopped, but areas at risk of flooding behind dedicated flood control structures that are not overtopped are identified as a protected flood fringe zone. There is no protected flood fringe zone for the ice jam design flood.

The high hazard flood fringe includes areas outside of the floodway that are directly inundated and deeper than 1 m. The additional areas determined to be high hazard flood fringe are insignificant.

Significant areas in the flood fringe include:

- Low-lying areas around the Cochrane Water Treatment Plant.
- Portions of the Riverfront Park Nature Playground.
- The Girl Guide Camp Jubilee, including several buildings on the property.

Outside of Cochrane, the majority of the areas in the flood fringe are presently undeveloped and have minimal infrastructure.

More information regarding infrastructure and property within the flood fringe can be found in the Flood Risk Assessment and Inventory Report (NHC, 2022), provided under separate cover.

7 ICE JAM WATER SURFACE ELEVATION GRIDS

Water surface elevation grids were prepared for each ice-affected flood scenario and provided with the GIS deliverables for this study component, along with the WSE TINs, flood depth grids, and inundation extent polygons. A description of the WSE grids is provided below.

7.1 Water Surface Elevation Grid Specification

For each of the flood scenarios, the adjusted WSE TINs described in Section 5.1 were converted to a tiled set of WSE grids matching the alignment, horizontal resolution, and tiling boundaries of the LiDAR-derived DTM supplied by AEP. Water surface elevations in metres are provided as 32-bit floating point grid cell values. The WSE grids at this stage were used to compute the flood depth grids, as described in Section 8.1.

As a final step, the inundation extent polygons were used to clip the WSE grids such that a value of NoData is provided for all dry areas and the water surface elevation values are indicated only where inundation is shown.

7.2 General Comments

WSE grids are provided for information only. Grid values are based on linear interpolation between cross sections, and as such, should be considered approximate. Since the adjusted WSE grids have been clipped using the smoothed inundation extent polygons, water's edge boundaries implied by the raster WSE grids correspond to the inundation extent boundaries presented on the inundation maps.

8 ICE JAM FLOOD DEPTH GRIDS

Flood depth grids were prepared for each ice-affected flood scenario and provided with the GIS deliverables for this study component, along with the WSE TINs, WSE grids, and inundation extent polygons. A description of the flood depth grids is provided below.

8.1 Flood Depth Grid Specifications

For each of the flood scenarios, each bare earth DTM grid tile was subtracted from the corresponding adjusted WSE grid tile (prior to clipping) to generate a set of flood depth grid tiles representing water depth in metres as 32-bit floating point values. All flood depth grids maintained the same alignment, horizontal resolution, and tiling boundaries as the LiDAR-derived bare earth DTM supplied by AEP. Grid cells with depth values less than 0 m, which represent dry areas, were assigned a value of NoData.

8.2 General Comments

The flood depth grids are provided for information only. Grid values are based on linear interpolation of water surface elevations between cross sections, and as such, should be considered approximate. Water's edge boundaries implied by the raster depth grids may deviate slightly from the inundation extent boundaries presented on the inundation maps. The depth grids are computed by subtracting the bare earth DTM grids from the adjusted water surface grids, whereas the mapped inundation extent boundaries, which were derived from the depth grids, have been further filtered and smoothed as discussed in Section 5.1.

Also, since the LiDAR-derived DTM indicates the approximate water surface elevation at the time of the LiDAR survey for submerged portions of river beds and other ground covered by water, depth values in those areas should not be considered accurate. Elsewhere, the depth grids may be used for many purposes, such as to identify areas in the floodplain that exceed a specified depth criteria. For example, these data were used to delineate the 1 m depth contour to support the flood hazard identification component of this study.

9 CONCLUSIONS

The objectives of this study were to assess river flood-related hazards along a 118 km long reach of the Bow River (including Policeman Creek), 1 km of Exshaw Creek, 6 km of Bighill Creek, and 5 km of Jumpingpound Creek. The Upper Bow River Hazard Study was divided into eight major project components. This report summarizes the work on the Ice Jam Modelling Assessment and Flood Hazard Identification component, which included documentation of the ice jam flood history, enhancement of the open water hydraulic model for ice conditions, hydraulic modelling of ice jams to assess ice jam flood frequencies, inundation mapping, a sensitivity analysis of model inputs, and production of ice jam floodway criteria maps. The reports for the four previous work components should be read in conjunction with this report, as they provide additional pertinent background information.

The effect of ice on the flood hazards varies throughout the study reach. Upstream of Ghost Dam, water levels can increase during the winter months due to ice accumulation, but the potential increase in water levels presents minimal risk of flooding and are much less severe than open water flooding. Downstream of Ghost Dam, ice-affected flooding is of similar magnitude to the open water flooding. Therefore, the ice jam analysis was limited to the reach downstream of Ghost Dam. The most severe ice-affected incident occurred in 1973 due to short term loss in thermal generating capacity, which resulted in an increase in discharge from the Ghost Plant. The maximum stage reported at River Avenue Bridge in 1973 was 1,119.36 m. The next highest stage observed, which occurred in 1970-71, was 1,119.18 m. Furthermore, there were several other observed stages at River Avenue Bridge within 1 m of the maximum stage.

Flood hazards due to ice jams are the result of a combination of both ice conditions and discharge. Monte Carlo simulations were carried out to simulate a large number of scenarios in order to determine the frequency distribution of the flood hazards between Ghost and Bearspaw dams. The input parameters for the Monte Carlo simulation were the maximum discharge during ice production, the annual maximum ice front location, and the deviation from the expected ice jam level. The HEC-RAS model was enhanced to facilitate ice jam modelling through modifications of the model geometry, the selection of ice specific model parameters from the literature, and the calibration of an ice roughness value of 0.035 to the maximum ice-affected water level measured in 1988-89. The ice-enhanced HEC-RAS model was used to convert the inputs for each Monte Carlo scenario to water levels along the study reach. An Ice production model was developed and calibrated to the observed annual maximum ice front locations to generate an unbiased record of annual maximum ice front location for the Monte Carlo simulation. Water level frequency curves generated from the Monte Carlo simulation results at each HEC-RAS model cross section were used to generate water surface profiles for the 50-, 100-, and 200-year return periods.

Sensitivity of several inputs to the Monte Carlo simulation were investigated to determine the effect on the 100-year water surface profile. The sensitivity of water levels due to ice roughness was found to be about ±0.10 m for a ±15% change in roughness. The Ice production model was analyzed for nine inputs and was found to be the most sensitive to the porosity of the ice accumulation, with a mean and standard deviation of the simulated mean varying by ±2,500 m and ±400 m, respectively. The sensitivity

results to the ice roughness and the Ice production model parameters were applied to the Monte Carlo simulation to determine the effect on the ice jam flood frequency profiles.

Flood inundation mapping was completed to show areas that would be inundated for the 50-, 100-, and 200-year flood scenarios. The inundation mapping addressed both direct and indirect areas affected by flooding. The 50-year ice jam flood and larger inundates area around the Cochrane Water Treatment Plant, the backyards of several residences in the Bow Meadows community and along Riverside Place, and recreational areas near the Jumpingpound Creek confluence, the Bighill Creek confluence, and the Girl Guide Camp Jubilee. The 100-year ice jam flood and larger partially inundates several camp buildings in the Girl Guide Camp Jubilee. Minor flooding of the area around the Spray Lake Sawmills Family Sports Centre occurs during the 50-year ice jam flood. The only bridge affected by inundation is the pedestrian bridge at the mouth of Bighill Creek at the 50-year ice jam flood level and higher.

The floodway criteria maps provided with this report document the ice jam floodway governing criteria and resulting floodway boundaries. The governing criterion for the majority of the study reach is 1m depth for the newly mapped areas and the previously defined floodway or the inundation limit (when the previously defined floodway is outside the extent of inundation) for previously mapped areas. The floodway includes recreational trails near the Cochrane Water Treatment Plant, near the Jumpingpound Creek Confluence, and upstream and downstream of the Highway 22 bridge on the north (left) floodplain. The floodway includes recreational trails and parks near the Cochrane Water Treatment Plant, the mouth of Jumpingpound and Bighill creeks, and the Girl Guide Camp Jubilee. The flood fringe includes additional parkland and trails around the Cochrane Water Treatment Plant, portions of the Riverfront Park Nature Playground, and several buildings at the Girl Guide Camp Jubilee.

10 REFERENCES

Acres International Ltd. (1996). Bow River – MD of Bighorn Flood Risk Mapping Study. Submitted to Alberta Environment, Alberta Environmental Protection River Engineering Branch for Canada-Alberta Flood Damage Reduction Program, February 1996.

Alberta Environment Water Management Operations, River Forecast Section (2011). Flood Hazard Identification Program Guidelines, July 2011.

Alberta Environment Water Resources Management Services, Technical Services Division (1990). Cochrane Floodplain Study, Addendum. River Engineering Branch for Canada – Alberta Flood Damage Reduction Program, November 1990.

Andres D.D. (1995a). A Case Study: Freeze-up and Jamming on the Peace River at Peace River in Beltaos S (Ed.), *River Ice Jams* (372 p). Highlands Ranch, Colorado: Water Resources Publications LLC.

Andres, D.D. (1995b). Frazil generation and ice floe formation on a regulated river. Proceedings of the Eighth Workshop of the Hydraulics of Ice Covered Rivers, Kamloops, BC. Canadian Committee of River Ice Processes and the Environment.

Beltaos, S. (1978). Equilibrium thickness of ice jams – discussion. Journal of the Hydraulics Division, ASCE, Vol. 104 (HY4), 578-581.

Beltaos, S. and Tang, P. (2013). Applying HEC-RAS to simulate river ice jams: snags and practical hints. Edmonton, AB. Committee on River Ice Processes and the Environment.

Flato, G., and Gerard R. (1986). Calculation of Ice Jam Thickness Profiles. Fourth Workshop on Hydraulics of River Ice. Montreal, June 1986.

Golder Associates (2017). Bow, Elbow, Highwood, and Sheep River Hydrology Assessment, February 2017.

Healy, D., and Hicks, F. (1997). A Comparison of the ICEJAM and RIVJAM Ice Jam Profile Models. MSc Thesis, Department of Civil and Environmental Engineering, University of Alberta, Edmonton, Alberta, 295 p.

Majewki, W., and M. Grzes (1986). Formation of ice cover on impounding reservoir and its influence on roughness coefficients and flow conditions. In Proceedings, IAHR Ice Symposium 1986, 18-22 August, Iowa City, Iowa, vol. 1, p. 489-502.

Neill, C.R. and Andres, D.D. (1984). Freeze-up flood stages associated with fluctuating reservoir releases. Cold Region Engineering Specialty Conference, Edmonton, Alberta, Canadian Society for Civil Engineering, Montreal, Canada, 249-264.

Nezhikhovskiy, R.A. (1964). Coefficient of roughness of bottom surfaces of slush ice cover. Soviet Hydrology, selected papers, no. 2, pp. 127-150.

Northwest Hydraulic Consultants (2011). Ice-Related Flood Levels: Riversong Development Bow River at Cochrane. Report submitted to Tamani Communities June 30, 2011.

Northwest Hydraulic Consultants (2018a). Upper Bow River Hazard Study – Hydraulic Model Creation and Calibration Report. Report for Alberta Environment and Parks.

Northwest Hydraulic Consultants (2018b). Upper Bow River Hazard Study – Open Water Flood Inundation Mapping. Report for Alberta Environment and Parks.

Northwest Hydraulic Consultants (2022). Upper Bow River Hazard Study – Flood Risk Assessment and Inventory. Report for Alberta Environment and Parks.

Pariset, E., Hausser, R., and Gagnon, A. (1966). Formation of ice covers and ice jams in rivers. Journal of the Hydraulic Division., ASCE, Vol. 92 (HY6), 1-24.

Shen, H.T. and Wang, D.S. (1992). Frazil jam evolution and cover load transport. In Proceedings, IAHR Ice Symposium 1992, 15-19 June 1992, Banff, Alberta, vol. 1, p. 418-429

Shen, H.T., Wang, D.E., and Wasnatha Lal, A.M. (1995). Numerical simulation of river ice processes. ASCE Journal of Cold Regions Engineering, Vol 9, No 3.

Uzner, M.S. and Kennedy, J.F. (1976). Theoretical model of river ice jams. Journal of the Hydraulics Division, ASCE, Vol. 102 (HY9), 1365-1383.

W-E-R Agra Ltd. (1993). Canmore Flood Risk Mapping Study. Submitted to Alberta Environment, Alberta Environmental Protection River Engineering Branch for Canada-Alberta Flood Damage Reduction Program, March 1993.

White, K. (1999). Hydraulic and Physical Properties Affecting Ice Jams. CRREL Report. US Army Corps of Engineers.

FIGURES

STUDY LIMIT

Ghost Dam

WSC 05BE006
BOW RIVER BELOW GHOST DAM
1933 - 1989

TransAlta/WSC 05BE999
GHOST TAILRACE
1988 - Present

TransAlta/WSC 05BE005
GHOST LAKE NEAR COCHRANE
1970 - Present
WL only

Jumpingpound Creek

WSC 05BH009
JUMPINGPOUND CREEK NEAR THE MOUTH
1965 - 2006

WSC 05BH005
BOW RIVER NEAR COCHRANE
1917 - 1930 (seasonal)

WSC 05BH015
JUMPINGPOUND AT TOWNSHIP ROAD No 252
2006 - Present

STUDY LIMIT

Bighill Creek

STUDY LIMIT

WSC 05BH005 (real-time)
BOW RIVER NEAR COCHRANE
2006 - Present (seasonal)

River Avenue Bridge

Highway 22 Bridge

Bow River

Bearspaw Dam

STUDY LIMIT

Alberta Government

nhc northwest hydraulic consultants

Model Stream Network (with stationing)
Dam
Bridge

Hydrometric Station
Active
Discontinued
Not Referenced in Study

Summer Village
Town
City

First Nation Reserve
County or Municipal District

DATA SOURCES: Basemap from Esri & NRCAN.

SCALE - 1:80,000
0 1 2 3 KM
N

Coordinate System: NAD 1983 3TM 114
Units: METRES

Job: 3001178 | Date: 17-NOV-2017

UPPER BOW RIVER HAZARD STUDY

STUDY AREA

FIGURE 1

MSN, \\mainfile-van\Projects\Active\3001178 Upper Bow River Flood Hazard Study\90 GIS\3001178_MSN_Fig_T5_StudyArea2.mxd

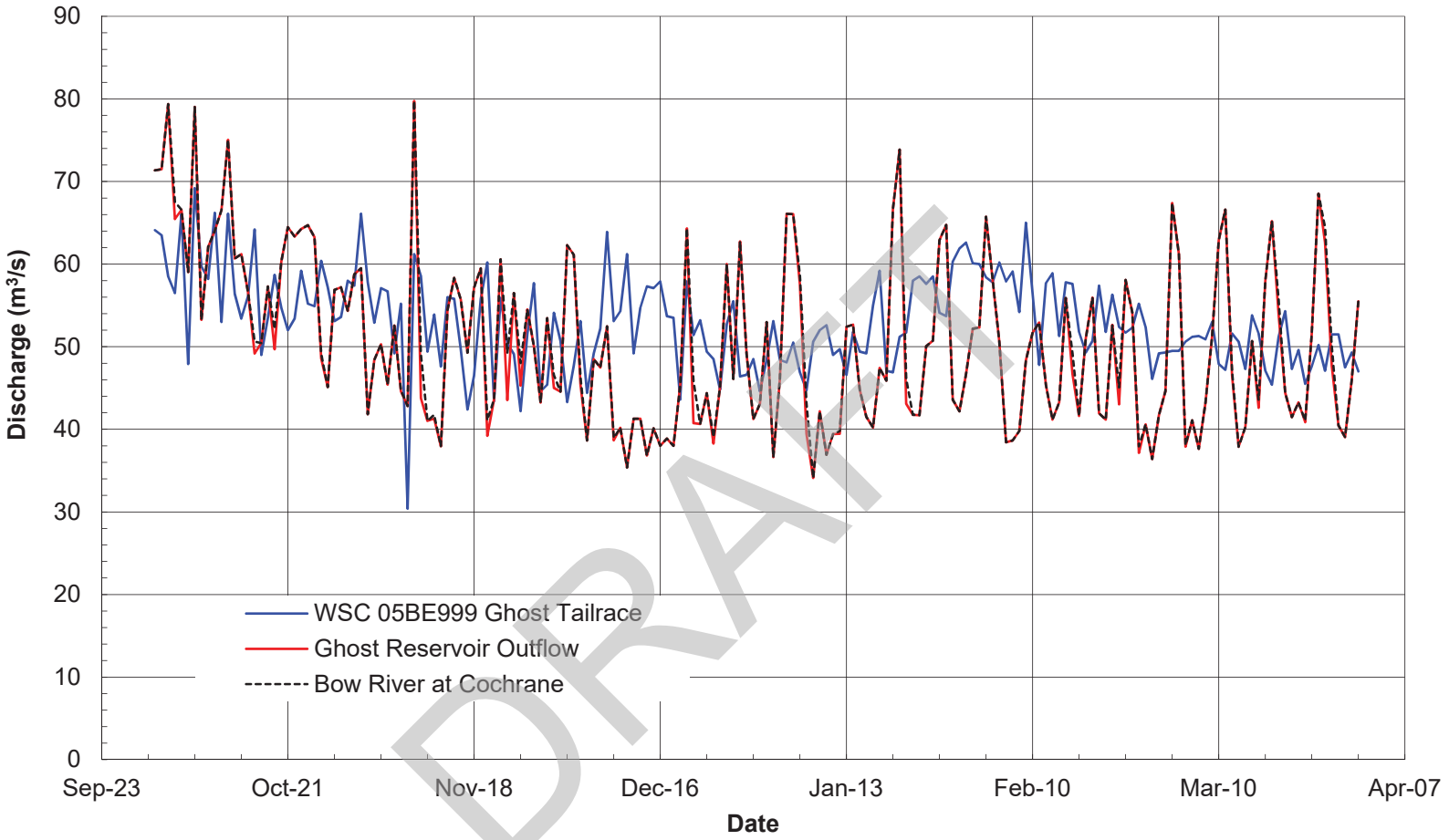

Note
Discharge hydrograph is for the year 2000.

nhc northwest hydraulic consultants

ALBERTA ENVIRONMENT AND PARKS		
UPPER BOW RIVER HAZARD STUDY ICE JAM MODELLING & FLOOD HAZARD IDENTIFICATION **Comparison of Simulated and Measured Daily Winter Discharge (October to March)**		
3001178	07 AUG 2018	**FIGURE 2**

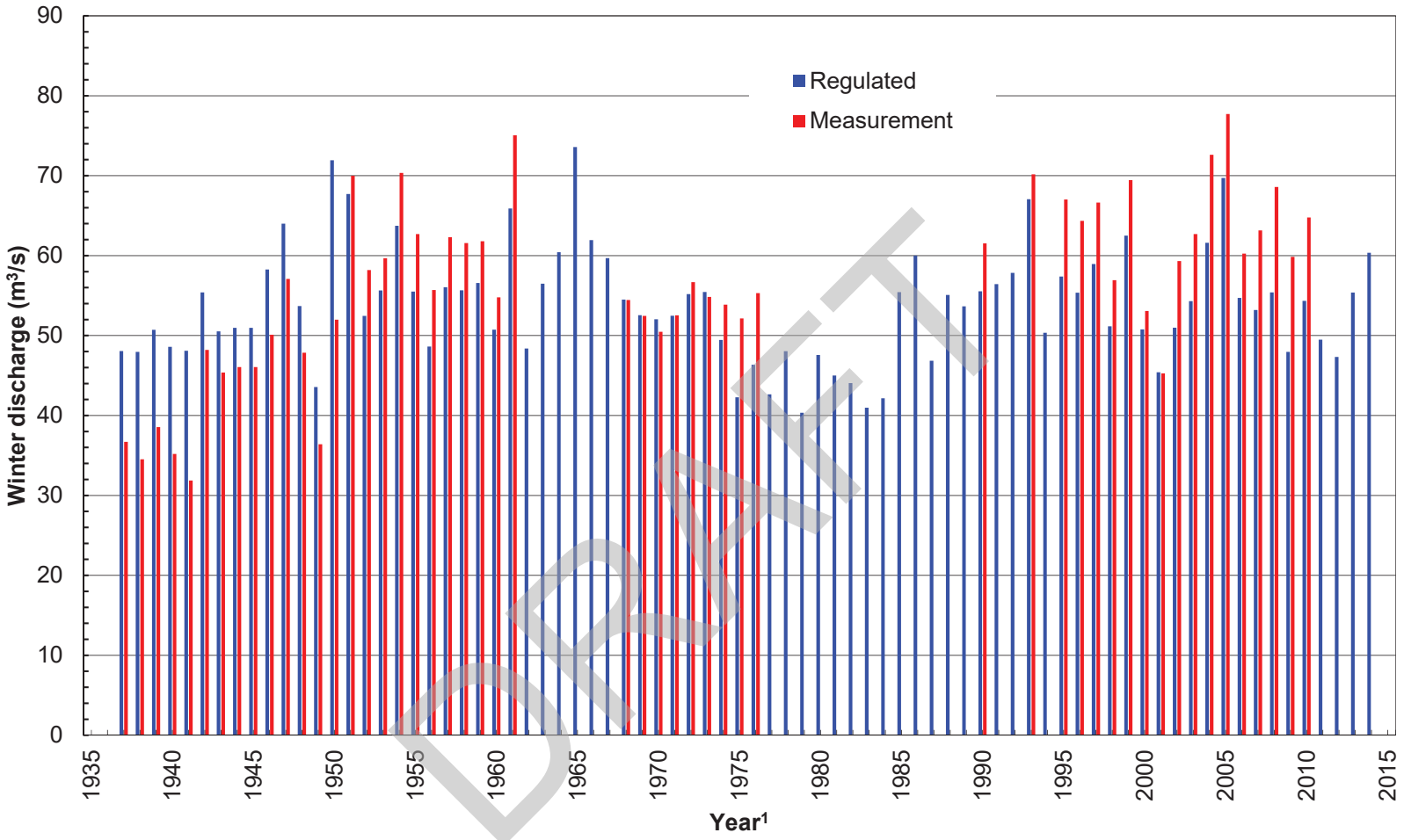

Notes

[1] Year refers the start of the winter year from October to March

[2] Winter discharge measurements are a combination of gauges WSC 05BE006, WSC 05BE999, and WSC 05BH005. Refer to Table 3 for a summary of the WSC gauges.

nhc northwest hydraulic consultants

ALBERTA ENVIRONMENT AND PARKS

UPPER BOW RIVER HAZARD STUDY
ICE JAM MODELLING & FLOOD HAZARD IDENTIFICATION

Comparison of Simulated and Measured Mean Winter Discharge

3001178	07 AUG 2018	**FIGURE 3**

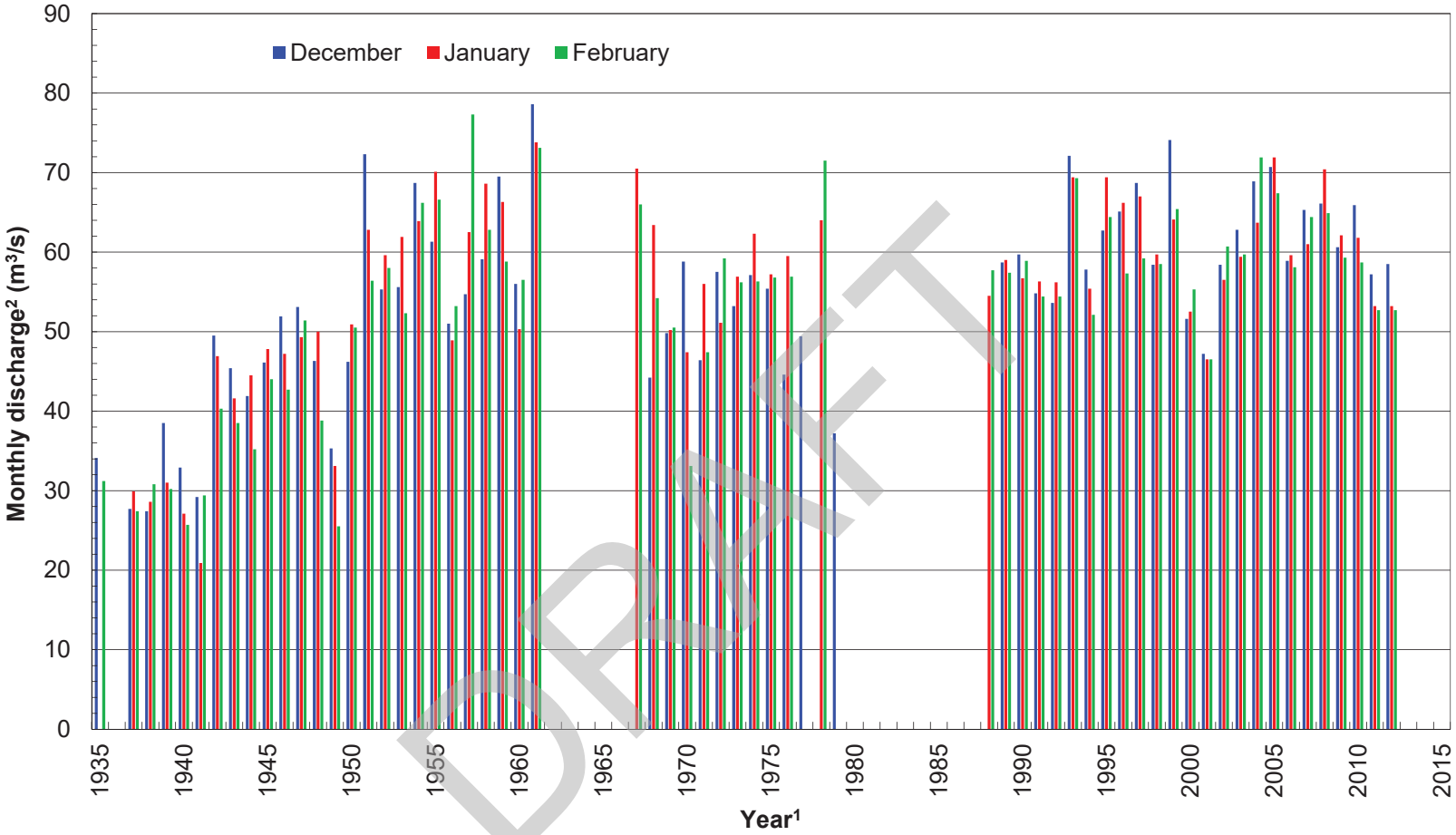

Notes

[1] Year refers the start of the winter year from October to March

[2] Monthly discharges are a combination of gauges WSC 05BE006, WSC 05BE999, and WSC 05BH005. Refer to Table 3 for a summary of the WSC gauges.

nhc northwest hydraulic consultants

ALBERTA ENVIRONMENT AND PARKS

UPPER BOW RIVER HAZARD STUDY
ICE JAM MODELLING & FLOOD HAZARD IDENTIFICATION

Mean Monthly Flows during December, January, and February

3001178	07 AUG 2018	**FIGURE 4**

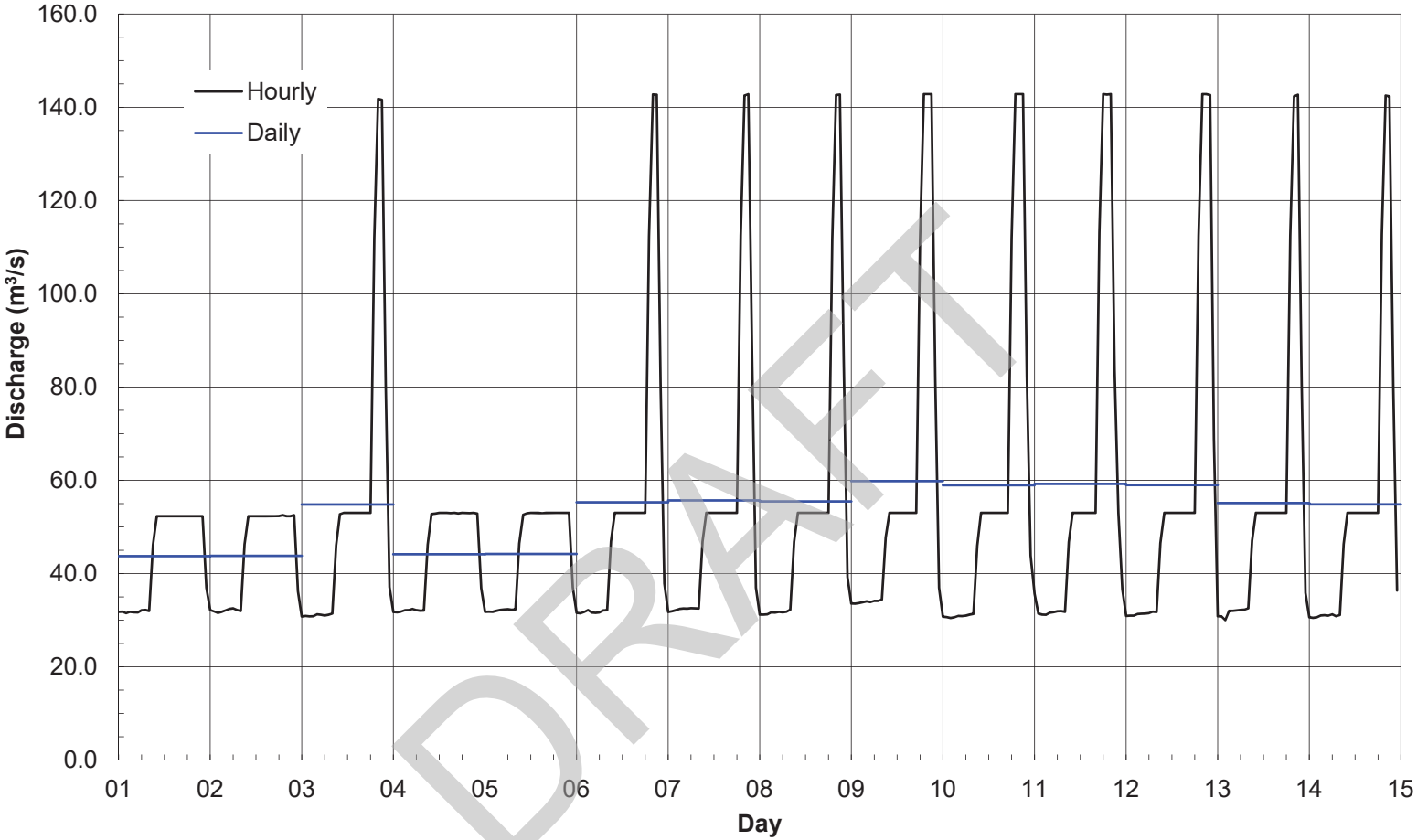

nhc northwest hydraulic consultants

ALBERTA ENVIRONMENT AND PARKS

UPPER BOW RIVER HAZARD STUDY
ICE JAM MODELLING & FLOOD HAZARD IDENTIFICATION

Variation in Hourly Discharge at the Ghost Dam Tailrace - January, 2015

3001178	07 AUG 2018	**FIGURE 5**

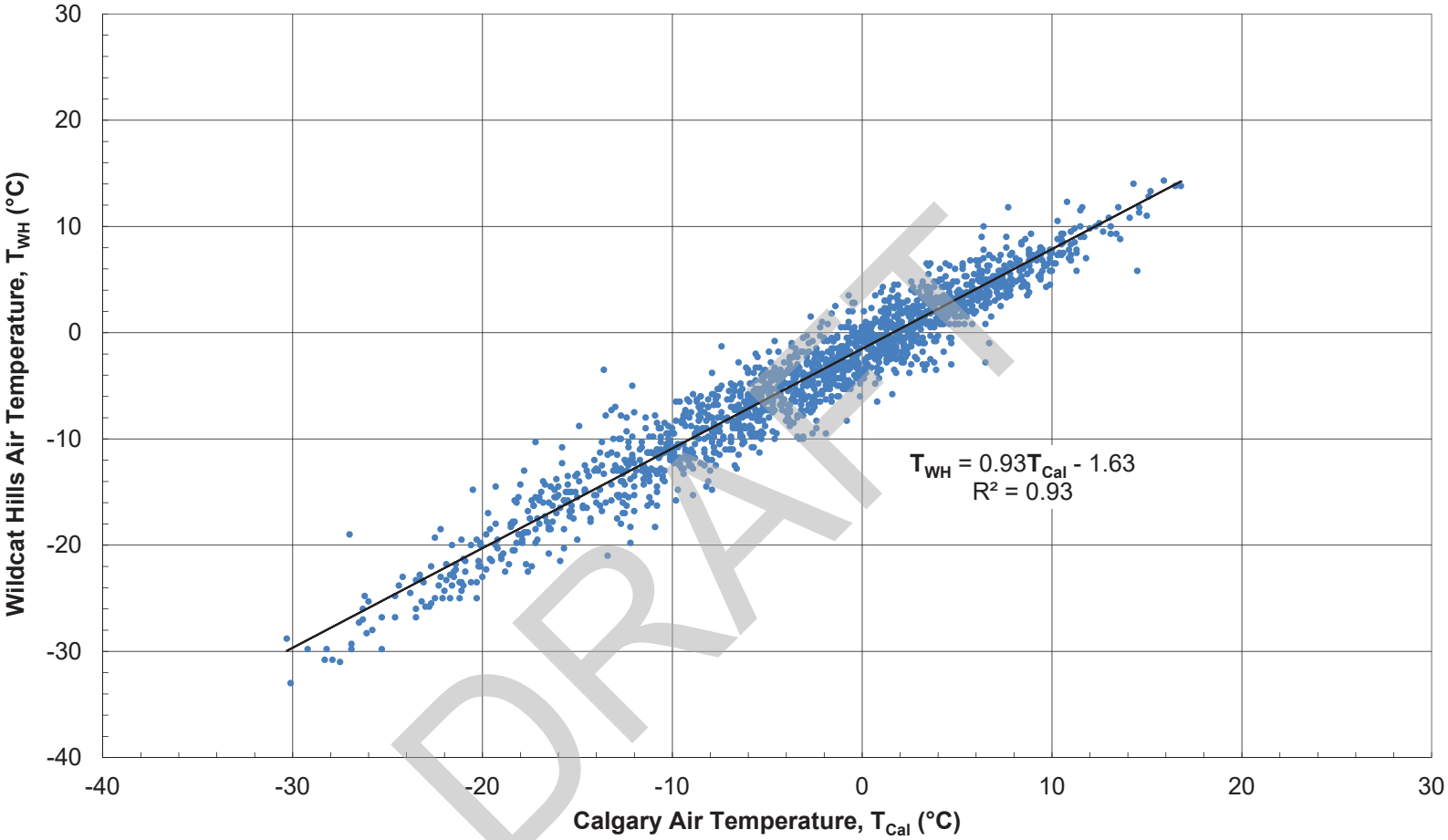

nhc northwest hydraulic consultants

ALBERTA ENVIRONMENT AND PARKS

UPPER BOW RIVER HAZARD STUDY
ICE JAM MODELLING & FLOOD HAZARD IDENTIFICATION

Daily Temperature Correlation from October to March between Calgary International Airport and Wildcat Hills

3001178	07 AUG 2018	**FIGURE 6**

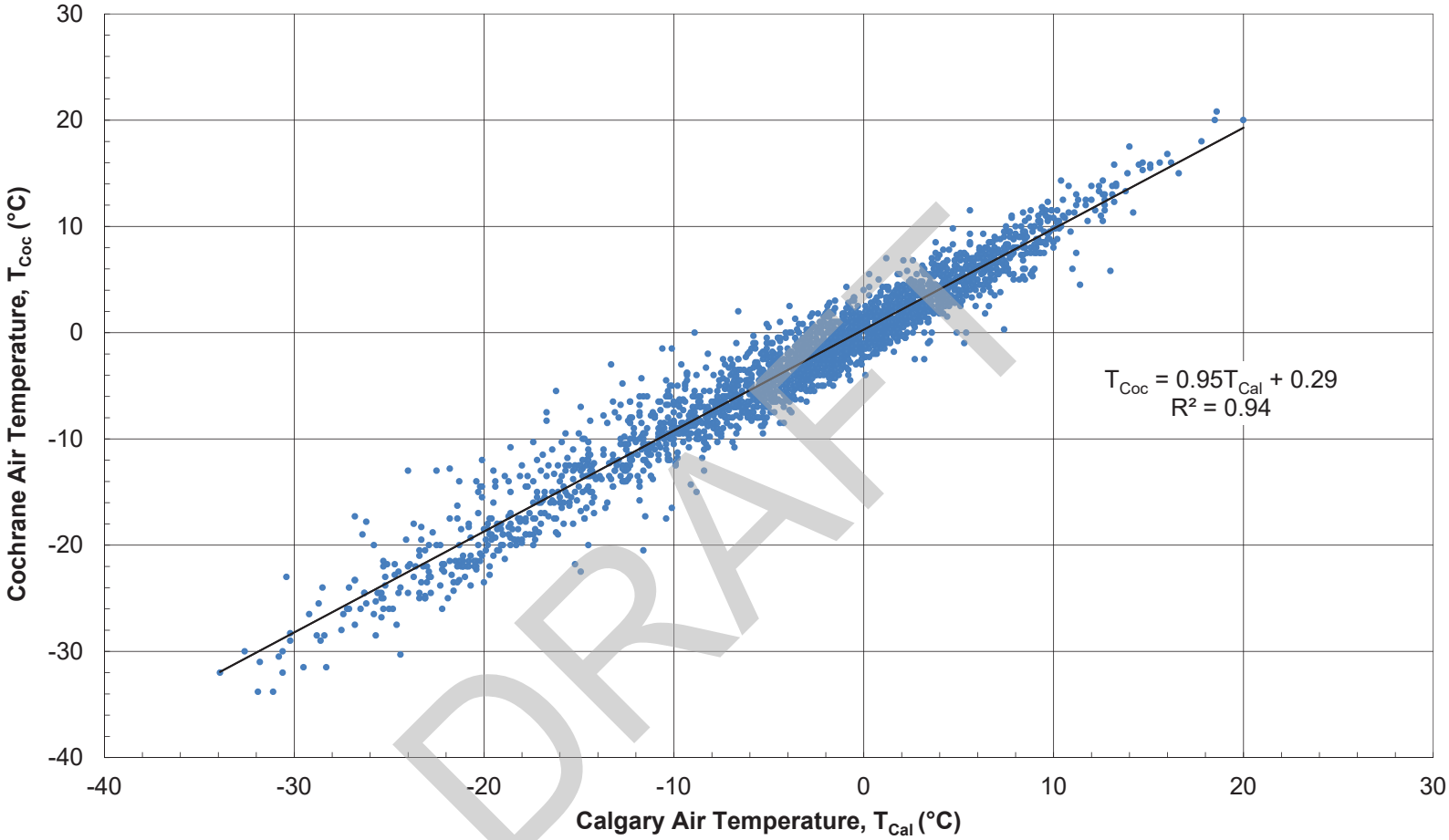

nhc northwest hydraulic consultants

ALBERTA ENVIRONMENT AND PARKS		
UPPER BOW RIVER HAZARD STUDY ICE JAM MODELLING & FLOOD HAZARD IDENTIFICATION **Daily Temperature Correlation from October to March between Calgary International Airport and Cochrane**		
3001178	07 AUG 2018	**FIGURE 7**

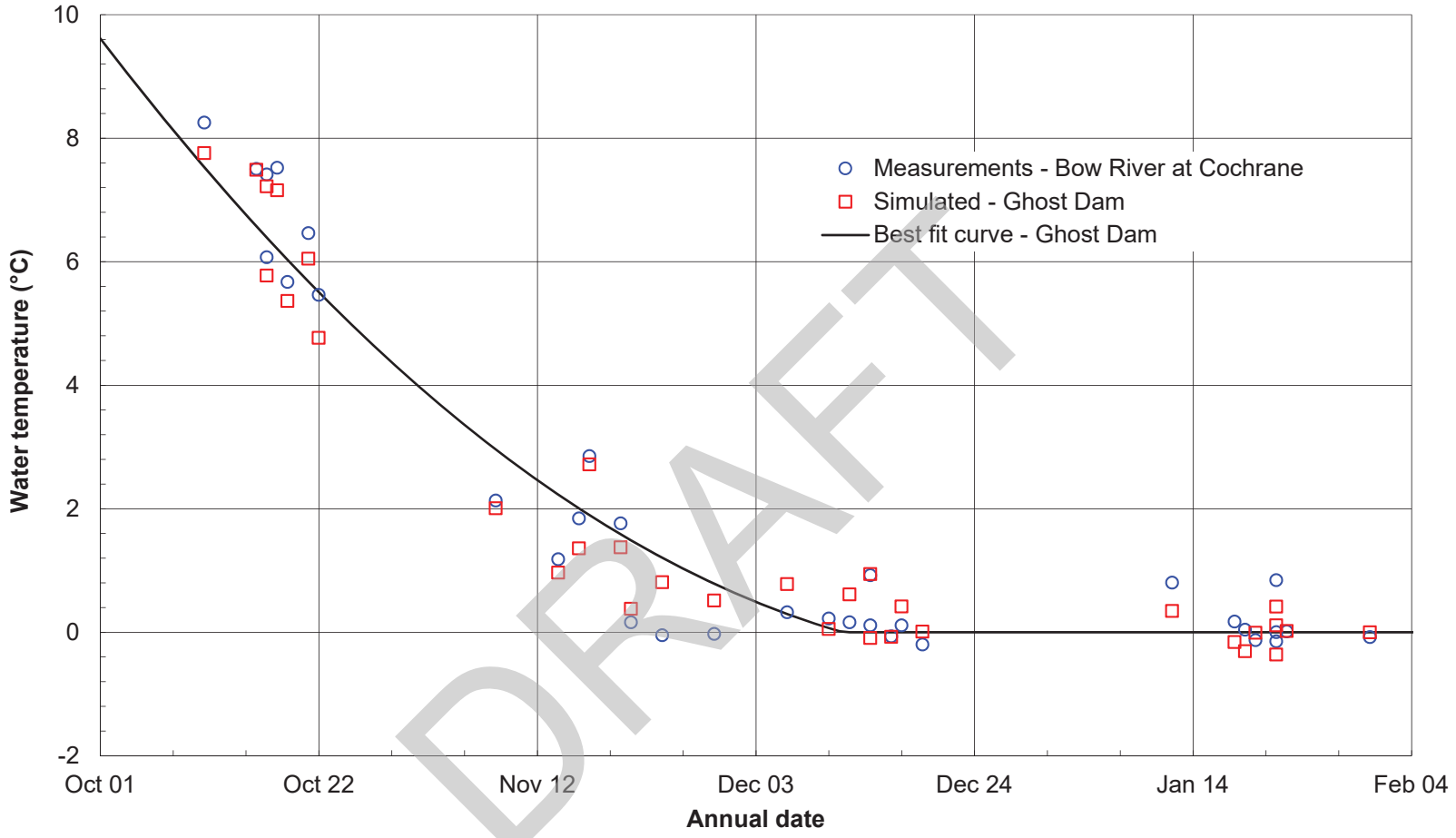

nhc northwest hydraulic consultants

ALBERTA ENVIRONMENT AND PARKS

UPPER BOW RIVER HAZARD STUDY
ICE JAM MODELLING & FLOOD HAZARD IDENTIFICATION

Water Temperature Measurements and Simulation
Bow River between Ghost Dam and Cochrane

3001178	07 AUG 2018	**FIGURE 8**

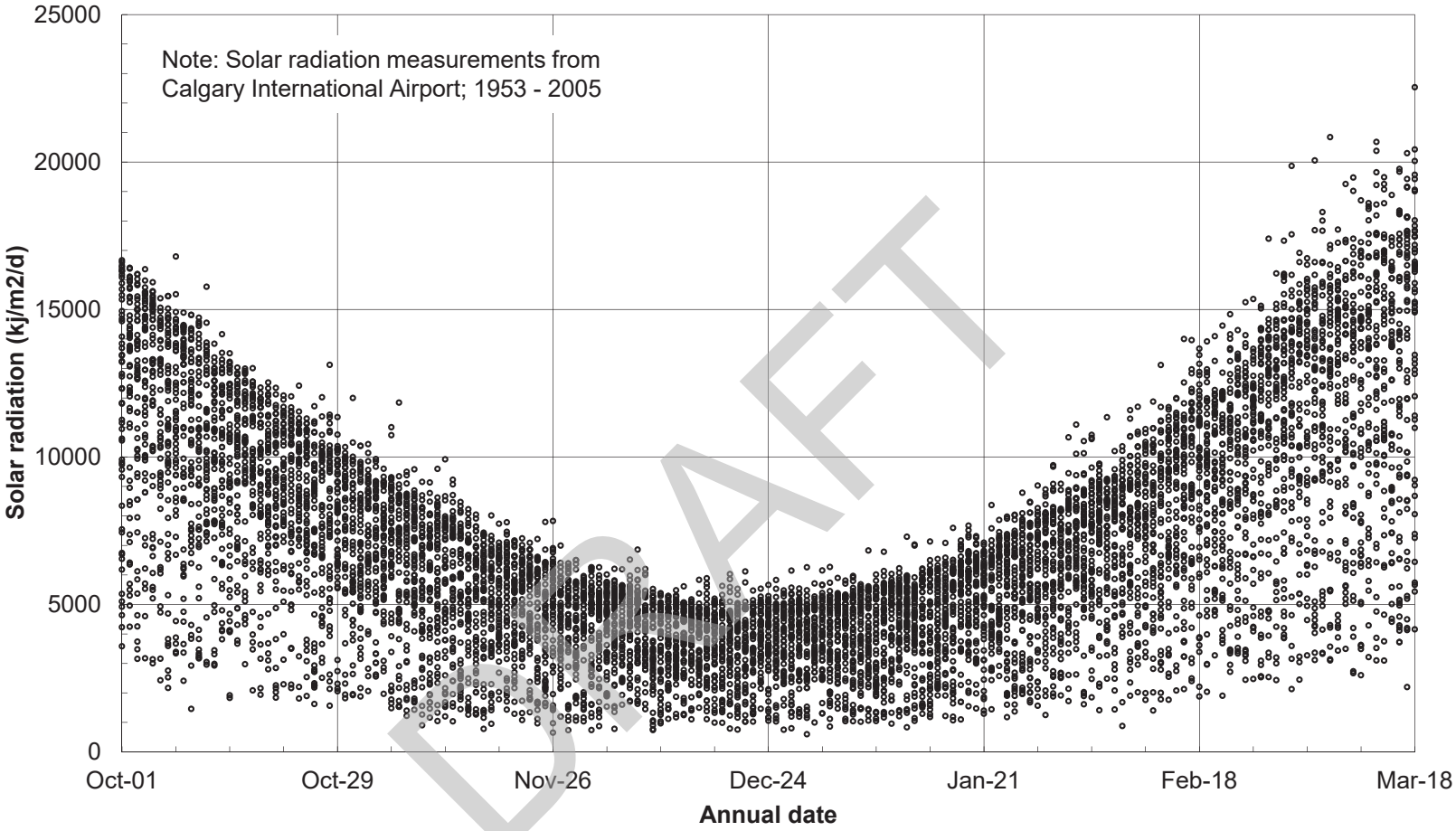

nhc northwest hydraulic consultants

ALBERTA ENVIRONMENT AND PARKS

UPPER BOW RIVER HAZARD STUDY
ICE JAM MODELLING & FLOOD HAZARD IDENTIFICATION

Solar Radiation Variation during Winter Months Calgary International Airport, 1953 - 2005

3001178	07 AUG 2018	**FIGURE 9**

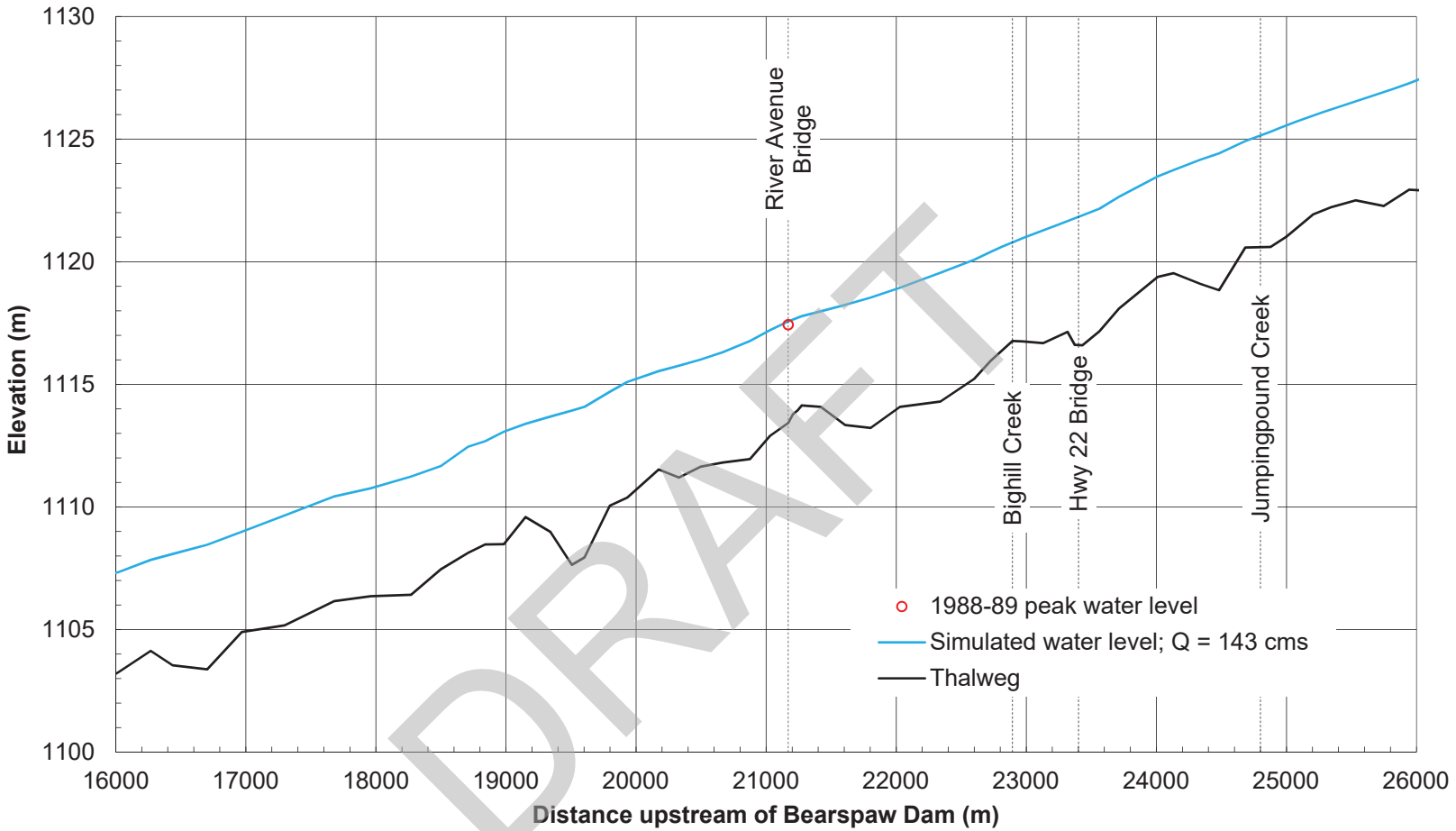

Note
The Manning's Roughness of the bed and the ice were 0.035.

nhc northwest hydraulic consultants

ALBERTA ENVIRONMENT AND PARKS

UPPER BOW RIVER HAZARD STUDY
ICE JAM MODELLING & FLOOD HAZARD IDENTIFICATION

Ice Jam Profile Simulation, 1988-89

3001178	07 AUG 2018	**FIGURE 10**

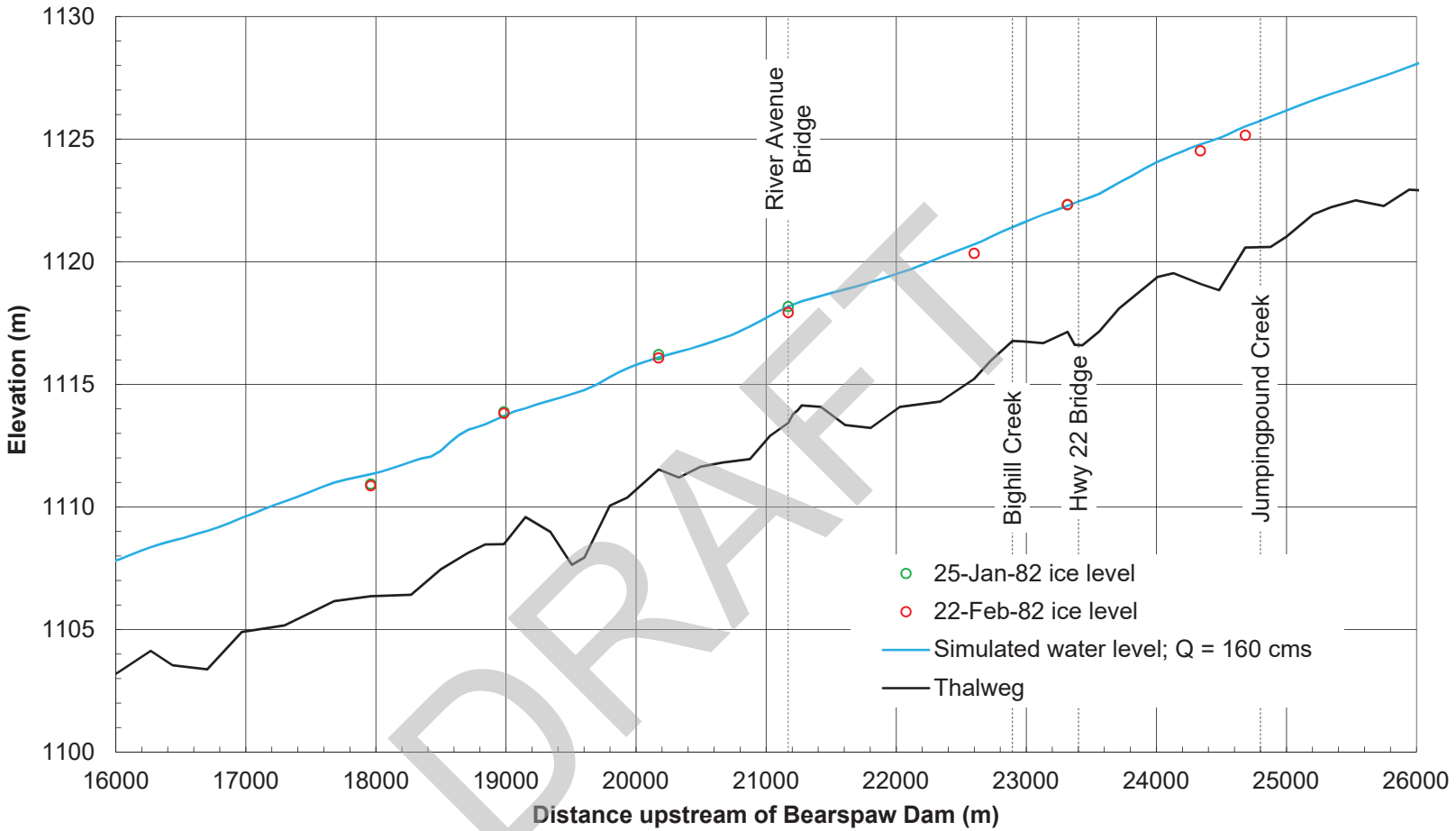

Note
The Manning's Roughness of the bed and the ice were 0.035.

nhc northwest hydraulic consultants

ALBERTA ENVIRONMENT AND PARKS

UPPER BOW RIVER HAZARD STUDY
ICE JAM MODELLING & FLOOD HAZARD IDENTIFICATION

Ice Jam Profile Simulation, 1981-82

3001178	07 AUG 2018	**FIGURE 11**

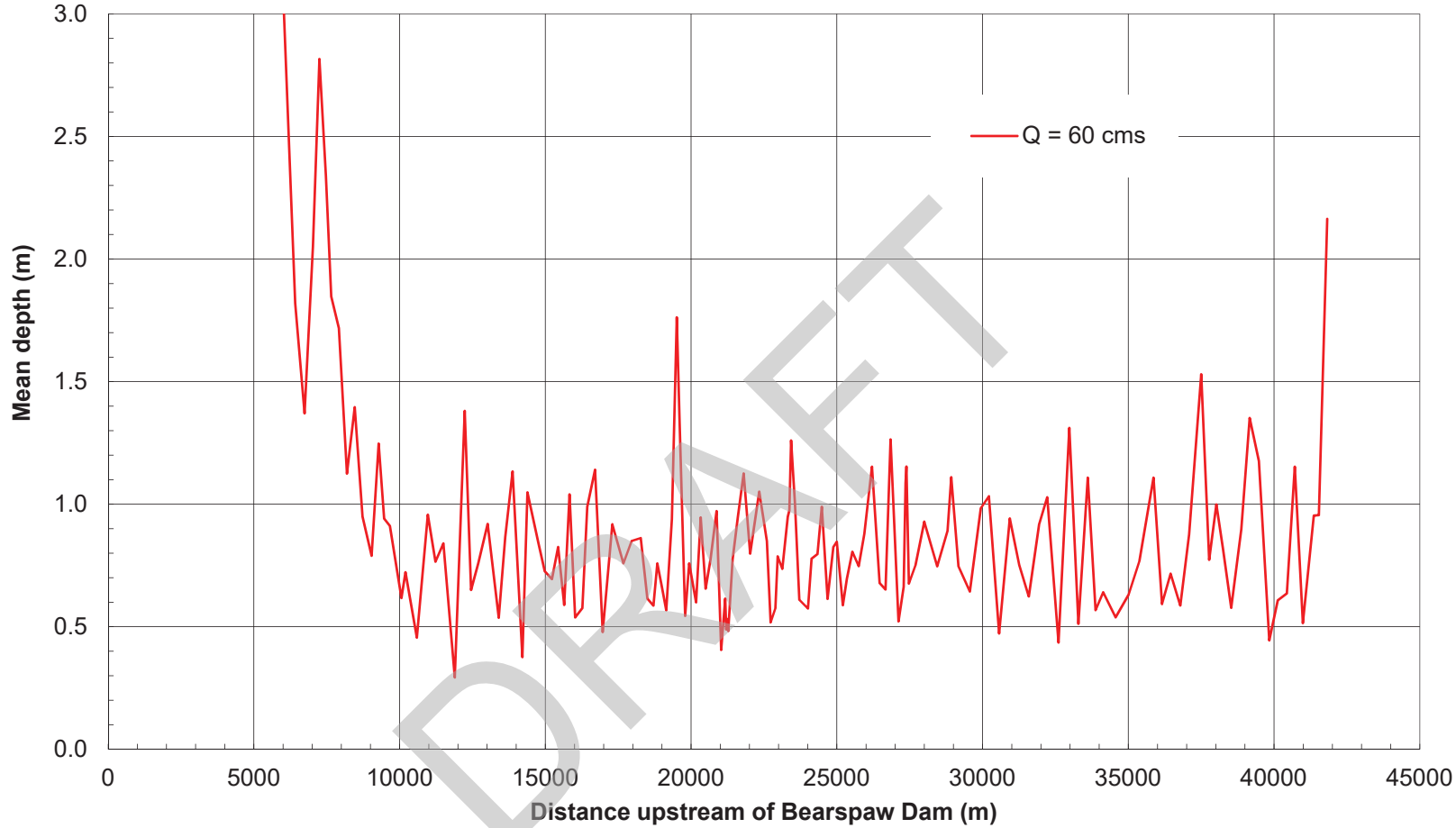

nhc northwest hydraulic consultants

ALBERTA ENVIRONMENT AND PARKS		
UPPER BOW RIVER HAZARD STUDY ICE JAM MODELLING & FLOOD HAZARD IDENTIFICATION **Mean Depth Variation during Typical Winter Discharge**		
3001178	07 AUG 2018	**FIGURE 12**

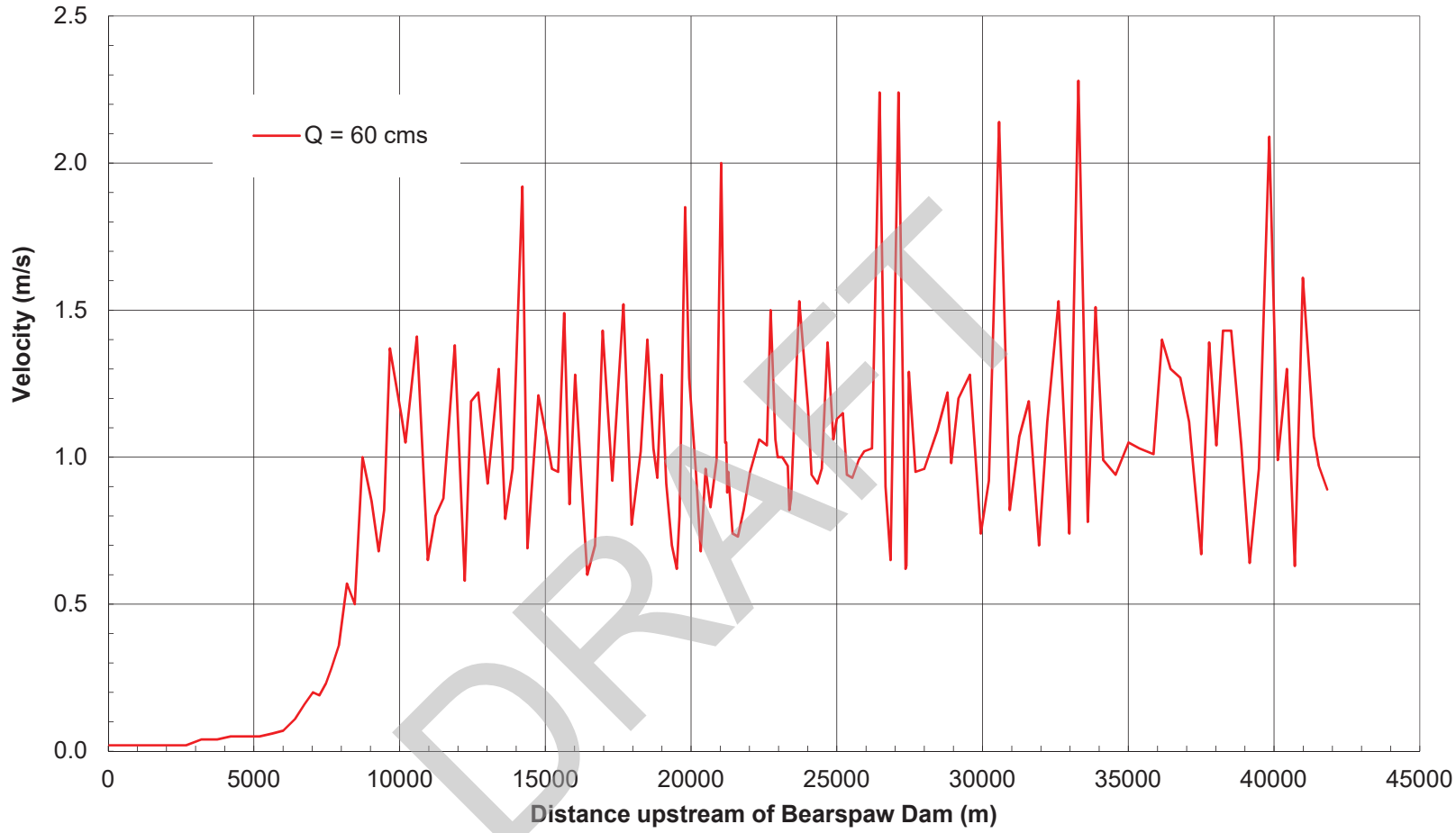

nhc northwest hydraulic consultants

ALBERTA ENVIRONMENT AND PARKS		
UPPER BOW RIVER HAZARD STUDY ICE JAM MODELLING & FLOOD HAZARD IDENTIFICATION **Mean Velocity Variation during Typical Winter Discharge**		
3001178	07 AUG 2018	**FIGURE 13**

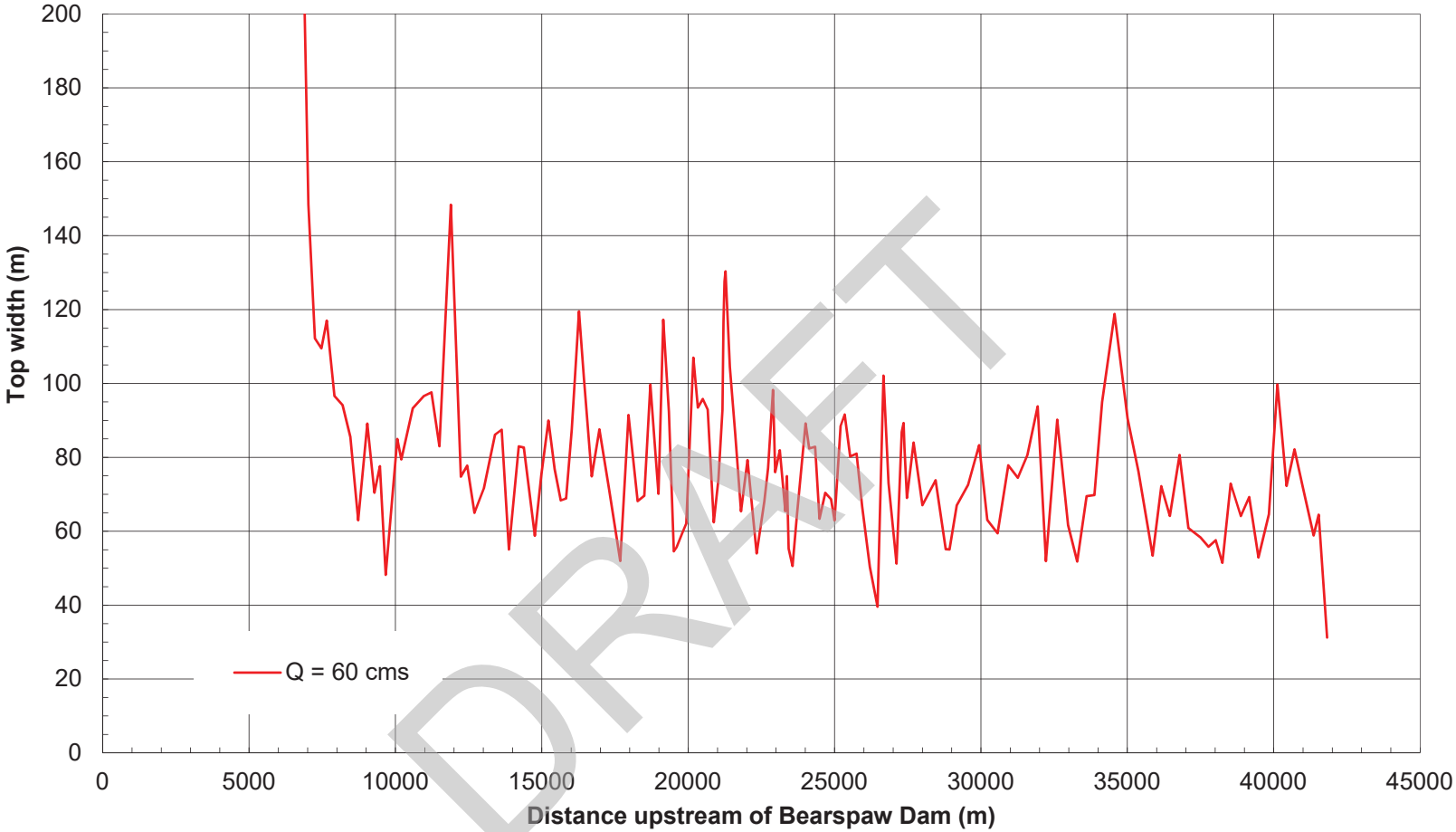

nhc northwest hydraulic consultants

ALBERTA ENVIRONMENT AND PARKS		
UPPER BOW RIVER HAZARD STUDY ICE JAM MODELLING & FLOOD HAZARD IDENTIFICATION **Top Width Variation during Typical Winter Discharge**		
3001178	07 AUG 2018	**FIGURE 14**

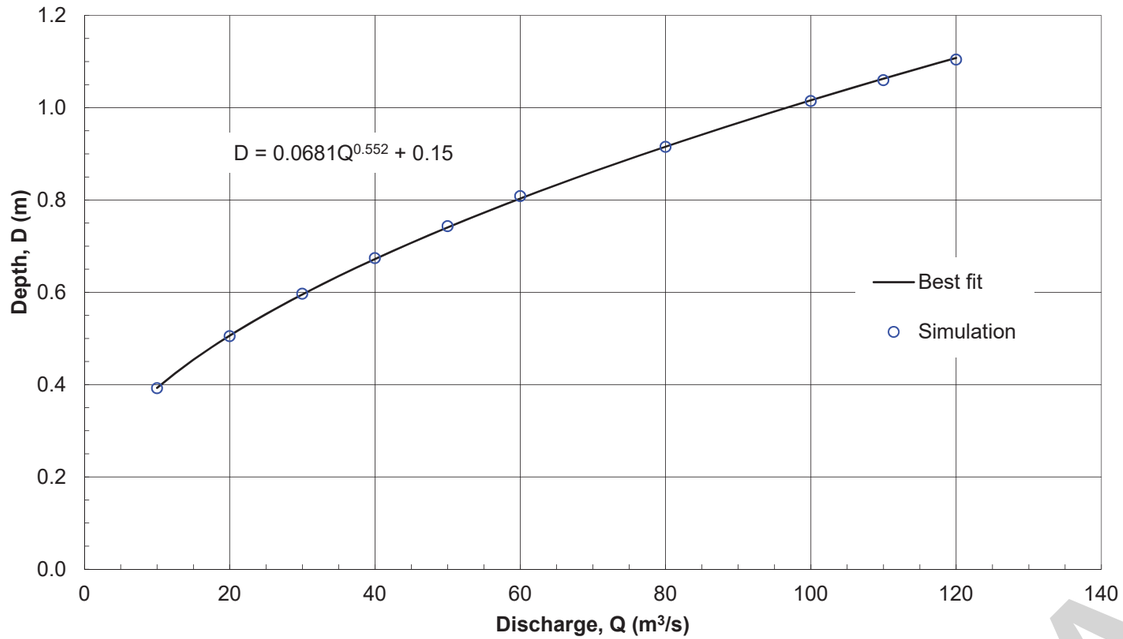

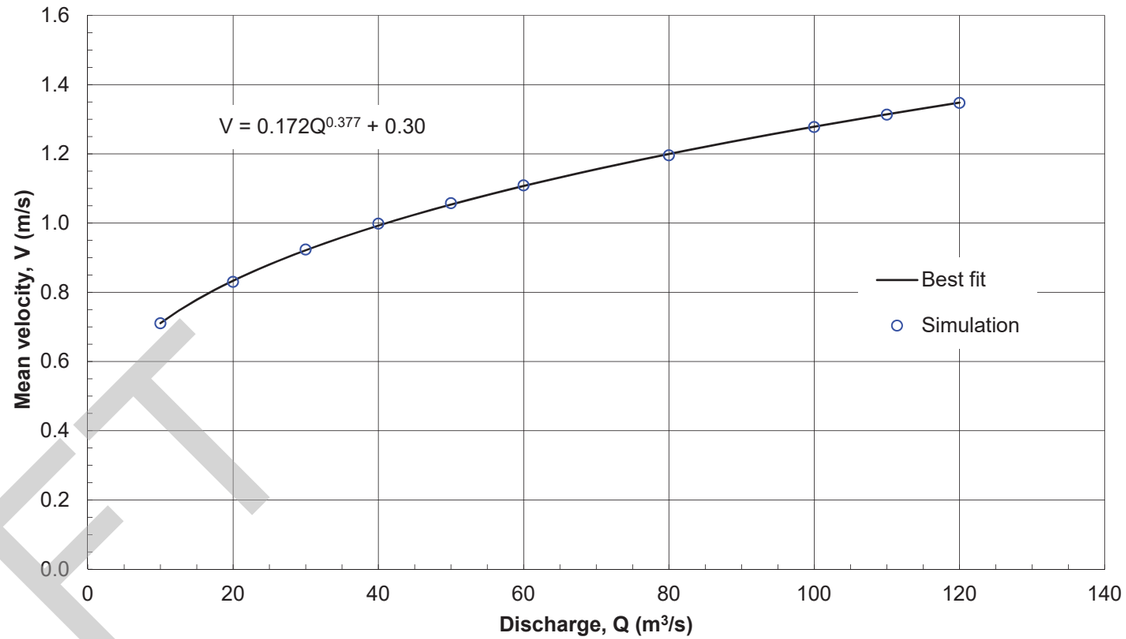

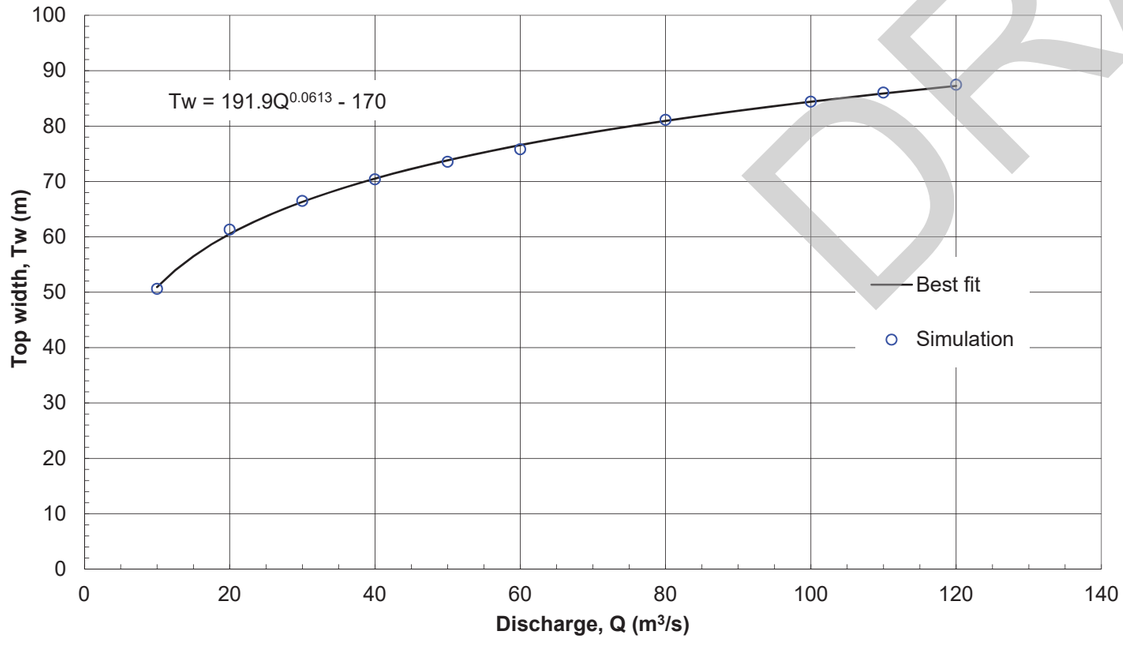

nhc northwest hydraulic consultants

ALBERTA ENVIRONMENT AND PARKS

UPPER BOW RIVER HAZARD STUDY
ICE JAM MODELLING & FLOOD HAZARD IDENTIFICATION

ADOPTED BEST FIT CURVES FOR HYDRAULIC PARAMETERS FOR ICE PRODUCTION SIMULATION

3001178	28 JULY 2017	**FIGURE 15**

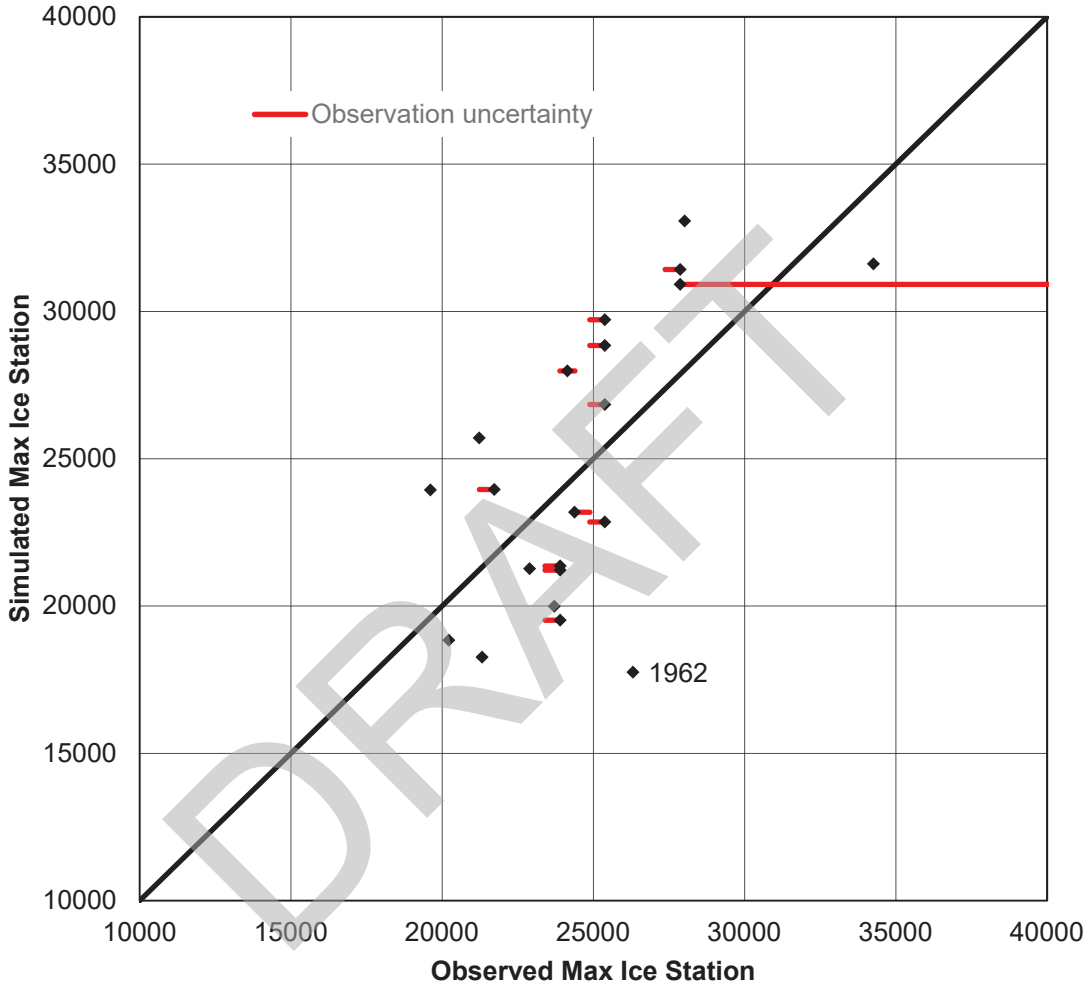

Note
Listed years are the start of each ice year (October to March).

nhc northwest hydraulic consultants

ALBERTA ENVIRONMENT AND PARKS		
UPPER BOW RIVER HAZARD STUDY ICE JAM MODELLING & FLOOD HAZARD IDENTIFICATION **Comparison of Observed and Simulated Maximum Annual Ice Station**		
3001178	07 AUG 2018	**FIGURE 16**

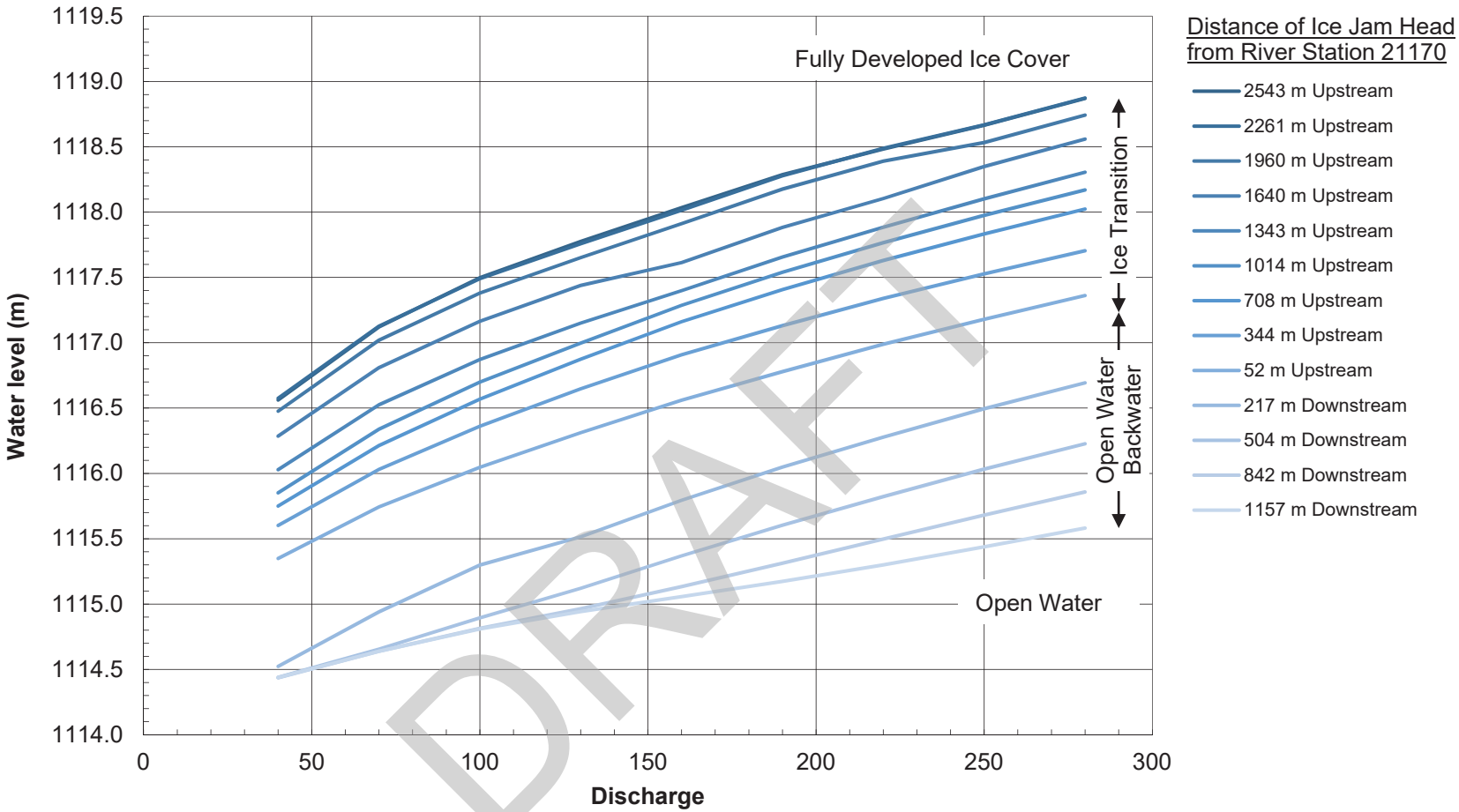

nhc northwest hydraulic consultants

ALBERTA ENVIRONMENT AND PARKS

UPPER BOW RIVER HAZARD STUDY
ICE JAM MODELLING & FLOOD HAZARD IDENTIFICATION

Simulated Rating Curve Variation at WSC Gauge Site River Avenue Bridge - River Station 21170

3001178	07 AUG 2018	**FIGURE 17**

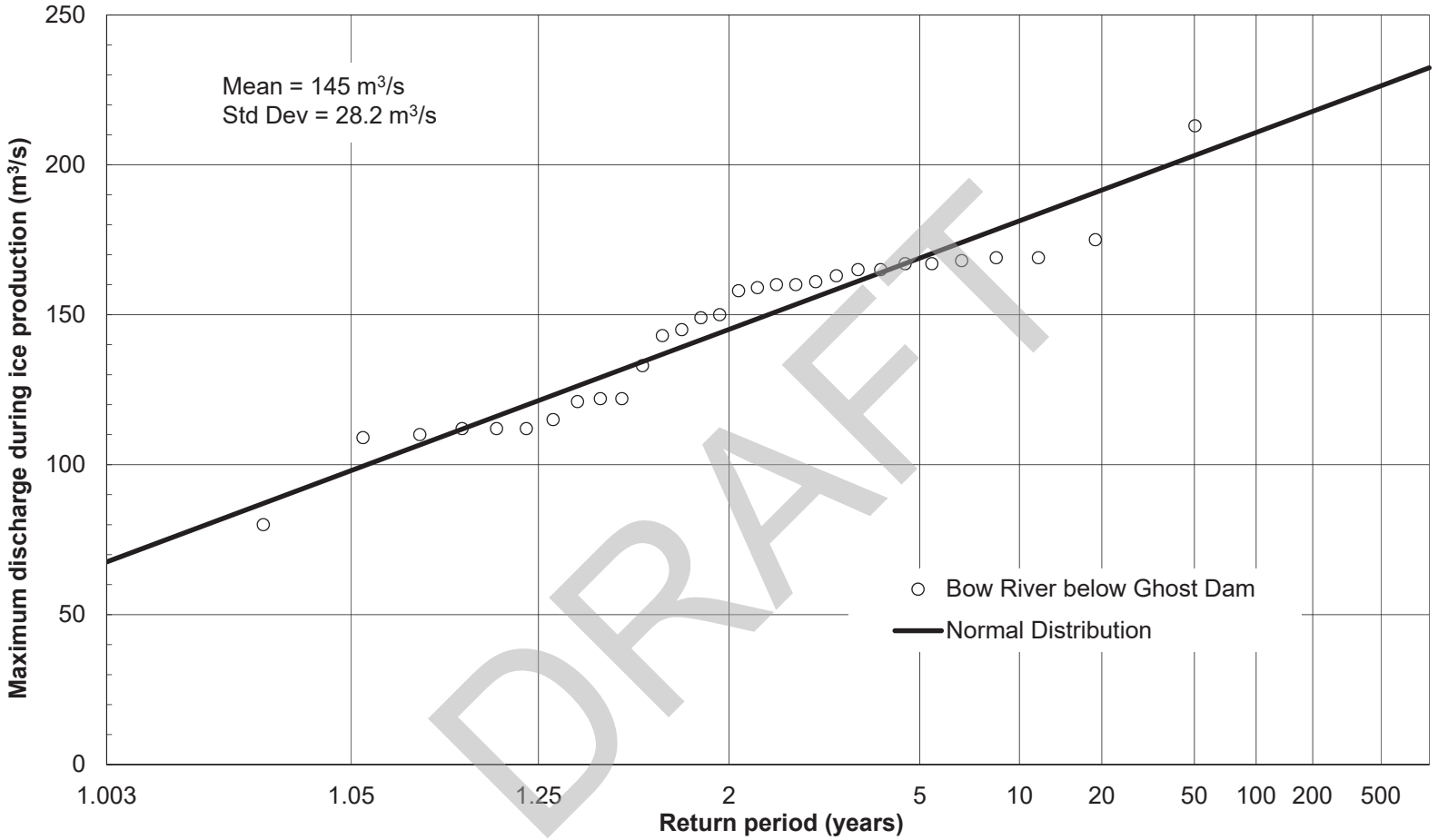

nhc northwest hydraulic consultants

ALBERTA ENVIRONMENT AND PARKS

UPPER BOW RIVER HAZARD STUDY
ICE JAM MODELLING & FLOOD HAZARD IDENTIFICATION

Maximum Discharge during Ice Production Frequency Distribution Bow River below Ghost Reservoir

3001178	07 AUG 2018	**FIGURE 18**

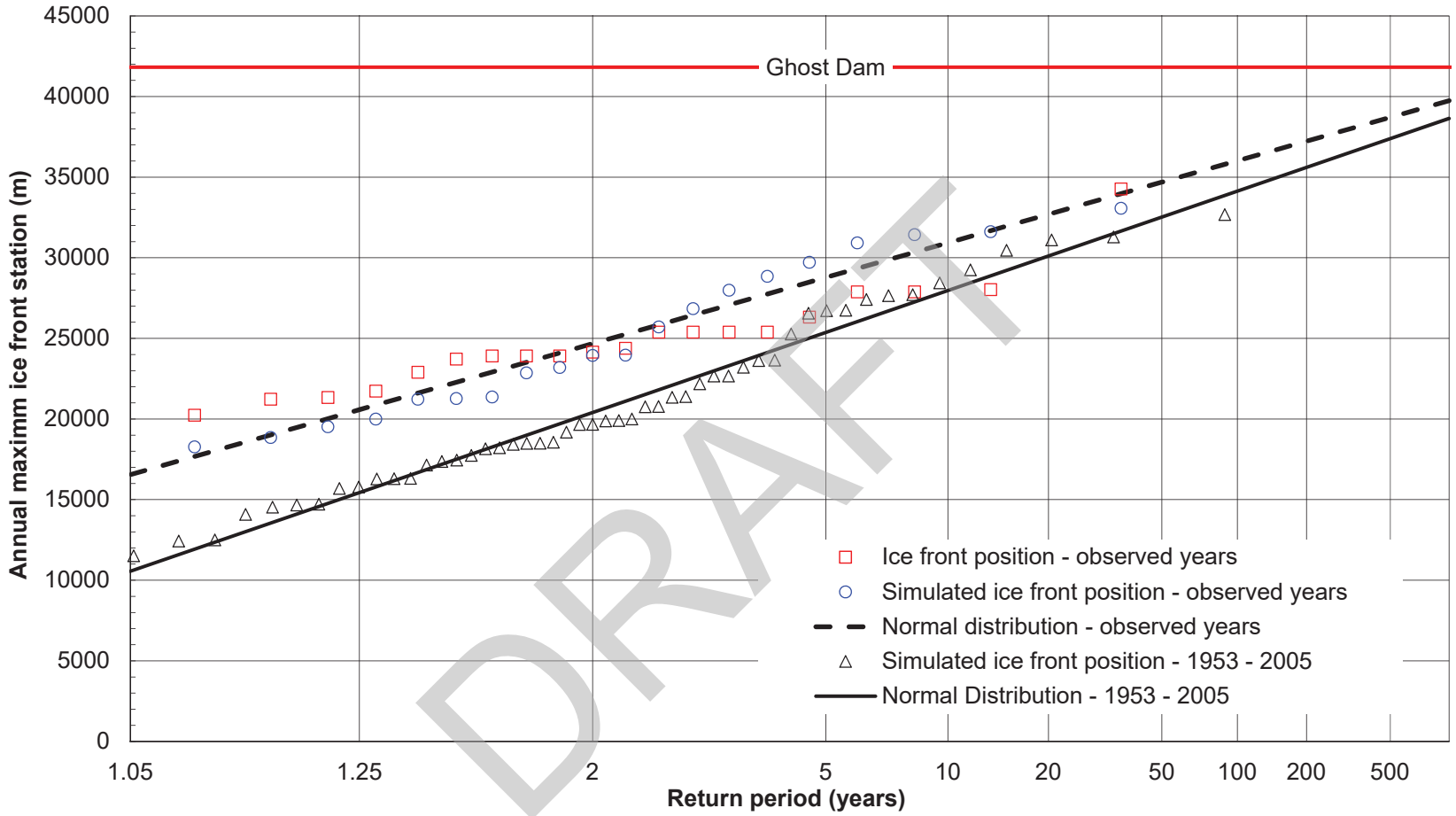

Note
Observed years refers to years during which the description of the annual maximum ice front location (Table 1) were useful for the calibration of the ice production model. The years were 1953 – 56, 58, 62, 64, 66, 68 – 75, 77 – 78, 81, 84, and 88.

nhc northwest hydraulic consultants

ALBERTA ENVIRONMENT AND PARKS		
UPPER BOW RIVER HAZARD STUDY ICE JAM MODELLING & FLOOD HAZARD IDENTIFICATION **Annual Maximum Ice Front Station Frequency Distribution Observed and Simulated Record**		
3001178	07 AUG 2018	**FIGURE 19**

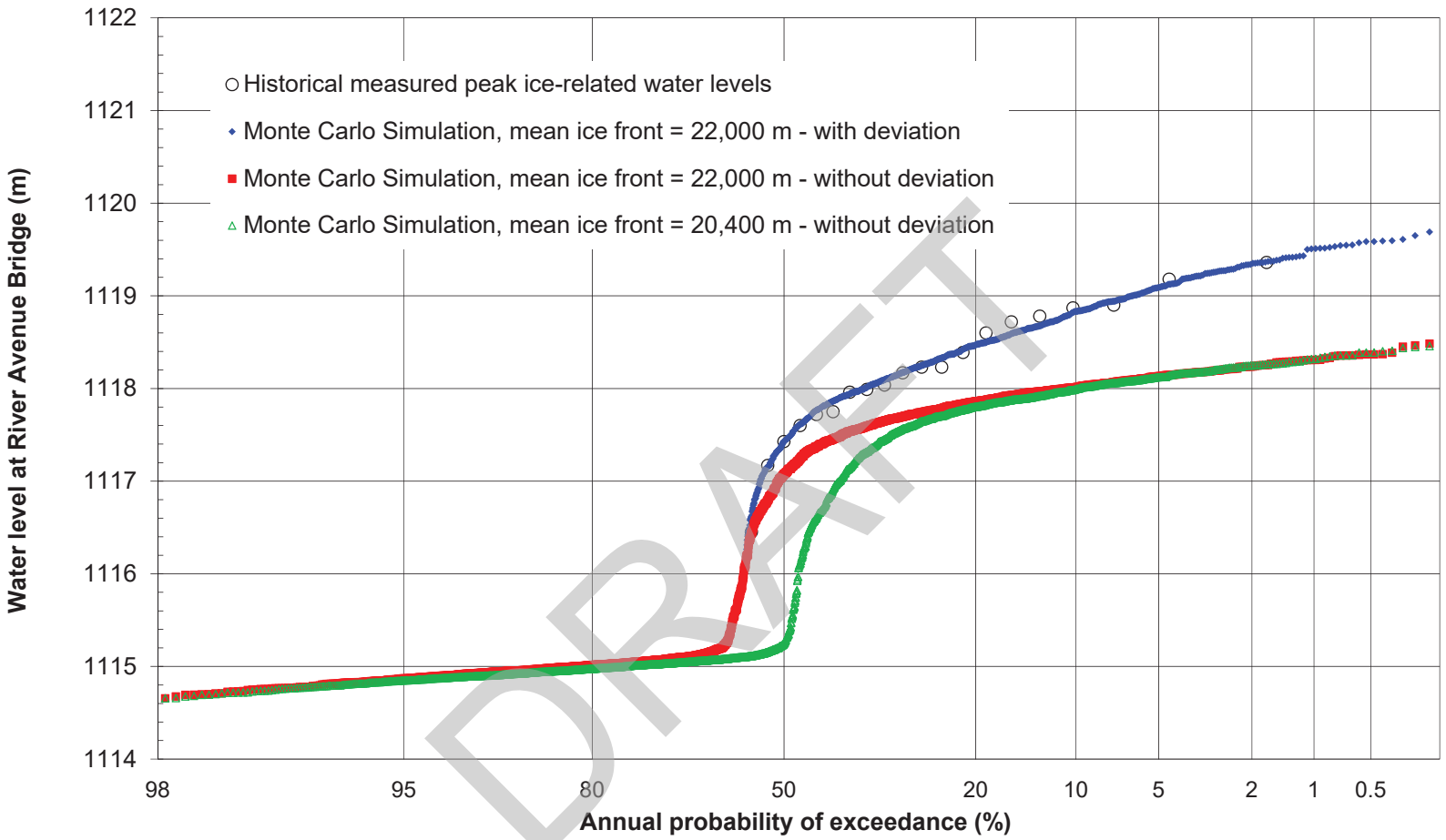

nhc northwest hydraulic consultants

ALBERTA ENVIRONMENT AND PARKS

UPPER BOW RIVER HAZARD STUDY
ICE JAM MODELLING & FLOOD HAZARD IDENTIFICATION

Monte Carlo Simulation Results at River Avenue Bridge River Station 21170

3001178	07 AUG 2018	**FIGURE 20**

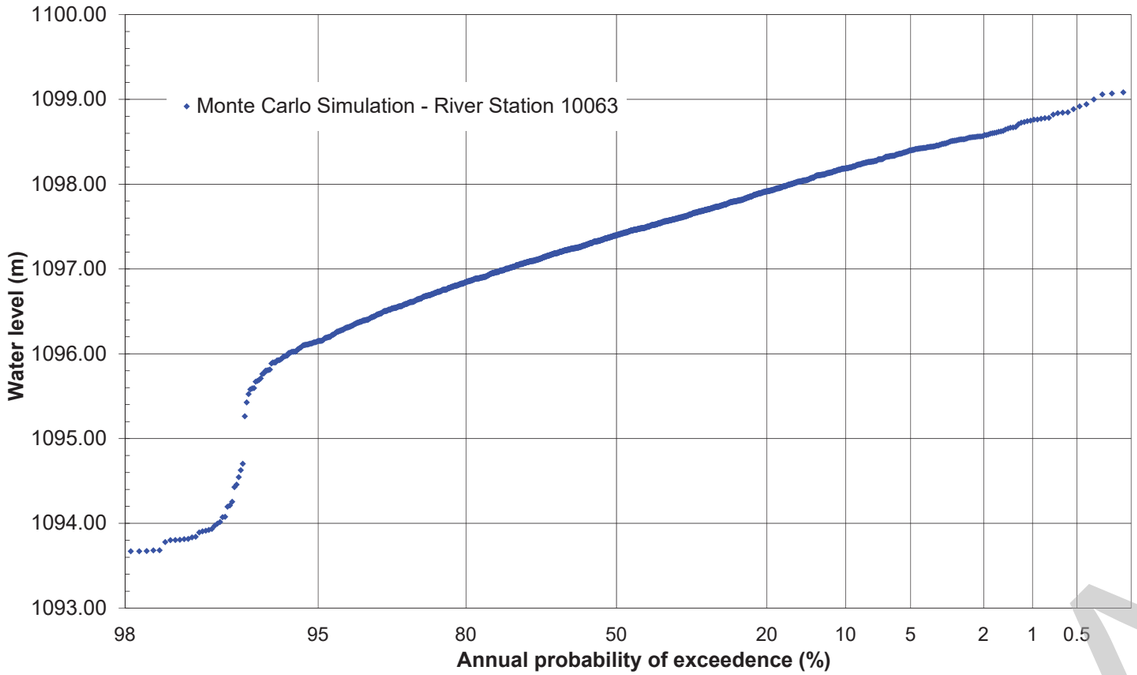

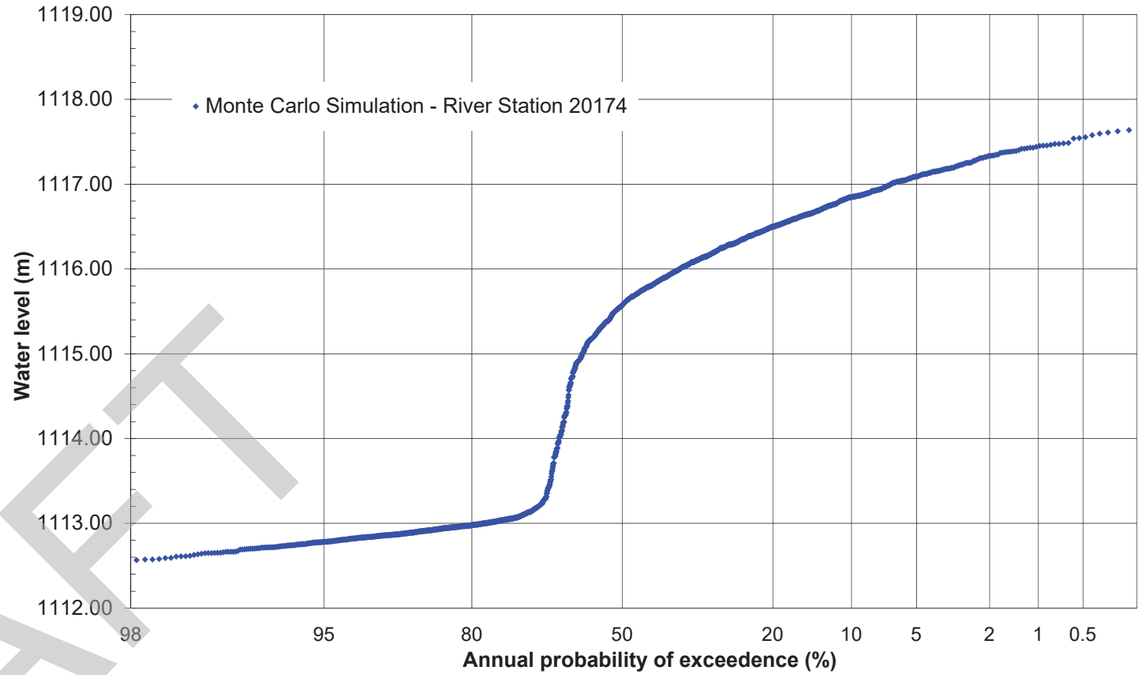

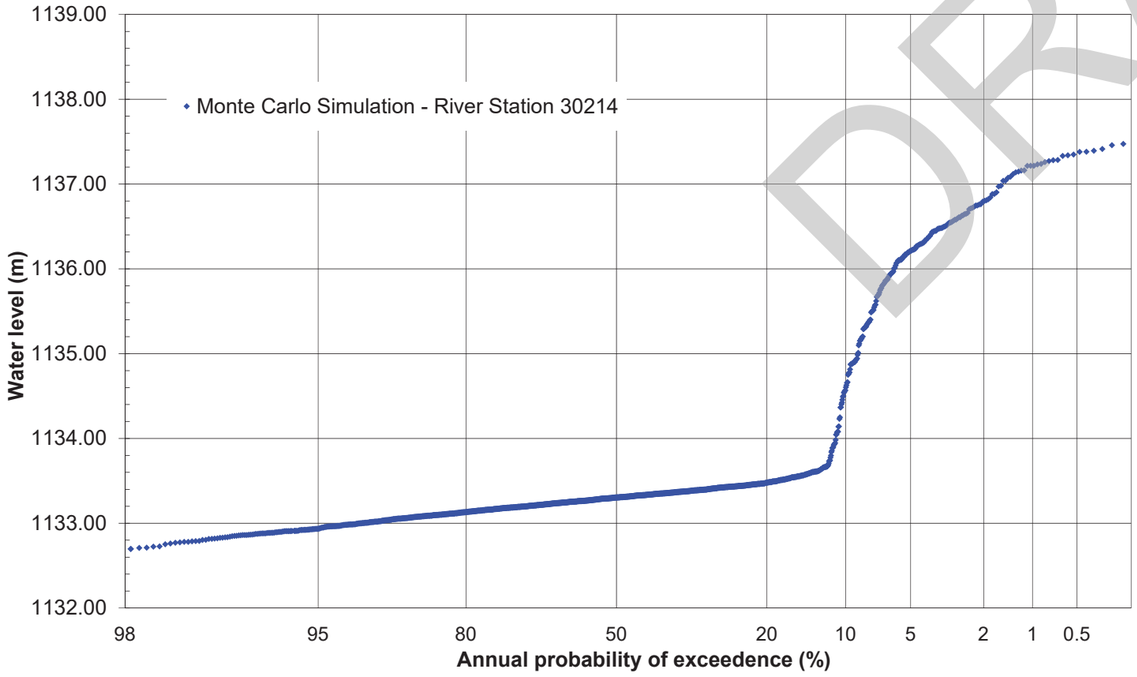

nhc northwest hydraulic consultants

ALBERTA ENVIRONMENT AND PARKS

UPPER BOW RIVER HAZARD STUDY
ICE JAM MODELLING & FLOOD HAZARD IDENTIFICATION

WATER LEVEL FREQUENCY CURVE VARIATION AT SELECTED RIVER STATIONS

3001178	28 JULY 2017	**FIGURE 21**

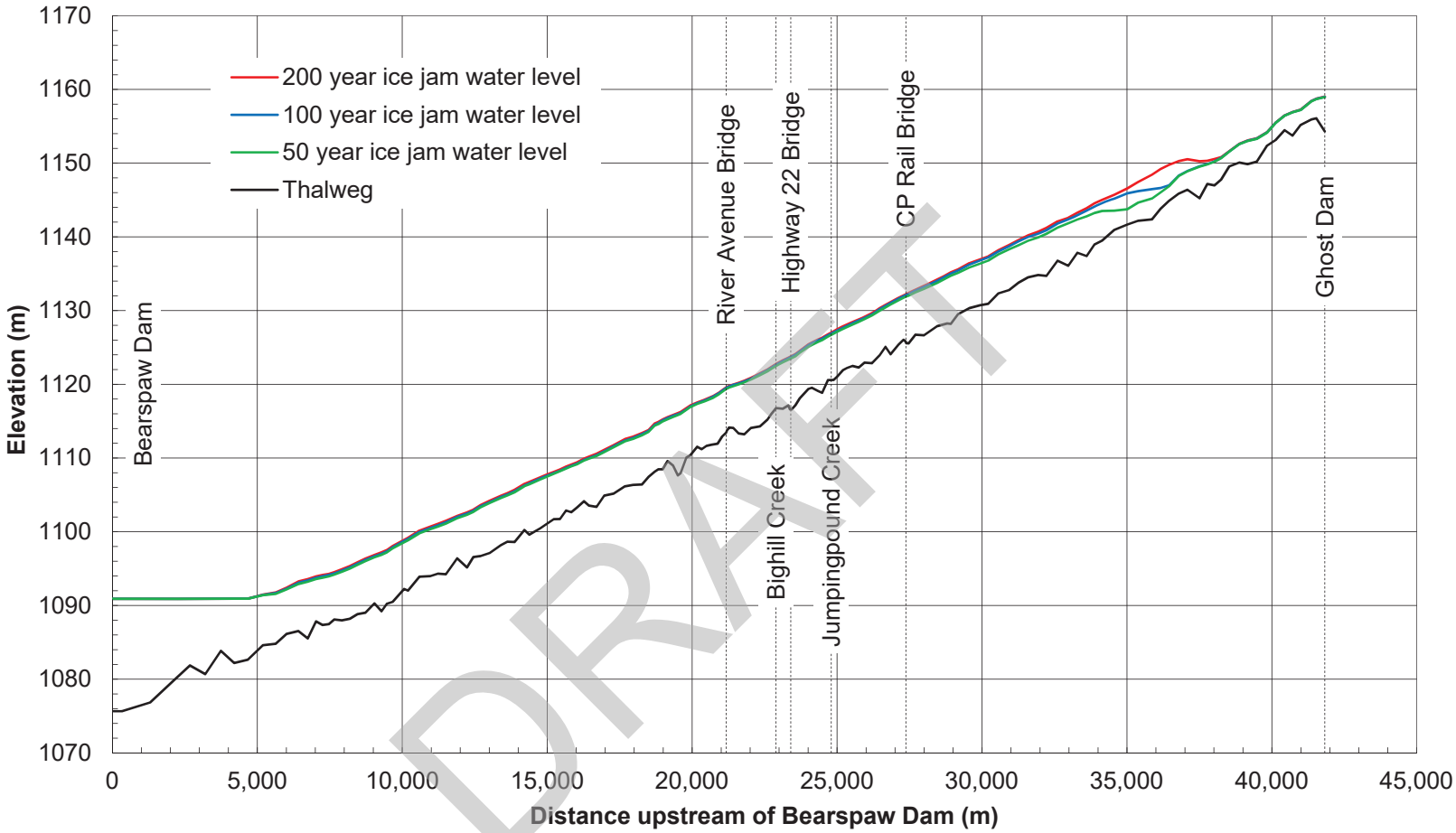

nhc northwest hydraulic consultants

ALBERTA ENVIRONMENT AND PARKS

UPPER BOW RIVER HAZARD STUDY
ICE JAM MODELLING & FLOOD HAZARD IDENTIFICATION

Ice Jam Flood Frequency Profiles

3001178	07 AUG 2018	**FIGURE 22**

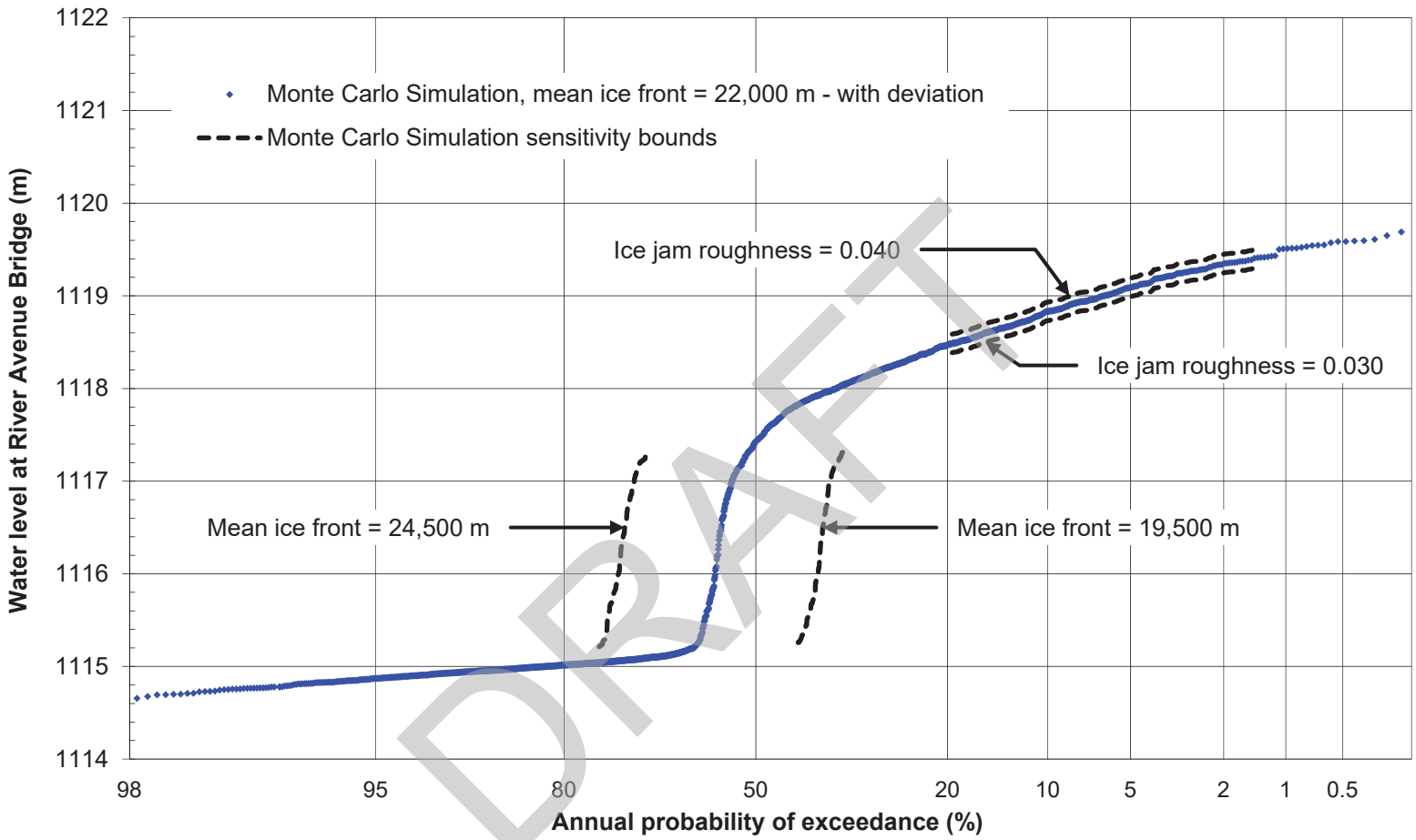

nhc northwest hydraulic consultants

ALBERTA ENVIRONMENT AND PARKS

UPPER BOW RIVER HAZARD STUDY
ICE JAM MODELLING & FLOOD HAZARD IDENTIFICATION

Sensitivity Analysis of Monte Carlo Simulation Results at River Avenue Bridge - River Station 21,170

3001178	07 AUG 2018	**FIGURE 23**

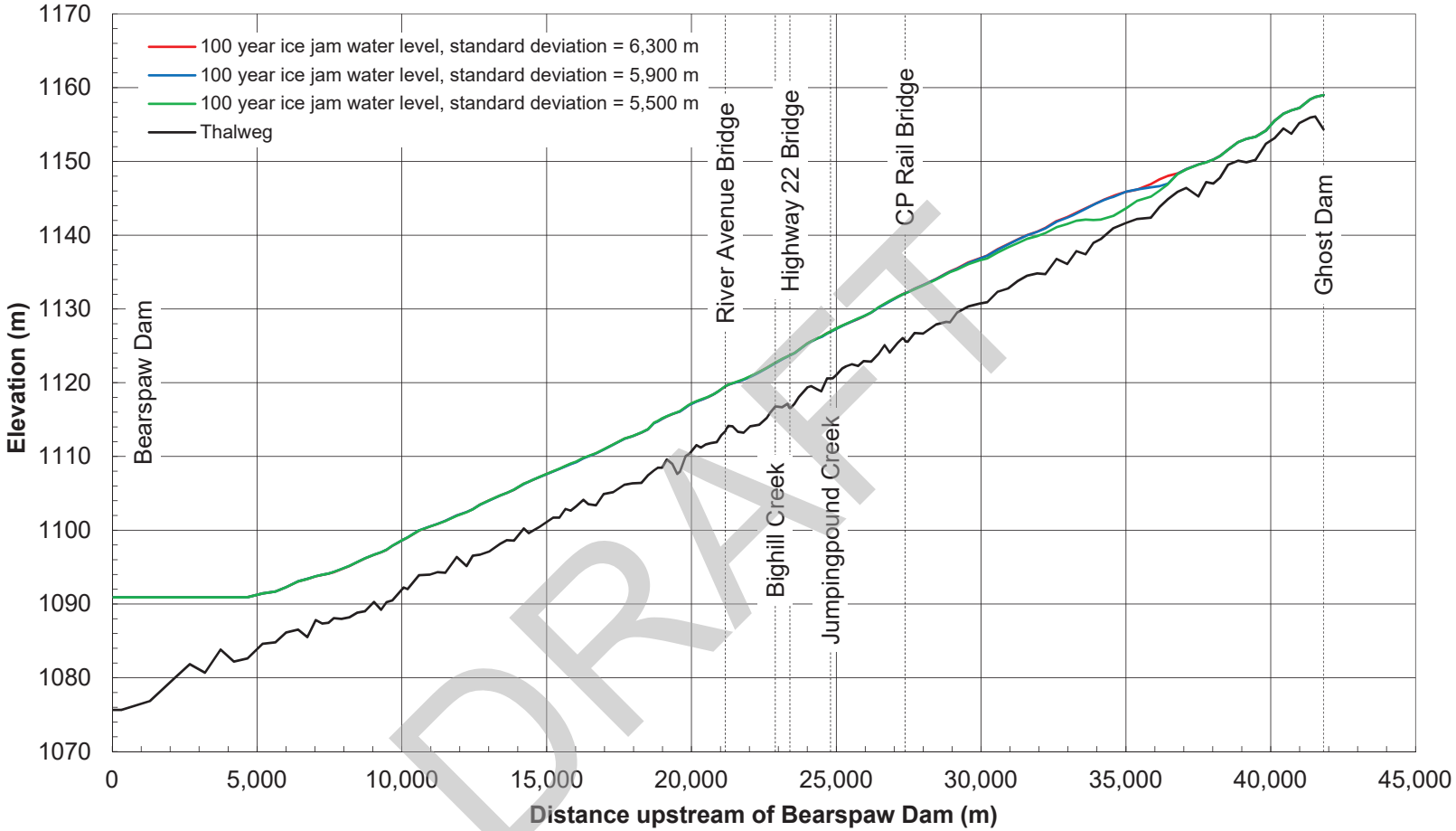

nhc northwest hydraulic consultants

ALBERTA ENVIRONMENT AND PARKS

UPPER BOW RIVER HAZARD STUDY
ICE JAM MODELLING & FLOOD HAZARD IDENTIFICATION

Sensitivity Analysis to Annual Maximum Ice Front Station Standard Deviation

3001178	07 AUG 2018	**FIGURE 24**

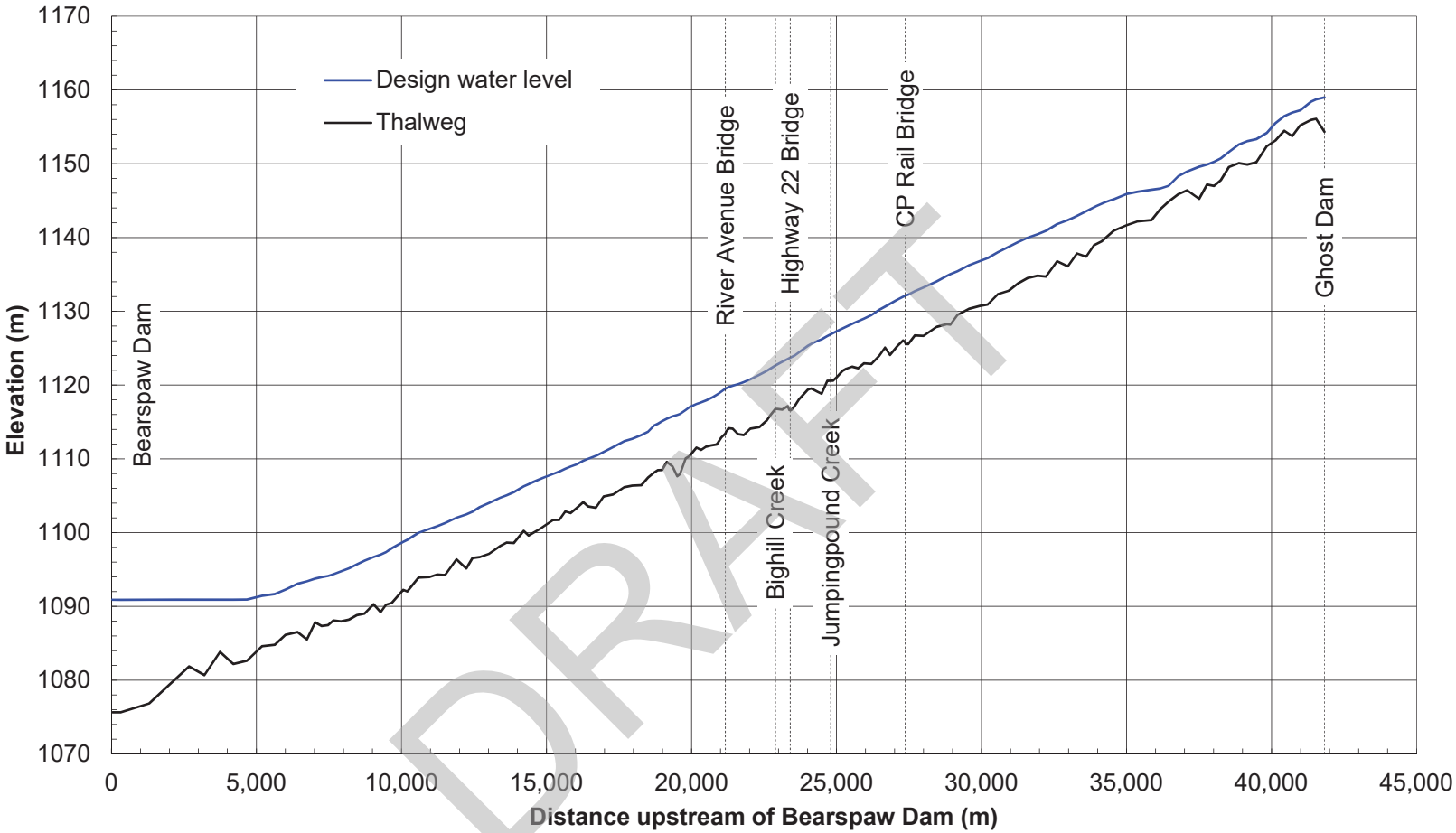

nhc northwest hydraulic consultants

ALBERTA ENVIRONMENT AND PARKS

UPPER BOW RIVER HAZARD STUDY
ICE JAM MODELLING & FLOOD HAZARD IDENTIFICATION

Ice Jam Design Flood Profile

3001178	20 MAR 2019	**FIGURE 25**

MAPS

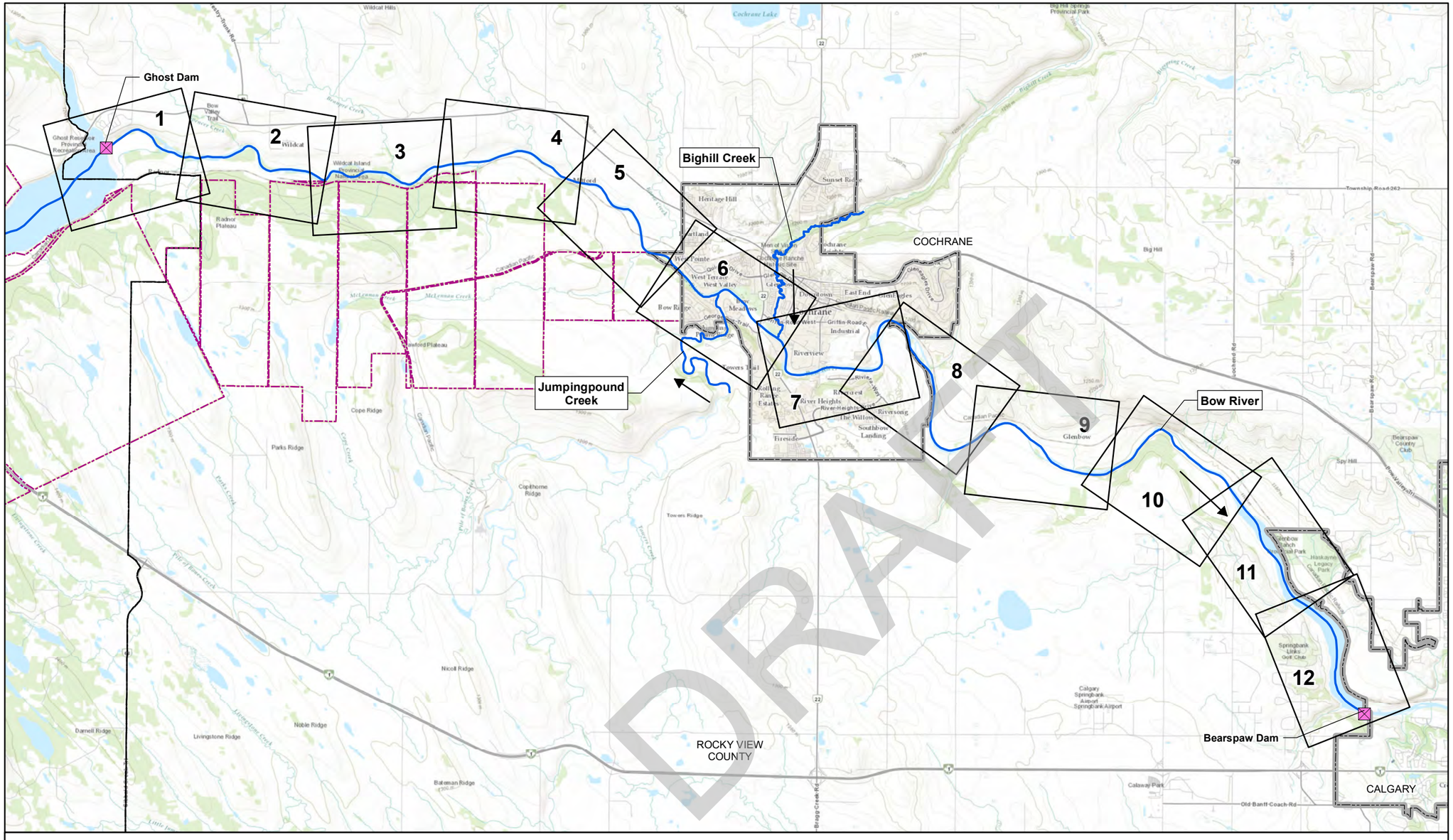

- Dam
- Summer Village
- Town
- City
- First Nation Reserve
- County or Municipal District

SCALE - 1:100,000

0 2 4 KM

N

Coordinate System: NAD 1983 3TM 114
Units: METRES

Engineer	GIS	Reviewer
RA	MSN/MMM	MM

Job Number	Date
3001178	02-NOV-2022

UPPER BOW RIVER HAZARD STUDY

ICE JAM FLOODWAY CRITERIA INDEX MAP

INDEX MAP

Notes to Users:

1. Please refer to the accompanying **Upper Bow River Hazard Study – Ice Jam Modelling Assessment and Flood Hazard Identification Report** for important information concerning these maps.
2. Within the flood inundation areas shown on this map, there may be isolated pockets of high ground. To determine whether or not a particular site is subject to flooding, reference should be made to the computed flood levels in conjunction with site-specific surveys where detailed definition is required.
3. Non-riverine and local sources of water have not been considered, and structures such roads, railways or barriers such as levees can restrict water flow and affect local flood levels. Channel obstruction, local stormwater inflow, groundwater seepage or other land drainage can cause flood levels to exceed those indicated on the map. Lands adjacent to a flooded area may be subject to flooding from tributary streams not indicated on the maps.
4. Backwater flood inundation along Bighill Creek and Jumpingpound Creek was determined using simulated water levels from the Bow River.
5. Line work for bridges and flood control structures is shown above flood inundation areas, even in cases where bridges or flood control structures are inundated.

Definitions:

Flood Hazard Map - A flood hazard map is a specific type of flood map that identifies the area flooded for the 1:100 design flood, and divides that flood hazard area into floodway and flood fringe zones. Flood hazard maps can also show additional flood hazard information, including the incremental areas at risk for more severe floods like the 1:200 and 1:500 floods. Flood hazard maps are typically used for long-term flood hazard area management and land-use planning.

Design Flood - The design flood standard in Alberta is the 1:100 flood, which is a flood that has a 1% chance of being equaled or exceeded in any given year. The design flood is typically based on the 1:100 open water flood, but it can also reflect 1:100 ice jam flood levels or be based on a historical flood event. Different sized floods have different chances of occurring – for example, a 1:200 flood has a 0.5% chance of occurring in any given year and a 1:500 flood has a 0.2% chance of occurring in any given year – but only the 1:100 design flood is used to define the floodway and flood fringe zones on flood hazard maps.

Floodway - When a floodway is first defined on a flood hazard map, it typically represents the area of highest flood hazard where flows are deepest, fastest, and most destructive during the 1:100 design flood. When a flood hazard map is updated, the floodway will not get larger in most circumstances to maintain long-term regulatory certainty, even if the flood hazard area gets larger or design flood levels get higher.

Flood Fringe - The flood fringe is the area outside of the floodway that is flooded or could be flooded during the 1:100 design flood. The flood fringe typically represents areas with

Definitions (continued):

shallower, slower, and less destructive flooding, but it may also include “high hazard flood fringe” areas. Areas at risk of flooding behind flood berms may also be mapped as “protected flood fringe” areas.

High Hazard Flood Fringe - The high hazard flood fringe identifies areas within the flood fringe with deeper or faster moving water than the rest of the flood fringe. High hazard flood fringe areas are likely to be most significant for flood maps that are being updated, but they may also be included in new flood maps.

Protected Flood Fringe - The protected flood fringe identifies areas that could be flooded if dedicated flood berms fail or do not work as designed during the 1:100 design flood, even if they are not overtopped. Protected flood fringe areas are part of the flood fringe and do not differentiate between areas with deeper or faster moving water and shallower or slower moving water.

Data Sources and References:

1. Orthophoto imagery acquired by ORTHOSHOP Geomatics Ltd. (3 June 2016) for Alberta Environment and Parks.
2. Base data from Town of Canmore, M.D. Bighorn, Town of Cochrane, Alberta Environment and Parks, AltaLIS and Natural Resources Canada.
3. Additional base mapping from Esri.

SHEET 2 ↓

Alberta Government

nhc
northwest hydraulic consultants

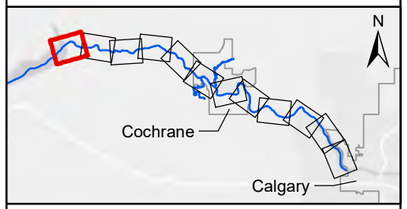

- FLOW DIRECTION
- BANK STATION
- PROPOSED FLOODWAY LIMIT
- PREVIOUS FLOODWAY
- PROPOSED FLOODWAY BOUNDARY
- BRIDGE
- CROSS SECTION
- RS 12,345 RIVER STATION
- STUDY LIMIT
- FLOOD CONTROL STRUCTURE
- OTHER FEATURE
- DAM
- 100-YEAR ICE JAM DESIGN FLOOD EXTENT
- DEPTH >= 1m
- RAILWAY
- MAJOR ROAD
- LOCAL ROAD
- CITY
- TOWN
- SUMMER VILLAGE
- COUNTY OR MUNICIPAL DISTRICT
- FIRST NATION RESERVE

SCALE - 1:10,000

0 100 200 300 400 M

N

Coordinate System: NAD 1983 3TM 114
Units: METRES

Engineer	GIS	Reviewer
RA	MSN/MMM	MM

Job Number	Date
3001178	01-NOV-2022

UPPER BOW RIVER HAZARD STUDY

ICE JAM FLOODWAY CRITERIA MAP

SHEET 1 OF 12

MMM_P:_Projects (Active)\3001178_Upper Bow River Hazard Study\2022_Municipal_Review_Update\90 GIS\UpperBowRHS_IJ_Floodway_Criteria_Map_2022MRUpdate.mxd

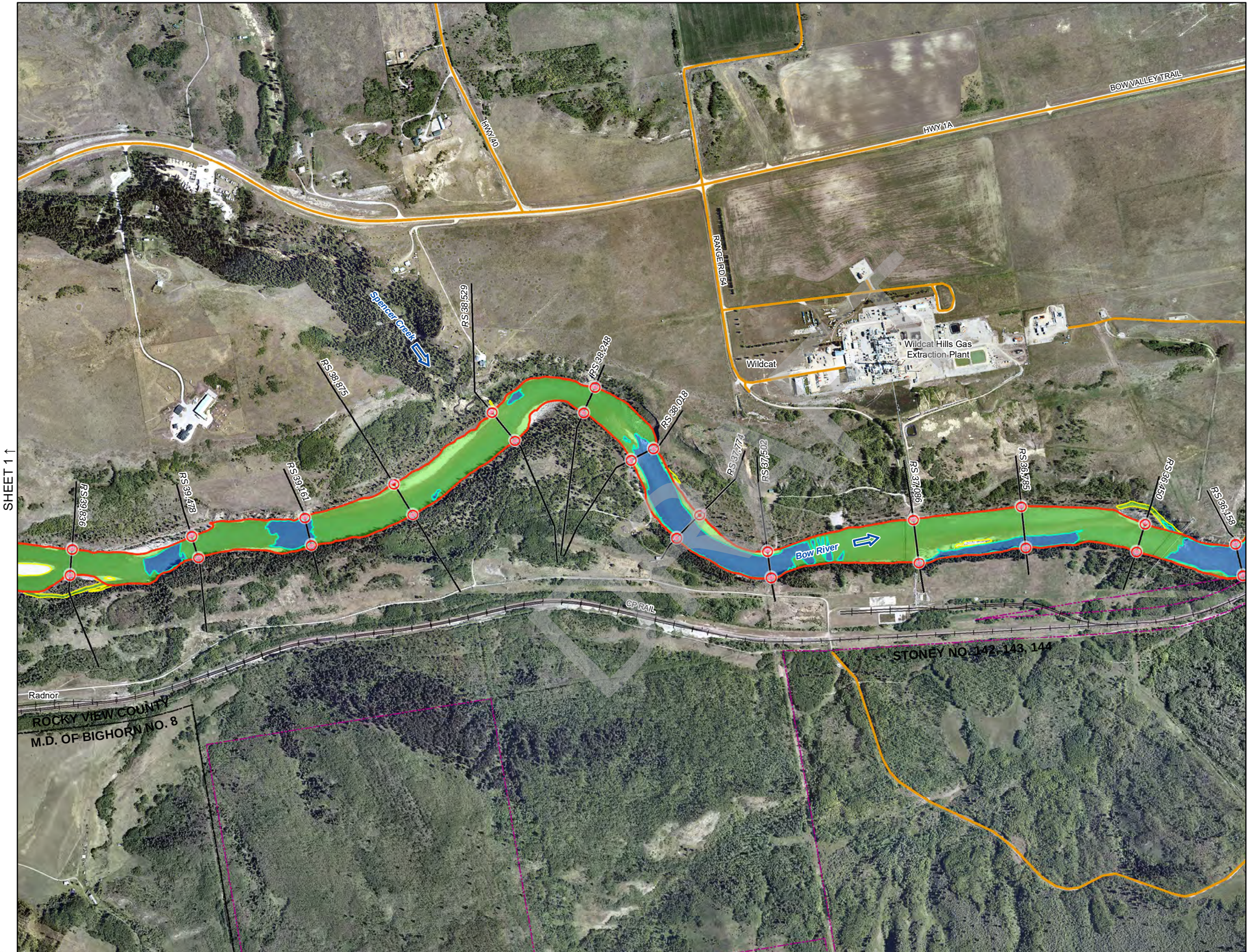

Alberta Government

nhc
northwest hydraulic consultants

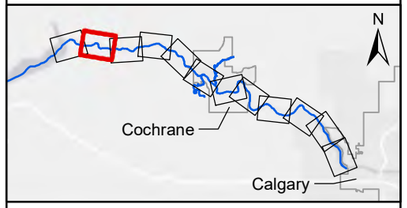

- FLOW DIRECTION
- BANK STATION
- PROPOSED FLOODWAY LIMIT
- PREVIOUS FLOODWAY
- PROPOSED FLOODWAY BOUNDARY
- BRIDGE
- CROSS SECTION
- RS 12,345 RIVER STATION
- STUDY LIMIT
- FLOOD CONTROL STRUCTURE
- OTHER FEATURE
- DAM
- 100-YEAR ICE JAM DESIGN FLOOD EXTENT
- DEPTH >= 1m
- RAILWAY
- MAJOR ROAD
- LOCAL ROAD
- CITY
- TOWN
- SUMMER VILLAGE
- COUNTY OR MUNICIPAL DISTRICT
- FIRST NATION RESERVE

SCALE - 1:10,000

0 100 200 300 400 M

N

Coordinate System: NAD 1983 3TM 114
Units: METRES

Engineer	GIS	Reviewer
RA	MSN/MMM	MM

Job Number	Date
3001178	01-NOV-2022

UPPER BOW RIVER HAZARD STUDY

ICE JAM FLOODWAY CRITERIA MAP

SHEET 2 OF 12

MMM, P:_Projects (Active)\3001178_Upper Bow River Hazard Study\2022_Municipal_Review_Update\90 GIS\UpperBowRHS_IJ_Floodway_Criteria_Map_2022MRUpdate.mxd

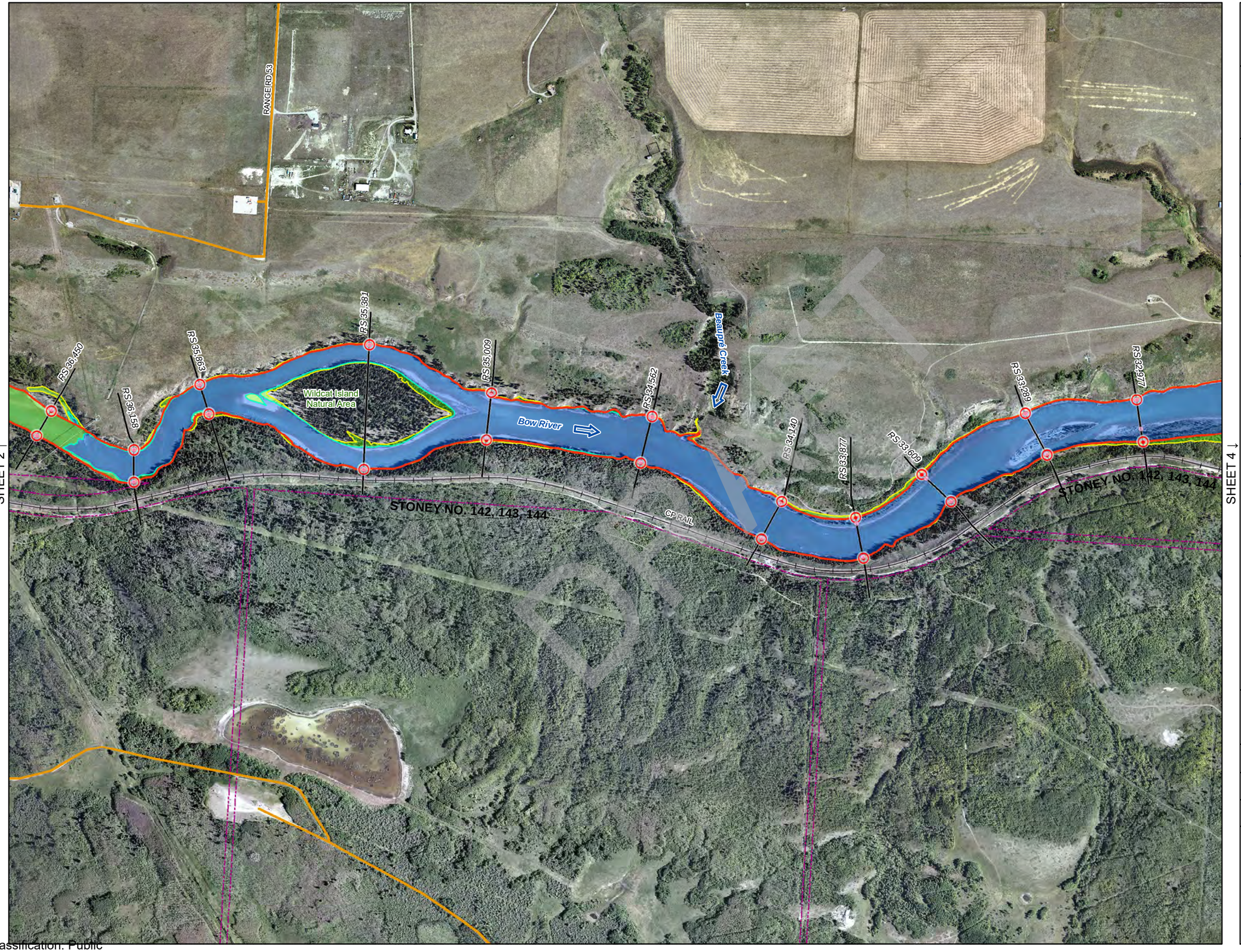

Alberta Government

nhc
northwest hydraulic consultants

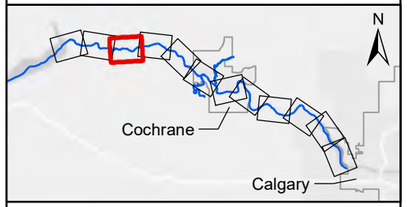

- FLOW DIRECTION
- BANK STATION
- PROPOSED FLOODWAY LIMIT
- PREVIOUS FLOODWAY
- PROPOSED FLOODWAY BOUNDARY
- BRIDGE
- CROSS SECTION
- RS 12,345 RIVER STATION
- STUDY LIMIT
- FLOOD CONTROL STRUCTURE
- OTHER FEATURE
- DAM
- 100-YEAR ICE JAM DESIGN FLOOD EXTENT
- DEPTH >= 1m
- RAILWAY
- MAJOR ROAD
- LOCAL ROAD
- CITY
- TOWN
- SUMMER VILLAGE
- COUNTY OR MUNICIPAL DISTRICT
- FIRST NATION RESERVE

SCALE - 1:10,000

0 100 200 300 400 M

N

Coordinate System: NAD 1983 3TM 114
Units: METRES

Engineer	GIS	Reviewer
RA	MSN/MMM	MM

Job Number	Date
3001178	01-NOV-2022

UPPER BOW RIVER HAZARD STUDY

ICE JAM FLOODWAY CRITERIA MAP

SHEET 3 OF 12

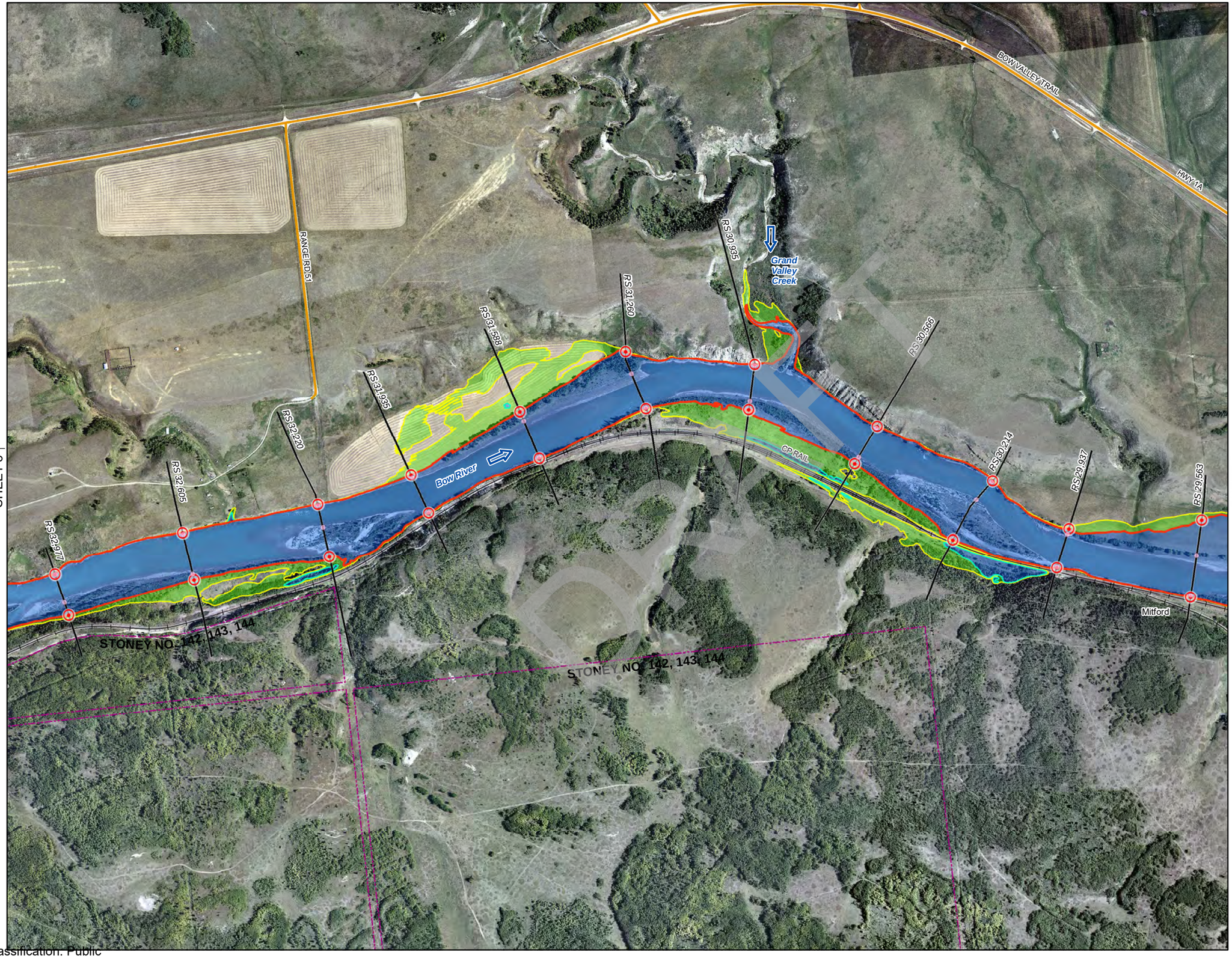

Alberta Government

nhc northwest hydraulic consultants

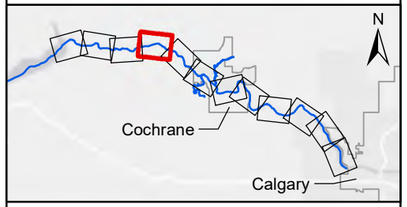

- FLOW DIRECTION
- BANK STATION
- PROPOSED FLOODWAY LIMIT
- PREVIOUS FLOODWAY
- PROPOSED FLOODWAY BOUNDARY
- BRIDGE
- CROSS SECTION
- RS 12,345 RIVER STATION
- STUDY LIMIT
- FLOOD CONTROL STRUCTURE
- OTHER FEATURE
- DAM
- 100-YEAR ICE JAM DESIGN FLOOD EXTENT
- DEPTH >= 1m
- RAILWAY
- MAJOR ROAD
- LOCAL ROAD
- CITY
- TOWN
- SUMMER VILLAGE
- COUNTY OR MUNICIPAL DISTRICT
- FIRST NATION RESERVE

SCALE - 1:10,000

0 100 200 300 400 M

N

Coordinate System: NAD 1983 3TM 114
Units: METRES

Engineer	GIS	Reviewer
RA	MSN/MMM	MM

Job Number	Date
3001178	01-NOV-2022

UPPER BOW RIVER HAZARD STUDY

ICE JAM FLOODWAY CRITERIA MAP

SHEET 4 OF 12

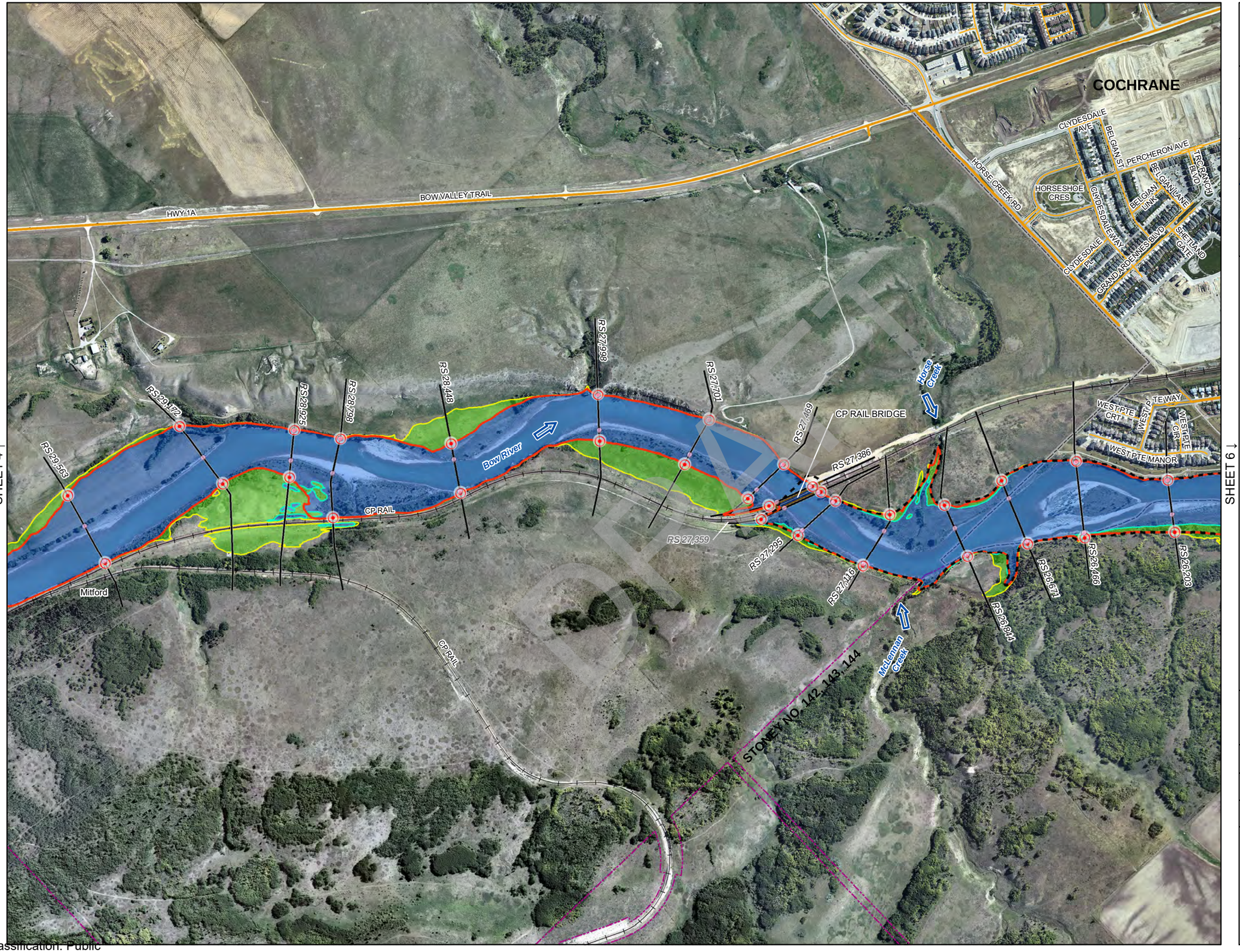

Alberta Government

nhc
northwest hydraulic consultants

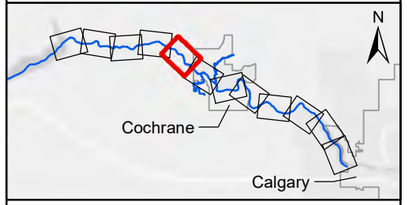

- FLOW DIRECTION
- BANK STATION
- PROPOSED FLOODWAY LIMIT
- PREVIOUS FLOODWAY
- PROPOSED FLOODWAY BOUNDARY
- BRIDGE
- CROSS SECTION
- RS 12,345 RIVER STATION
- STUDY LIMIT
- FLOOD CONTROL STRUCTURE
- OTHER FEATURE
- DAM
- 100-YEAR ICE JAM DESIGN FLOOD EXTENT
- DEPTH >= 1m
- RAILWAY
- MAJOR ROAD
- LOCAL ROAD
- CITY
- TOWN
- SUMMER VILLAGE
- COUNTY OR MUNICIPAL DISTRICT
- FIRST NATION RESERVE

SCALE - 1:10,000

0 100 200 300 400 M

Coordinate System: NAD 1983 3TM 114
Units: METRES

Engineer	GIS	Reviewer
RA	MSN/MMM	MM

Job Number	Date
3001178	01-NOV-2022

UPPER BOW RIVER HAZARD STUDY

ICE JAM FLOODWAY CRITERIA MAP

SHEET 5 OF 12

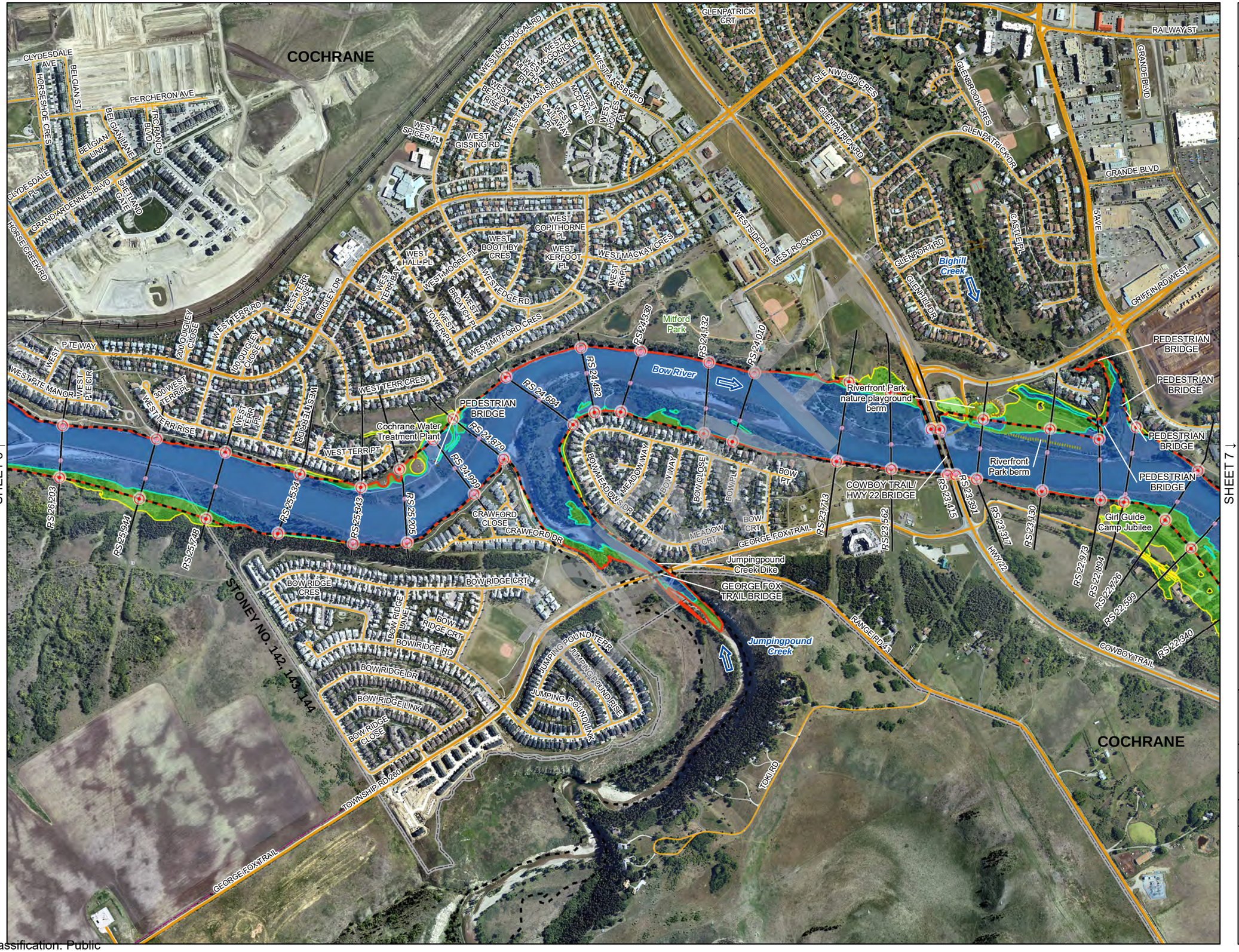

Alberta Government

nhc northwest hydraulic consultants

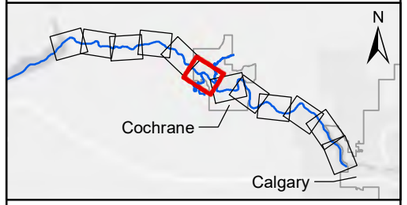

- FLOW DIRECTION
- BANK STATION
- PROPOSED FLOODWAY LIMIT
- PREVIOUS FLOODWAY
- PROPOSED FLOODWAY BOUNDARY
- BRIDGE
- CROSS SECTION
- RS 12,345 RIVER STATION
- STUDY LIMIT
- FLOOD CONTROL STRUCTURE
- OTHER FEATURE
- DAM
- 100-YEAR ICE JAM DESIGN FLOOD EXTENT
- DEPTH >= 1m
- RAILWAY
- MAJOR ROAD
- LOCAL ROAD
- CITY
- TOWN
- SUMMER VILLAGE
- COUNTY OR MUNICIPAL DISTRICT
- FIRST NATION RESERVE

SCALE - 1:10,000

0 100 200 300 400 M

N

Coordinate System: NAD 1983 3TM 114
Units: METRES

Engineer	GIS	Reviewer
RA	MSN/MMM	MM

Job Number	Date
3001178	01-NOV-2022

UPPER BOW RIVER HAZARD STUDY

ICE JAM FLOODWAY CRITERIA MAP

SHEET 6 OF 12

Alberta Government

nhc
northwest hydraulic consultants

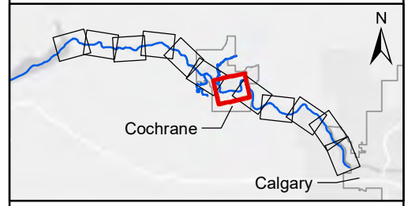

- FLOW DIRECTION
- BANK STATION
- PROPOSED FLOODWAY LIMIT
- PREVIOUS FLOODWAY
- PROPOSED FLOODWAY BOUNDARY
- BRIDGE
- CROSS SECTION
- RS 12,345 RIVER STATION
- STUDY LIMIT
- FLOOD CONTROL STRUCTURE
- OTHER FEATURE
- DAM
- 100-YEAR ICE JAM DESIGN FLOOD EXTENT
- DEPTH >= 1m
- RAILWAY
- MAJOR ROAD
- LOCAL ROAD
- CITY
- TOWN
- SUMMER VILLAGE
- COUNTY OR MUNICIPAL DISTRICT
- FIRST NATION RESERVE

SCALE - 1:10,000

0 100 200 300 400 M

N

Coordinate System: NAD 1983 3TM 114
Units: METRES

Engineer	GIS	Reviewer
RA	MSN/MMM	MM

Job Number	Date
3001178	01-NOV-2022

UPPER BOW RIVER HAZARD STUDY

ICE JAM FLOODWAY CRITERIA MAP

SHEET 7 OF 12

SHEET 7 ↑

SHEET 9 ↓

Glenbow Ranch Provincial Park

Bow River

COCHRANE

RS 18,270
RS 17,960
RS 17,630
RS 18,500
RS 18,709
RS 18,840
RS 18,984
RS 19,150
RS 17,298
RS 16,939
RS 19,342
RS 19,507
RS 19,603
RS 16,703
RS 16,437
RS 16,209
RS 19,798
RS 16,024
RS 19,933
RS 15,830
RS 20,174
RS 15,648
RS 20,329
RS 15,440
RS 15,224
RS 14,981
RS 14,763
RS 13,626
RS 13,874
RS 14,213
RS 14,383

CP RAIL

Glenbow Ranch Provincial Park

Alberta Government

nhc
northwest hydraulic consultants

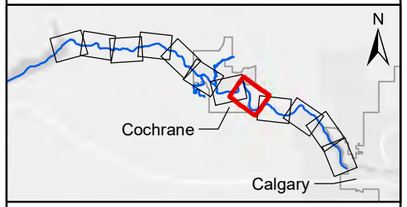

- FLOW DIRECTION
- BANK STATION
- PROPOSED FLOODWAY LIMIT
- PREVIOUS FLOODWAY
- PROPOSED FLOODWAY BOUNDARY
- BRIDGE
- CROSS SECTION
- RS 12,345 RIVER STATION
- STUDY LIMIT
- FLOOD CONTROL STRUCTURE
- OTHER FEATURE
- DAM
- 100-YEAR ICE JAM DESIGN FLOOD EXTENT
- DEPTH >= 1m
- RAILWAY
- MAJOR ROAD
- LOCAL ROAD
- CITY
- TOWN
- SUMMER VILLAGE
- COUNTY OR MUNICIPAL DISTRICT
- FIRST NATION RESERVE

SCALE - 1:10,000

0 100 200 300 400 M

Coordinate System: NAD 1983 3TM 114
Units: METRES

Engineer	GIS	Reviewer
RA	MSN/MMM	MM

Job Number	Date
3001178	01-NOV-2022

UPPER BOW RIVER HAZARD STUDY

ICE JAM FLOODWAY CRITERIA MAP

SHEET 8 OF 12

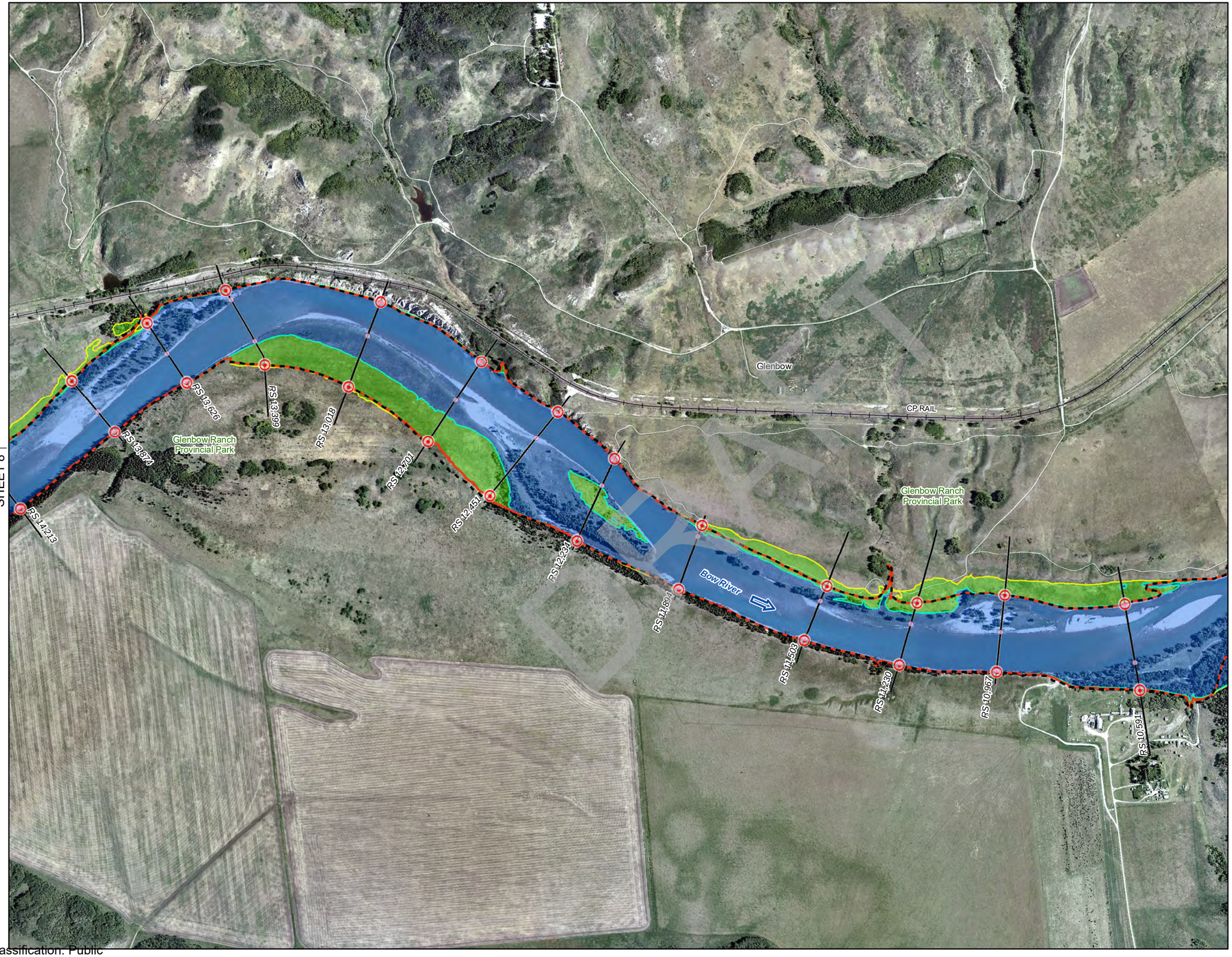

Alberta Government

nhc northwest hydraulic consultants

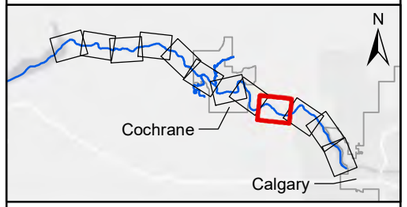

- FLOW DIRECTION
- BANK STATION
- PROPOSED FLOODWAY LIMIT
- PREVIOUS FLOODWAY
- PROPOSED FLOODWAY BOUNDARY
- BRIDGE
- CROSS SECTION
- RS 12,345 RIVER STATION
- STUDY LIMIT
- FLOOD CONTROL STRUCTURE
- OTHER FEATURE
- DAM
- 100-YEAR ICE JAM DESIGN FLOOD EXTENT
- DEPTH >= 1m
- RAILWAY
- MAJOR ROAD
- LOCAL ROAD
- CITY
- TOWN
- SUMMER VILLAGE
- COUNTY OR MUNICIPAL DISTRICT
- FIRST NATION RESERVE

SCALE - 1:10,000

0 100 200 300 400 M

N

Coordinate System: NAD 1983 3TM 114
Units: METRES

Engineer	GIS	Reviewer
RA	MSN/MMM	MM

Job Number	Date
3001178	01-NOV-2022

UPPER BOW RIVER HAZARD STUDY

ICE JAM FLOODWAY CRITERIA MAP

SHEET 9 OF 12

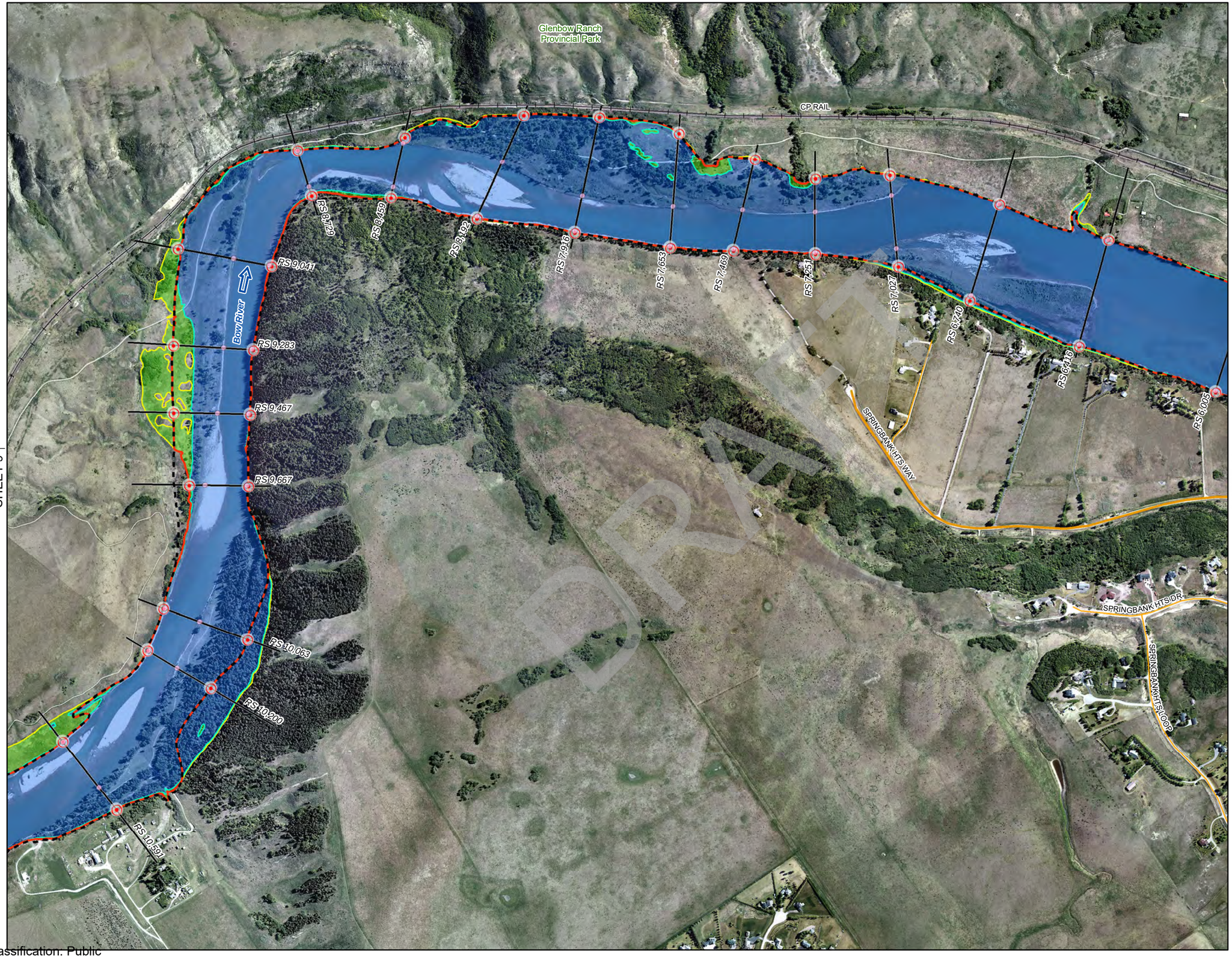

Alberta Government

nhc
northwest hydraulic consultants

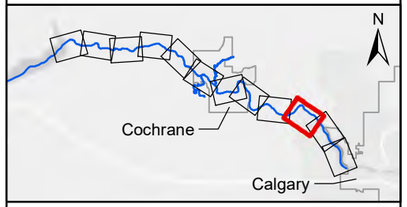

- FLOW DIRECTION
- BANK STATION
- PROPOSED FLOODWAY LIMIT
- PREVIOUS FLOODWAY
- PROPOSED FLOODWAY BOUNDARY
- BRIDGE
- CROSS SECTION
- RS 12,345 RIVER STATION
- STUDY LIMIT
- FLOOD CONTROL STRUCTURE
- OTHER FEATURE
- DAM
- 100-YEAR ICE JAM DESIGN FLOOD EXTENT
- DEPTH >= 1m
- RAILWAY
- MAJOR ROAD
- LOCAL ROAD
- CITY
- TOWN
- SUMMER VILLAGE
- COUNTY OR MUNICIPAL DISTRICT
- FIRST NATION RESERVE

SCALE - 1:10,000

0 100 200 300 400 M

Coordinate System: NAD 1983 3TM 114
Units: METRES

Engineer	GIS	Reviewer
RA	MSN/MMM	MM

Job Number	Date
3001178	01-NOV-2022

UPPER BOW RIVER HAZARD STUDY

ICE JAM FLOODWAY CRITERIA MAP

SHEET 10 OF 12

MMM_P:_Projects (Active)\3001178_Upper Bow River Hazard Study\2022_Municipal_Review_Update\90 GIS\UpperBowRHS_IJ_Floodway_Criteria_Map_

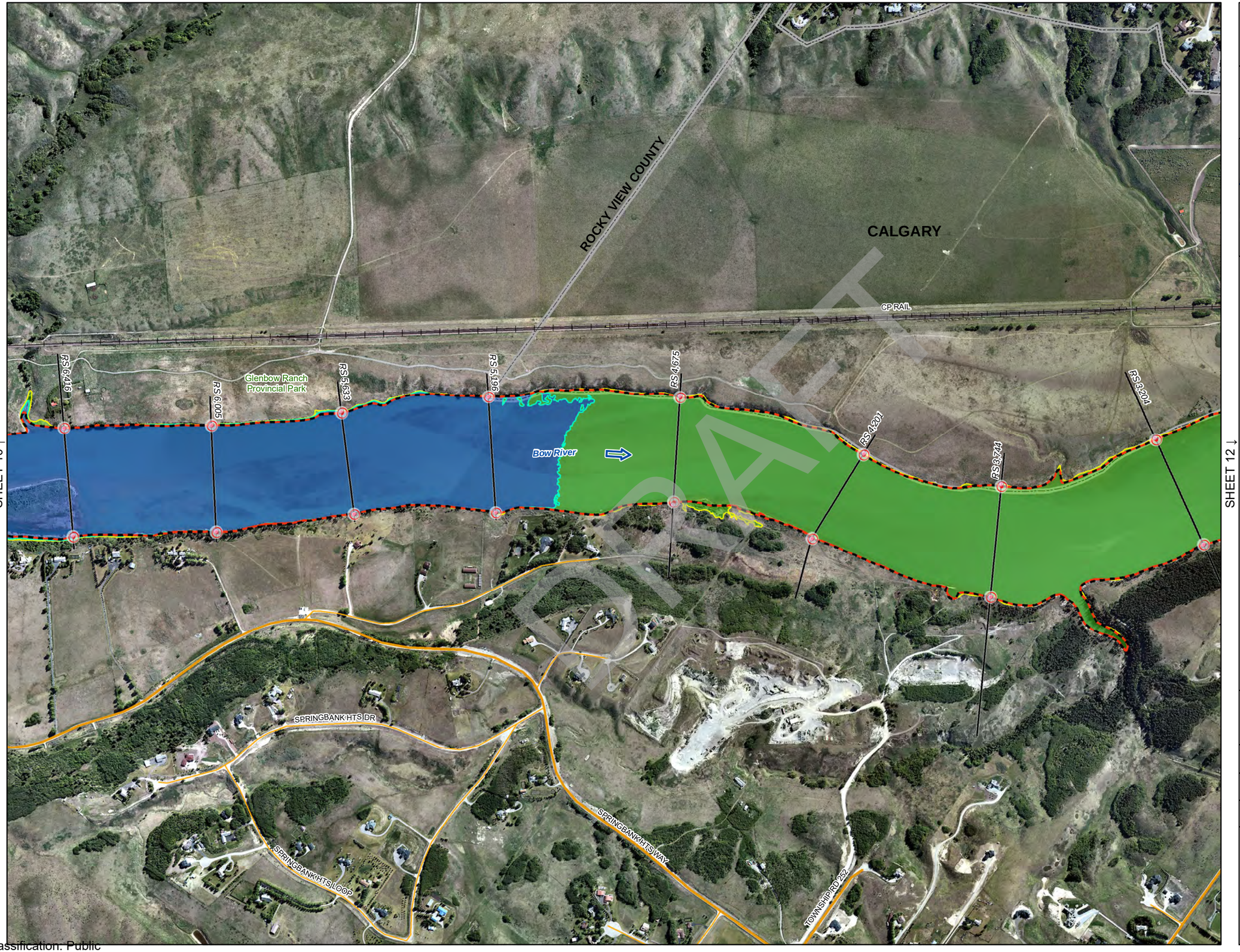

Alberta Government

nhc
northwest hydraulic consultants

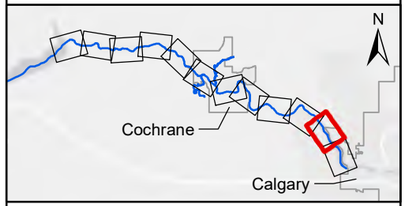

- FLOW DIRECTION
- BANK STATION
- PROPOSED FLOODWAY LIMIT
- PREVIOUS FLOODWAY
- PROPOSED FLOODWAY BOUNDARY
- BRIDGE
- CROSS SECTION
- RS 12,345 RIVER STATION
- STUDY LIMIT
- FLOOD CONTROL STRUCTURE
- OTHER FEATURE
- DAM
- 100-YEAR ICE JAM DESIGN FLOOD EXTENT
- DEPTH >= 1m
- RAILWAY
- MAJOR ROAD
- LOCAL ROAD
- CITY
- TOWN
- SUMMER VILLAGE
- COUNTY OR MUNICIPAL DISTRICT
- FIRST NATION RESERVE

SCALE - 1:10,000

0 100 200 300 400 M

Coordinate System: NAD 1983 3TM 114
Units: METRES

Engineer	GIS	Reviewer
RA	MSN/MMM	MM

Job Number	Date
3001178	01-NOV-2022

UPPER BOW RIVER HAZARD STUDY

ICE JAM FLOODWAY CRITERIA MAP

SHEET 11 OF 12

SHEET 11 ↑

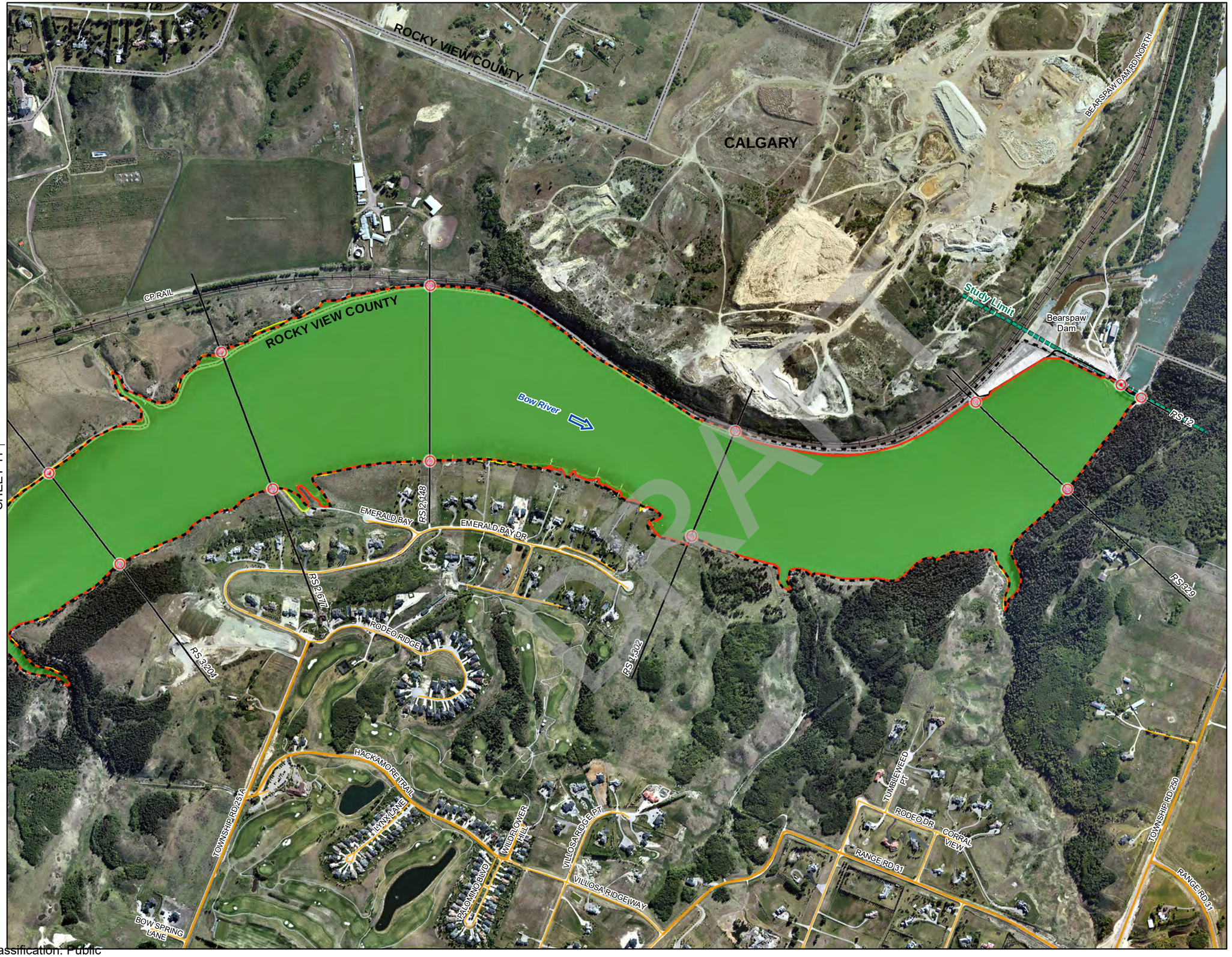

Alberta Government

nhc
northwest hydraulic consultants

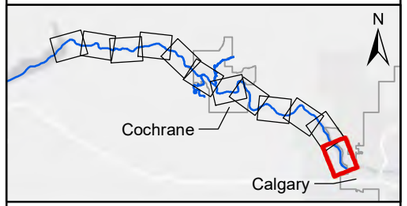

- FLOW DIRECTION
- BANK STATION
- PROPOSED FLOODWAY LIMIT
- PREVIOUS FLOODWAY
- PROPOSED FLOODWAY BOUNDARY
- BRIDGE
- CROSS SECTION
- RS 12,345 RIVER STATION
- STUDY LIMIT
- FLOOD CONTROL STRUCTURE
- OTHER FEATURE
- DAM
- 100-YEAR ICE JAM DESIGN FLOOD EXTENT
- DEPTH >= 1m
- RAILWAY
- MAJOR ROAD
- LOCAL ROAD
- CITY
- TOWN
- SUMMER VILLAGE
- COUNTY OR MUNICIPAL DISTRICT
- FIRST NATION RESERVE

SCALE - 1:10,000

0 100 200 300 400 M

N

Coordinate System: NAD 1983 3TM 114
Units: METRES

Engineer	GIS	Reviewer
RA	MSN/MMM	MM

Job Number	Date
3001178	01-NOV-2022

UPPER BOW RIVER HAZARD STUDY

ICE JAM FLOODWAY CRITERIA MAP

SHEET 12 OF 12

APPENDIX A
COMPUTED ICE JAM FLOOD FREQUENCY WATER LEVELS

River Station (m)	Computed Water Surface Elevation (m)		
	200-Year	100-Year	50-Year
41,824	1158.96	1158.99	1159.03
41,537	1158.70	1158.73	1158.76
41,361	1158.38	1158.41	1158.44
40,989	1157.20	1157.23	1157.26
40,712	1156.88	1156.91	1156.94
40,439	1156.43	1156.46	1156.48
40,129	1155.46	1155.48	1155.50
39,836	1154.14	1154.18	1154.21
39,478	1153.29	1153.33	1153.37
39,161	1153.02	1153.05	1153.09
38,875	1152.57	1152.60	1152.63
38,529	1151.55	1151.59	1151.64
38,248	1150.68	1150.73	1150.81
38,018	1150.19	1150.25	1150.56
37,774	1149.83	1149.89	1150.31
37,502	1149.52	1149.59	1150.26
37,086	1148.88	1148.95	1150.53
36,785	1148.25	1148.33	1150.28
36,450	1146.88	1147.00	1149.77
36,158	1146.02	1146.64	1149.20
35,863	1145.21	1146.48	1148.43
35,381	1144.64	1146.19	1147.44
35,009	1143.75	1145.91	1146.58
34,562	1143.55	1145.18	1145.72
34,140	1143.52	1144.60	1145.02
33,877	1143.25	1144.11	1144.56
33,609	1142.79	1143.55	1143.90
33,289	1142.35	1142.96	1143.28
32,977	1141.85	1142.37	1142.60
32,605	1141.26	1141.82	1142.10
32,220	1140.41	1140.91	1141.23
31,935	1139.92	1140.44	1140.72
31,588	1139.48	1139.98	1140.21
31,260	1138.88	1139.39	1139.57
30,935	1138.33	1138.74	1138.91
30,566	1137.64	1138.02	1138.20
30,214	1136.80	1137.22	1137.36
29,937	1136.39	1136.80	1136.96
29,563	1135.85	1136.24	1136.44
29,172	1135.13	1135.43	1135.59
28,925	1134.74	1135.03	1135.20
28,798	1134.48	1134.78	1134.93

River Station (m)	Computed Water Surface Elevation (m)		
	200-Year	100-Year	50-Year
28,448	1133.76	1134.03	1134.19
27,998	1132.95	1133.22	1133.37
27,701	1132.47	1132.73	1132.86
27,469	1132.03	1132.26	1132.37
27,386	1131.91	1132.14	1132.24
27,359*	1131.86*	1132.09*	1132.19*
27,295	1131.75	1131.97	1132.08
27,116	1131.40	1131.61	1131.75
26,844	1130.84	1131.02	1131.15
26,671	1130.43	1130.63	1130.77
26,466	1129.99	1130.17	1130.32
26,203	1129.35	1129.49	1129.68
25,944	1128.85	1129.01	1129.15
25,748	1128.48	1128.65	1128.81
25,534	1128.10	1128.29	1128.46
25,343	1127.77	1127.95	1128.13
25,205	1127.52	1127.69	1127.87
24,999	1127.11	1127.28	1127.45
24,879	1126.86	1127.02	1127.18
24,684	1126.47	1126.65	1126.79
24,482	1126.00	1126.19	1126.32
24,338	1125.75	1125.98	1126.07
24,132	1125.34	1125.58	1125.67
24,010	1125.09	1125.31	1125.41
23,713	1124.27	1124.46	1124.55
23,562	1123.81	1124.01	1124.10
23,415*	1123.52*	1123.72*	1123.81*
23,391*	1123.47*	1123.67*	1123.77*
23,317	1123.33	1123.52	1123.62
23,130	1122.99	1123.16	1123.26
22,973	1122.66	1122.83	1122.92
22,894	1122.49	1122.65	1122.74
22,726	1122.08	1122.23	1122.33
22,599	1121.77	1121.92	1122.01
22,340	1121.24	1121.40	1121.49
22,028	1120.65	1120.77	1120.87
21,803	1120.27	1120.39	1120.49
21,608	1119.98	1120.12	1120.22
21,421	1119.75	1119.91	1119.98
21,274	1119.55	1119.71	1119.79
21,235*	1119.47*	1119.64*	1119.71*
21,217*	1119.44*	1119.60*	1119.68*

River Station (m)	Computed Water Surface Elevation (m)		
	200-Year	100-Year	50-Year
21,170	1119.35	1119.51	1119.59
21,030	1118.97	1119.12	1119.20
20,876	1118.53	1118.69	1118.76
20,666	1118.06	1118.22	1118.30
20,496	1117.78	1117.92	1118.01
20,329	1117.55	1117.66	1117.77
20,174	1117.33	1117.44	1117.55
19,933	1116.90	1117.00	1117.14
19,798	1116.53	1116.62	1116.79
19,603	1115.98	1116.09	1116.25
19,507	1115.83	1115.96	1116.10
19,342	1115.58	1115.75	1115.85
19,150	1115.27	1115.44	1115.56
18,984	1114.96	1115.11	1115.25
18,840	1114.61	1114.75	1114.91
18,709	1114.39	1114.52	1114.68
18,500	1113.54	1113.68	1113.81
18,270	1113.08	1113.24	1113.39
17,960	1112.59	1112.73	1112.90
17,680	1112.25	1112.38	1112.56
17,298	1111.47	1111.61	1111.77
16,969	1110.81	1110.93	1111.12
16,703	1110.28	1110.40	1110.59
16,437	1109.90	1110.01	1110.19
16,269	1109.64	1109.75	1109.92
16,024	1109.13	1109.23	1109.41
15,830	1108.86	1108.95	1109.13
15,648	1108.58	1108.66	1108.85
15,440	1108.19	1108.27	1108.45
15,224	1107.86	1107.97	1108.12
14,981	1107.47	1107.59	1107.76
14,763	1107.08	1107.23	1107.40
14,383	1106.44	1106.56	1106.76
14,213	1106.17	1106.28	1106.49
13,874	1105.36	1105.49	1105.69
13,626	1104.91	1105.06	1105.23
13,399	1104.57	1104.71	1104.87
13,018	1103.91	1104.03	1104.22
12,701	1103.32	1103.47	1103.62
12,451	1102.68	1102.85	1102.99
12,234	1102.30	1102.47	1102.63
11,894	1101.82	1102.01	1102.16

River Station (m)	Computed Water Surface Elevation (m)		
	200-Year	100-Year	50-Year
11,503	1101.10	1101.29	1101.48
11,230	1100.68	1100.87	1101.08
10,967	1100.33	1100.51	1100.71
10,591	1099.79	1099.98	1100.15
10,200	1098.84	1099.02	1099.17
10,063	1098.57	1098.75	1098.90
9,667	1097.73	1097.89	1098.05
9,467	1097.20	1097.35	1097.52
9,283	1096.87	1097.03	1097.21
9,041	1096.52	1096.69	1096.87
8,729	1096.02	1096.19	1096.37
8,459	1095.51	1095.69	1095.86
8,192	1094.99	1095.17	1095.34
7,916	1094.57	1094.74	1094.92
7,653	1094.17	1094.36	1094.52
7,469	1093.94	1094.13	1094.29
7,251	1093.77	1093.96	1094.13
7,027	1093.58	1093.77	1093.94
6,740	1093.21	1093.41	1093.58
6,416	1092.90	1093.07	1093.26
6,005	1092.18	1092.28	1092.40
5,633	1091.57	1091.68	1091.76
5,196	1091.39	1091.43	1091.48
4,675	1090.92	1090.92	1090.92
4,201	1090.91	1090.91	1090.91
3,744	1090.91	1090.91	1090.91
3,204	1090.90	1090.90	1090.90
2,677	1090.90	1090.90	1090.90
2,148	1090.90	1090.90	1090.90
1,302	1090.90	1090.90	1090.90
329	1090.90	1090.90	1090.90
12	1090.90	1090.90	1090.90

Note:

Cross sections denoted by an * were omitted from the ice enhanced model for improved model performance (refer to Section 4.1.2). The computed water surface elevations presented in the table were interpolated between the closest upstream and downstream cross sections.

APPENDIX B
ICE JAM FLOODWAY DETERMINATION CRITERIA SUMMARY

River Station (m)	Left		Right	
	Floodway Limit (m)	Governing Criteria	Floodway Limit (m)	Governing Criteria
41,824	299.9	Main Channel	336.5	Main Channel
41,537	142.3	Main Channel	231.1	Main Channel
41,361	124.1	Main Channel	205.7	Main Channel
40,989	36.3	Main Channel	122.3	Main Channel
40,712	73.8	Main Channel	289.0	Main Channel
40,439	152.4	Main Channel	326.9	Main Channel
40,129	155.8	Main Channel	276.3	Main Channel
39,836	187.0	Main Channel	259.6	Main Channel
39,478	149.2	Main Channel	211.7	Main Channel
39,161	148.3	Main Channel	225.3	Main Channel
38,875	398.3	Main Channel	498.6	Main Channel
38,529	373.9	Main Channel	474.6	Main Channel
38,248	67.4	Main Channel	145.5	Main Channel
38,018	136.3	Main Channel	204.8	Main Channel
37,774	222.3	Main Channel	312.5	Main Channel
37,502	262.2	Main Channel	336.5	Main Channel
37,086	166.6	Main Channel	287.3	Main Channel
36,785	140.5	Main Channel	254.5	Main Channel
36,450	138.1	Main Channel	217.7	Main Channel
36,158	168.0	Main Channel	258.0	Main Channel
35,863	84.2	Main Channel	171.4	Main Channel
35,381	91.1	1m Depth	442.3	1m Depth
35,009	148.8	1m Depth	283.3	1m Depth
34,562	124.6	1m Depth	258.9	1m Depth
34,140	241.7	1m Depth	360.7	1m Depth
33,877	225.4	1m Depth	341.8	1m Depth
33,609	69.5	1m Depth	181.0	1m Depth
33,289	84.1	1m Depth	216.3	1m Depth
32,977	78.7	1m Depth	198.6	1m Depth
32,605	203.8	1m Depth	337.9	1m Depth
32,220	281.9	1m Depth	431.2	1m Depth
31,935	316.4	1m Depth	433.5	1m Depth
31,588	251.9	1m Depth	392.7	1m Depth
31,260	217.2	1m Depth	389.7	1m Depth
30,935	417.4	1m Depth	544.5	1m Depth
30,566	341.4	1m Depth	462.6	1m Depth
30,214	107.4	1m Depth	306.3	1m Depth
29,937	226.9	1m Depth	340.7	1m Depth
29,563	126.1	1m Depth	343.7	1m Depth
29,172	119.4	1m Depth	322.5	1m Depth
28,925	120.0	1m Depth	253.3	1m Depth
28,798	169.2	1m Depth	393.4	1m Depth
28,448	169.2	1m Depth	309.5	1m Depth
27,998	212.6	1m Depth	344.5	1m Depth
27,701	141.2	1m Depth	284.3	1m Depth

River Station (m)	Left		Right	
	Floodway Limit (m)	Governing Criteria	Floodway Limit (m)	Governing Criteria
27,469	191.3	1m Depth	330.4	1m Depth
27,386	193.6	Inundation Limit[1]	327.2	1m Depth
27,359	180.3	Inundation Limit[1]	364.5	Previous Floodway
27,295	161.1	Inundation Limit[1]	303.6	Previous Floodway
27,116	164.9	Previous Floodway	330.2	Previous Floodway
26,844	218.2	Inundation Limit[1]	375.5	Previous Floodway
26,671	204.5	Inundation Limit[2]	395.7	Inundation Limit[1]
26,466	223.2	Inundation Limit[1]	438.6	Inundation Limit[1]
26,203	164.4	Inundation Limit[1]	311.5	Previous Floodway
25,944	120.7	Previous Floodway	294.5	Previous Floodway
25,748	70.0	Inundation Limit[1]	263.7	Previous Floodway
25,534	255.4	Previous Floodway	433.3	Previous Floodway
25,343	299.4	Inundation Limit[1]	457.9	Previous Floodway
25,205	214.9	Inundation Limit[1]	423.0	Inundation Limit[1]
24,999	126.6	Previous Floodway	316.8	Inundation Limit[1]
24,879	90.4	Previous Floodway	272.0	Inundation Limit[1]
24,684	38.3	Inundation Limit[1]	269.8	Previous Floodway
24,482	40.1	Inundation Limit[1]	226.9	Inundation Limit[1]
24,338	35.5	Inundation Limit[1]	216.5	Inundation Limit[1]
24,132	13.6	Inundation Limit[1]	212.6	Inundation Limit[1]
24,010	53.1	Inundation Limit[1]	256.6	Inundation Limit[1]
23,713	145.5	Previous Floodway	371.7	Inundation Limit[1]
23,562	164.0	Previous Floodway	381.0	Previous Floodway
23,415	216.9	Inundation Limit[1]	352.8	Previous Floodway
23,391	220.5	Inundation Limit[1]	356.2	Previous Floodway
23,317	104.7	Previous Floodway	273.9	Previous Floodway
23,130	157.6	Previous Floodway	333.5	Inundation Limit[1]
22,973	122.4	Previous Floodway	292.3	Inundation Limit[1]
22,894	42.3	Previous Floodway	255.7	Inundation Limit[1]
22,726	149.9	Inundation Limit[1]	316.2	Previous Floodway
22,599	261.4	Inundation Limit[1]	440.6	Previous Floodway
22,340	434.5	Previous Floodway	631.6	Previous Floodway
22,028	589.6	Previous Floodway	723.7	Inundation Limit[1]
21,803	574.1	Previous Floodway	677.9	Previous Floodway
21,608	467.2	Inundation Limit[1]	620.2	Inundation Limit[1]
21,421	392.4	Previous Floodway	548.6	1 m Depth
21,274	125.2	Previous Floodway	294.2	Previous Floodway
21,235	91.3	Previous Floodway	255.1	Inundation Limit[2]
21,217	90.2	Previous Floodway	245.4	Inundation Limit[1]
21,170	149.2	Previous Floodway	312.2	Inundation Limit[1]
21,030	161.5	Previous Floodway	347.8	Inundation Limit[1]
20,876	213.5	Previous Floodway	383.9	Inundation Limit[1]
20,666	216.3	Inundation Limit[1]	370.8	Inundation Limit[1]
20,496	207.9	Inundation Limit[1]	369.9	Inundation Limit[1]
20,329	202.1	Previous Floodway	361.4	Inundation Limit[1]

River Station (m)	Left		Right	
	Floodway Limit (m)	Governing Criteria	Floodway Limit (m)	Governing Criteria
20,174	295.9	Inundation Limit[1]	458.6	Inundation Limit[1]
19,933	463.5	Inundation Limit[1]	628.2	Previous Floodway
19,798	524.1	Inundation Limit[1]	676.1	Previous Floodway
19,603	462.6	Inundation Limit[1]	587.1	Inundation Limit[1]
19,507	351.1	Inundation Limit[1]	499.9	Inundation Limit[1]
19,342	232.8	Previous Floodway	458.7	1 m Depth
19,150	240.7	1 m Depth	565.7	Inundation Limit[1]
18,984	185.2	Previous Floodway	470.3	Inundation Limit[1]
18,840	140.9	Previous Floodway	372.2	Inundation Limit[1]
18,709	121.1	Inundation Limit[2]	344.6	Inundation Limit[2]
18,500	72.4	Inundation Limit[2]	249.6	Previous Floodway
18,270	50.9	Inundation Limit[2]	189.9	Previous Floodway
17,960	43.8	Inundation Limit[1]	222.5	Previous Floodway
17,680	47.8	Inundation Limit[1]	313.0	Previous Floodway
17,298	51.4	Inundation Limit[1]	330.5	Inundation Limit[1]
16,969	53.8	Previous Floodway	234.2	Inundation Limit[1]
16,703	31.0	Inundation Limit[1]	191.6	Inundation Limit[1]
16,437	25.9	1 m Depth	192.0	Inundation Limit[1]
16,269	24.7	Inundation Limit[1]	197.7	Previous Floodway
16,024	39.1	Inundation Limit[1]	196.6	Previous Floodway
15,830	43.7	Inundation Limit[1]	210.1	Previous Floodway
15,648	59.8	Previous Floodway	268.7	Previous Floodway
15,440	106.6	Previous Floodway	277.9	Previous Floodway
15,224	149.0	Previous Floodway	322.8	Previous Floodway
14,981	133.2	Previous Floodway	314.5	Previous Floodway
14,763	144.4	Previous Floodway	318.9	Previous Floodway
14,383	119.1	Previous Floodway	259.7	Inundation Limit[1]
14,213	122.8	Previous Floodway	282.1	Inundation Limit[1]
13,874	118.6	Previous Floodway	305.6	Inundation Limit[1]
13,626	89.4	Inundation Limit[1]	288.6	Inundation Limit[1]
13,399	74.6	Previous Floodway	311.5	Previous Floodway
13,018	62.1	Previous Floodway	314.6	Previous Floodway
12,701	76.1	Inundation Limit[1]	344.7	Inundation Limit[1]
12,451	57.5	Inundation Limit[1]	358.7	Inundation Limit[1]
12,234	57.5	Inundation Limit[1]	308.9	Inundation Limit[1]
11,894	29.5	Previous Floodway	218.6	Previous Floodway
11,503	162.4	Previous Floodway	328.3	Inundation Limit[1]
11,230	211.5	Previous Floodway	391.0	Inundation Limit[1]
10,967	164.1	Previous Floodway	379.5	Inundation Limit[1]
10,591	105.4	Previous Floodway	348.5	Inundation Limit[1]
10,200	67.8	Inundation Limit[1]	273.3	Previous Floodway
10,063	73.1	Inundation Limit[1]	323.1	Previous Floodway
9,667	158.9	Inundation Limit[1]	323.4	Previous Floodway
9,467	125.7	Previous Floodway	339.0	Inundation Limit[1]
9,283	125.2	Previous Floodway	348.0	Inundation Limit[1]

River Station (m)	Left		Right	
	Floodway Limit (m)	Governing Criteria	Floodway Limit (m)	Governing Criteria
9,041	121.0	Previous Floodway	385.7	Inundation Limit[1]
8,729	102.8	Previous Floodway	235.6	Inundation Limit[1]
8,459	77.3	Previous Floodway	249.2	Inundation Limit[1]
8,192	29.2	Previous Floodway	345.4	Inundation Limit[1]
7,916	31.1	Inundation Limit[1]	359.9	Inundation Limit[1]
7,653	53.2	Inundation Limit[1]	372.8	Previous Floodway
7,469	41.1	1 m Depth	305.0	Inundation Limit[1]
7,251	76.5	Previous Floodway	288.0	Inundation Limit[1]
7,027	74.0	Previous Floodway	330.6	Previous Floodway
6,740	158.8	Previous Floodway	439.0	Previous Floodway
6,416	208.9	Inundation Limit[1]	515.2	Previous Floodway
6,005	80.9	Previous Floodway	380.3	Inundation Limit[1]
5,633	375.3	1 m Depth	374.1	Previous Floodway
5,196	64.2	Inundation Limit[1]	389.5	Previous Floodway
4,675	65.8	Previous Floodway	359.4	Inundation Limit[1]
4,201	65.0	Previous Floodway	340.4	Inundation Limit[2]
3,744	92.6	Previous Floodway	405.1	Inundation Limit[1]
3,204	208.2	Previous Floodway	530.2	Inundation Limit[1]
2,677	233.2	Previous Floodway	642.1	Inundation Limit[2]
2,148	114.2	Inundation Limit[1]	603.7	Previous Floodway
1,302	127.7	Inundation Limit[2]	445.4	Previous Floodway
329	109.5	Inundation Limit[1]	461.9	Inundation Limit[1]
12	565.0	Previous Floodway	634.1	Inundation Limit[1]

Notes:

1. Previous floodway is outside inundation limit.
2. No viable flood fringe.

APPENDIX C
ICE JAM DESIGN FLOOD WATER LEVELS

River Station (m)	Ice Jam Design Flood Water Level (m)
41,824	1158.99
41,537	1158.73
41,361	1158.41
40,989	1157.23
40,712	1156.91
40,439	1156.46
40,129	1155.48
39,836	1154.18
39,478	1153.33
39,161	1153.05
38,875	1152.60
38,529	1151.59
38,248	1150.73
38,018	1150.25
37,774	1149.89
37,502	1149.59
37,086	1148.95
36,785	1148.33
36,450	1147.00
36,158	1146.64
35,863	1146.48
35,381	1146.19
35,009	1145.91
34,562	1145.18
34,140	1144.60
33,877	1144.11
33,609	1143.55
33,289	1142.96
32,977	1142.37
32,605	1141.82
32,220	1140.91
31,935	1140.44
31,588	1139.98
31,260	1139.39
30,935	1138.74
30,566	1138.02
30,214	1137.22
29,937	1136.80
29,563	1136.24
29,172	1135.43
28,925	1135.03
28,798	1134.78
28,448	1134.03

River Station (m)	Ice Jam Design Flood Water Level (m)
27,998	1133.22
27,701	1132.73
27,469	1132.26
27,386	1132.14
27,359*	1132.09
27,295	1131.97
27,116	1131.61
26,844	1131.02
26,671	1130.63
26,466	1130.17
26,203	1129.49
25,944	1129.01
25,748	1128.65
25,534	1128.29
25,343	1127.95
25,205	1127.69
24,999	1127.28
24,879	1127.02
24,684	1126.65
24,482	1126.19
24,338	1125.98
24,132	1125.58
24,010	1125.31
23,713	1124.46
23,562	1124.01
23,415*	1123.72
23,391*	1123.67
23,317	1123.52
23,130	1123.16
22,973	1122.83
22,894	1122.65
22,726	1122.23
22,599	1121.92
22,340	1121.40
22,028	1120.77
21,803	1120.39
21,608	1120.12
21,421	1119.91
21,274	1119.71
21,235*	1119.64
21,217*	1119.60
21,170	1119.51
21,030	1119.12

River Station (m)	Ice Jam Design Flood Water Level (m)
20,876	1118.69
20,666	1118.22
20,496	1117.92
20,329	1117.66
20,174	1117.44
19,933	1117.00
19,798	1116.62
19,603	1116.09
19,507	1115.96
19,342	1115.75
19,150	1115.44
18,984	1115.11
18,840	1114.75
18,709	1114.52
18,500	1113.68
18,270	1113.24
17,960	1112.73
17,680	1112.38
17,298	1111.61
16,969	1110.93
16,703	1110.40
16,437	1110.01
16,269	1109.75
16,024	1109.23
15,830	1108.95
15,648	1108.66
15,440	1108.27
15,224	1107.97
14,981	1107.59
14,763	1107.23
14,383	1106.56
14,213	1106.28
13,874	1105.49
13,626	1105.06
13,399	1104.71
13,018	1104.03

River Station (m)	Ice Jam Design Flood Water Level (m)
12,701	1103.47
12,451	1102.85
12,234	1102.47
11,894	1102.01
11,503	1101.29
11,230	1100.87
10,967	1100.51
10,591	1099.98
10,200	1099.02
10,063	1098.75
9,667	1097.89
9,467	1097.35
9,283	1097.03
9,041	1096.69
8,729	1096.19
8,459	1095.69
8,192	1095.17
7,916	1094.74
7,653	1094.36
7,469	1094.13
7,251	1093.96
7,027	1093.77
6,740	1093.41
6,416	1093.07
6,005	1092.28
5,633	1091.68
5,196	1091.43
4,675	1090.92
4,201	1090.91
3,744	1090.91
3,204	1090.90
2,677	1090.90
2,148	1090.90
1,302	1090.90
329	1090.90
12	1090.90

Notes:

1. Cross sections denoted by an * were omitted from the ice enhanced model for improved model performance (refer to Section 4.1.2). The computed water levels presented in the table were interpolated between the closest upstream and downstream cross sections.
2. Design flood water level 1122.83 m at RS 22,973 was applied to Bighill Creek (RS 185 through 454) due to backwater inundation from the Bow River.
3. Design flood water level 1127.02 m at RS 24,879 was applied to Jumpingpound Creek (RS 116 through 1,056) due to backwater inundation from the Bow River.

nhc
northwest hydraulic consultants
water resource specialists